



Fahrtbericht und Abschlußbericht

SITKAP

Submersible Investigations of the
Tonga – Kermadec Arc using *PISCES*

Untersuchung des Tonga – Kermadec
Inselbogens mit dem Tauchboot *PISCES*

Stoffers, P.; Worthington, T.; Schwarz-Schampera, U.;
Evans, L.; Hannington, M.; Hekinian, R.; Lundsten, L.;
Massoth, G.; Schmidt, M.; Vaiomo'unga, R.

Auckland, New Zealand – Pago Pago, American Samoa
06 – 29 June 2005

BMBF 03G0632A
DFG STO 110/42-1

Projektleiter:
Prof. P. Stoffers, Christian-Albrechts-Universität zu Kiel
Dr. U. Schwarz-Schampera, BGR

June 2006

INHALTSVERZEICHNIS / TABLE OF CONTENTS

	Page
1 Aufgabenstellung und Zusammenfassung der Ergebnisse.....	1
1.1 Aufgabenstellung	1
1.2 Voraussetzungen, unter denen das Vorhaben durchgeführt wurde	1
1.3 Planung und Ablauf des Vorhabens	1
1.4 Zusammenarbeit mit anderen Stellen	2
1.5 Ergebnisse	2
1.6 Nutzen und Verwertbarkeit der Ergebnisse	5
1.7 Publikationen und Konferenzbeiträge	5
2 Summary.....	15
3 Acknowledgements.....	22
4 Participants.....	23
5 Cruise Narrative.....	24
6 Smoker Mineralization and Hydrothermal Precipitates.....	29
6.1 Introduction	29
6.2 Chimney Mineralogy	29
6.3 Chimney Geochemistry	34
6.4 Conclusions	35
7 Vent Fluid Analyses.....	37
7.1 Sampling and <i>in situ</i> Analyses	37
7.2 Post-Cruise Fluid Analyses	39
7.3 Conclusions	41
8 Volcano Evolution and Caldera Development.....	42
8.1 Caldera Formation	42
8.2 Volcano 1: Progressive Volcano Growth and a Sector Collapse	43
8.3 Mineralogy and Geochemistry	46
8.4 Volcano 18s: Basaltic Trigger for a Voluminous Eruption	50
8.5 Conclusions	52
Appendices.....	55

List of Appendices	No. of Pages
Appendix 1: Shipboard Scientific Party Contact Details	1
Appendix 2: Full Sample Listing	4
Appendix 3: Photologs of Recovered Samples	30
Appendix 4: Quick Look Reports and Biology Notes	22

List of Figures	Page
Fig. 2.1: Overview of the Tonga–Kermadec subduction system, SW Pacific	16
Fig. 2.2: Bathymetric images of Volcano 1, Volcano 18s and Volcano 19	17
Fig. 2.3: Composite of key hydrothermal and geological observations	19
Fig. 2.4: Composite of key hydrothermal (mineralised) samples	20
Fig. 6.1 Map of the active hydrothermal field at the summit of Volcano 19	30
Fig. 6.2 Map of the active hydrothermal field in the western caldera of Volcano 19	31
Fig. 6.3: Two-phase venting at 265 °C in a pit crater at the summit of Volcano 19	32
Fig. 6.4: Sulfide mineralization from a two-phase venting chimney	33
Fig. 6.5: Hydrothermal induration and argillic alteration of volcanoclastic sediment	34
Fig. 8.1: Key stratigraphic observations from the Volcano 1 caldera	44
Fig. 8.2 Key stratigraphic observations from the Volcano 18s caldera	51

List of Tables	Page
Table 2.1: Summary of <i>PISCES</i> and <i>RCV-150</i> dives	18
Table 6.1: Composition of the P4-137-2 two-phase chimney	35
Table 7.1: Water and gas samples (<i>in situ</i> and shipboard measurements)	38
Table 7.2: Vent fluid analyses	40
Table 8.1: Petrography of Volcano 1 lavas	47
Table 8.2: Mineralogy of Volcano 1 lavas	48
Table 8.3: Glass analyses of lava P4-143-R7	48
Table 8.4: Geochemistry of Volcano 1 lavas	49

1 AUFGABENSTELLUNG UND ZUSAMMENFASSUNG DER ERGEBNISSE

1.1 Aufgabenstellung

Während der Forschungsfahrt SITKAP wurden mit Hilfe der Forschungstauchboote *PISCES 4* und *5* an drei verschiedenen Vulkanen des Tonga Inselbogens aktive Hydrothermalsysteme untersucht. Die erst kürzlich in 2002 auf der Forschungsfahrt SO-167 (Louisville) entdeckten untermeerischen Vulkane wiesen Zeichen von hydrothermalen Aktivität auf. Daraus resultierten die folgenden Ziele des SITKAP Projektes (2005):

- 1) Lokalisierung der Hydrothermalfelder, deren Vermessung und eine erste Beprobung an den Vulkanen 1, 18s und 19.
- 2) Zur Klärung von Erz-Lagerstättenbildung und Hydrothermalen Fluidzirkulation an Inselbogensvulkanen werden Mineralpräzipitate, Massivsulfide, alterierte Gesteine und Fluide an den Hydrothermalfeldern beprobt.
- 3) Die Biodiversität des hydrothermalen Ökosystems wird anhand der beobachtbaren und der beprobten Fauna bestimmt.
- 4) Zur Klärung der Entwicklungsgeschichte der Vulkan bzw. Calderenbildung wird die Stratigraphie der Laven und Pyroklastischen Ablagerungen aufgenommen und beprobt.

1.2 Voraussetzungen, unter denen das Vorhaben durchgeführt wurde

Da die Arbeitsgebiete in der EEZ von Tonga lagen, war die Arbeitsgenehmigung dieses Staates eine wichtige Voraussetzung für die Durchführung der Forschungskampagne. Mit der Arbeitserlaubnis war die Auflage verbunden, Information über die Ergebnisse der Reise (Kartenmaterial, Fahrtbericht) weiterzureichen.

1.3 Planung und Ablauf des Vorhabens

Die Forschungsfahrt SITKAP fand im Zeitraum 06. – 29. Juni 2005 statt. Ausgangs- bzw. Endhafen waren Auckland (Neuseeland) und Pago Pago (Amerikanisch-Samoa). Es wurden 10 Tauchgänge für das Projekt beantragt, aufgrund der unerwartet günstigen Wetterbedingungen im Zielgebiet konnten aber 13 *PISCES* Tauchgänge mit insgesamt 79 h Bodenkontakt und 10 RCV-150 Videoschlitten-Einsätze durchgeführt werden. Neben den Arbeiten zur Vermessung und Erforschung der unbekannt Hydrothermalfelder konnten 14 Hochdruck-Gasproben, 13 Fluid-Proben, 58 Mineralpräzipitate und Smokerproben, 73 Lavaproben, und 99 biologische Proben erfolgreich geborgen werden.

BMBF als Träger des Projektes 03G0632A ermöglichte die Charter des Forschungsschiffes RV *KA'IMIKAI-O-KANALOA* inklusive der Tauchboote *PISCES 4* und *5*, und dem Unterwasser-Videosystem *RCV-150*.

Die DFG (STO 110/42-1) finanzierte die Transportkosten für die deutschen Wissenschaftler und deren Proben- und Ausrüstungstransport.

1.4 Zusammenarbeit mit anderen Stellen

Die SITKAP Reise war ein internationales Projekt, an dem neben der Universität Kiel, die BGR in Hannover, die University of Ottawa (Kanada), das Institute of Geological and Nuclear Sciences (Neuseeland), das Pacific Marine Environmental Laboratory (USA), das Monterey Bay Aquarium Research Institute (USA), und das Ministry of Lands, Survey and Natural Resources (Tonga) beteiligt waren.

1.5 Ergebnisse

Die wichtigsten Ergebnisse des SITKAP-Projektes sind im folgendem zusammen gefasst. Diese beinhalten im Wesentlichen die direkt während der Fahrt gewonnenen Erkenntnisse und erste geochemische Analysen an Land. Eine Finanzierung der nun notwendigen und aufwendigeren geochemischen Analysen, der in der sehr erfolgreichen Probennahmekampagne SITKAP gewonnenen Proben, wird versucht z.T. über Drittmittelanträge zu gewährleisten.

1) Entdeckung von Hochtemperatur-Hydrothermalfeldern

Vier bisher unbekannte aber sehr aktive Hydrothermalfelder wurden an untermeerischen Vulkanen des Tonga-Inselbogens entdeckt, z.T. beschrieben, und erste geologische und biologische Beprobungen wurden vorgenommen. Zwei der Felder wurden am erst kürzlich entdeckten Vulkan 19 entdeckt, wobei sich ein Feld im Gipfelbereich und das zweite Feld sich innerhalb der westlichen Caldera befindet. Das erste Hydrothermalfeld bedeckt eine Gipfelfläche von 800 x 800 m in einer Wassertiefe von 385–540 mbsl. Mit seinen Hochtemperaturfluiden (<265 °C), Phasenseparation in den Fluidaustrittsstellen, Sulfid-Sulfat Chimneys bis zu 10 m hoch, ist es das größte und heißeste Hydrothermalfeld, welches bisher entlang des gesamten Tonga-Kermadec Bogens gefunden wurde. Das Feld im westlichen Bereich der Caldera ist von vergleichbarer Größe in einer Wassertiefe von 850–985 mbsl, aber weist eher diffuses Fluid-Venting, und niedrigere Temperaturen in wenigen fokussierten Austritten (<112 °C), und zahlreiche kleinere Fe-oxyhydroxid- und Silikat-Chimneys auf.

Ein 250 x 600 m großes Feld mit schwachen hydrothermalen Fluidaustritten, deren Temperaturen um ca. 2 °C gegenüber den Umgebungstemperaturen leicht erhöht waren, wurde an der westlichen Flanke der östlichen Spitze des Vulkan 18s in einer Tiefe von 270–440 mbsl entdeckt. Dieses wahrscheinlich vor kurzem noch aktivere Feld war bedeckt von Fe-oxyhydroxiden, Silikatkrusten und Bakterienmatten.

Das vierte neu entdeckte Hydrothermalfeld liegt in der Caldera von Vulkan 1 nahe zweier jüngerer kleinerer Krater. Mittlere Temperaturen von bis zu 152 °C wurden in den austretenden Fluiden gemessen. Die Fläche von 400 x 600 m in einer Tiefe von 160–210 mbsl ist bedeckt von dichten Muschelfeldern, zwischen denen intensive Gasblasenströme aufsteigen und plastischer elementarer Schwefel auftritt.

2) **Sulfidmineralisation und Alterationsprodukte**

Sulfid-Sulfat Chimneys von bis zu 10 m Höhe am Vulkan 19 bestehen aus grobkristallinem Pyrit, Sphalerit und Wurtzit mit geringen Anteilen an Markasit, Zinkblende und Chalcopyrit, eingebettet in eine Anhydrit/Baryt-Matrix. Die kristallinen Strukturen der beprobten Chimneys lassen sich zurückführen auf übersättigte Lösungen welche durch Phasenseparation and den Austritten entstehen. Es ist daher sehr wahrscheinlich, dass sich signifikante Mengen an Sulfiden nahe der Sedimentoberfläche abgelagert haben. Die Metallkonzentrationen der Proben weisen maximale Werte von 22 wt.% Zn, 2.1 wt.% Pb und 0.6 wt.% Cu auf. Erhöhte Konzentrationen von Au (< 12 ppm), Ag (< 210 ppm), Sb und As in den Chimneys, liegen im Bereich für Epithermale Lagerstätten. Die Chimneys sind von Flächen umgeben, die intensive Tonmineralalteration anhand des Auftretens von Illit-Kaolinit- und anderen Mixed-Layer Tonmineralen, sowie amorpher Kieselsäure anzeigen. Das Auftreten dieses Hydrothermalfeldes ist aber eher unüblich bezüglich der basaltischen Struktur des Vulkan 19, da die Hydrothermalfelder des Tonga–Kermadec (und anderer Inselbögen) eher an andesitisch-dazitischen Calderen auftreten.

3) **Hydrothermale Fluide und Gase**

Die am intensivsten ausströmenden hydrothermalen Fluide wurden an den Chimneys des Vulkan 19 beobachtet. Die Temperaturen dieser Fluide liegen auf der Siedekurve von Seewasser bei den entsprechenden Tiefen. Daraus resultiert die beobachtete Phasenseparation in klare Fluide mit pH = 4.6–6.1 und niedrigen Gasgehalten, und flammenartige Dampfphasen (i.w. Wasserdampf). Hauptelementanalysen (z.B. Cl) bestätigen den konjugativen Zusammenhang dieser Phasen. Die hohen Konzentrationen von Li (~ 5x Seewasserkonzentration) und Ca zeigen intensive Wasser-Gesteinsreaktionen in tieferen Gesteinsschichten an. Die außergewöhnlich hohen Ca Konzentrationen (relative zu anderen Hydrothermalfluiden des Tonga–Kermadec Gebietes) könnten auf eine Zersetzung der ~3 km dicken Kalkablagerungen, welche unter dem Vulkan liegen (Tonga Ridge Platform),

hindeuten, oder dem ausschließlich basaltischen Charakter des Vulkan 19 zugesprochen werden. Im Gegensatz dazu besitzen die Fluide, die am Vulkan 1 austreten eine nahezu reine Meerwasserzusammensetzung, wobei die Gasblasen im wesentlichen CO₂ beinhalten. Dieses kann vorläufig durch tiefe Phasenseparation und einer unabhängig voneinander aufsteigenden wässrigen- und einer Gasphase interpretiert werden. Im Vergleich zu Mittelozeanischen Rücken-Fluiden weisen die submarinen Inselbogenvulkane sehr hohe CO₂/³He Verhältnisse auf, und könnten somit einen entscheidenden Beitrag zum globalen CO₂ Budget der Ozeane leisten.

4) Hydrothermalfauna

Diverse hydrothermale Fauna, wie Krebse (Bythograeidia), Shrimps, Polychaeten (Alvinellidae, Siboglinidae), Muscheln (Bathymodiolus, Gigantidas) und Seesterne (Asteroidea) besiedelt die Hydrothermalfelder am Vulkan 19, wobei das obere Feld starker besiedelt ist als das untere in der westlichen Caldera. Vulkan 1 ist bedeckt von dichten Muschelkolonien (Bathymodiolus), weißen Bakterienmatten, Schnecken, Brachyuran Krebsen und verschiedenen Polychaeten Arten. Diese Fauna kann mit der kürzlich im Laue Becken (Valu Fa Ridge) beprobten Fauna verglichen werden, um Hinweise auf Artenverteilung und Entwicklung in diesem Gebiet zu bekommen.

5) Entwicklung der Vulkane und Ausbildung der Calderen

Es werden durch den Vulkan 1 und 18s zwei sehr unterschiedliche Typen der Vulkanentwicklung und der Calderenausbildung repräsentiert. Die steilen Wände der Caldera von Vulkan 18s, die einem Durchmesser von 6.5 km und eine Tiefe von 1130 m besitzt, zeigen eine komplexe Abfolge von pyroklastischen Strömen, die aus alternierenden 30–100 m dicken Bändern von fein- bis Lapilli-Aschepartikeln und dazitischen Bimsen bestehen. Einige der massiven Bimslagen zeigen säulenartige Verwachsungen und andere Verschmelzungsstrukturen. Dieses weist wahrscheinlich auf einen schlagartigen und großvolumigen Ausstoß von dazitischer Magma hin. Ein Ausstoß der gesamten Magmakammer, getriggert durch eine basaltische Intrusion könnte der Grund für die die pyroklastischen Sequenzen bedeckenden basaltisch-andesitischen Klasten sein. Daran dann anschließend eruptierende basaltisch-andesitische Laven sind an den Flanken des Vulkans zu finden (östliche Vulkanspitze).

Aufschlüsse der inneren Calderwand des Vulkans 1 hingegen, zeigen eine Abfolge von sedimentierten vulkanischen Klasten. Diese sind typischerweise 20–30 m dick, und bestehen aus abwechselnd dünnen (<10 cm) fein und groben Aschelagen, z.T. gemischt mit Geröllablagerungen. Zusätzlich sind 5–10 m dicke, kissenförmige andesitische Laven eingeschaltet. Es wurden keine pyroklastischen Lavaflüsse beobachtet. Innerhalb der Gesteinslagen wurde alterierter Diorit, Hornblende und Biotit identifiziert. Die geordneten Ablagen werden von zahlreichen 1–3 m breiten

Dykes nahezu vertikal durchschnitten. Wechselnde Eruptionen am Vulkan 1 zwischen andesitischem Ausstrom und Bildung von Kissenlaven, und einem eher explosiven Ausstoß von Pyroklastika und Schlacken (auch andesitischen Ursprungs) ist wahrscheinlich. Die Caldera des Vulkan 1 hat sich wahrscheinlich eher durch einen Teilkollaps im Bereich der westlichen Kraterwand, ähnlich wie 1980 beim Vulkan Mount St Helens, als durch eine einzige katastrophale Eruption wie z.B. am Vulkan 18s gebildet.

1.6 Nutzen und Verwertbarkeit der Ergebnisse

Das Forschungsprojekt SITKAP markiert die erste erfolgreiche systematische Kartierungs- und Beprobungskampagne von Hydrothermalfeldern an aktiven submarinen Inselbogen Vulkanen mittels Tauchbooten. In Zusammenarbeit mit den internationalen Kollegen resultierte daraus eine Special Session auf der AGU 2005 (Fall) mit dem Fokus auf Hydrothermales Venting und Mineralisationen entlang des Tonga–Kermadec Arc.

Unser Projekt hat dazu geführt, dass das bisher größte und heißeste Hydrothermalfeld des Tonga–Kermadec Bogens und zwei weitere aktive Systeme entdeckt und beprobt wurden. Eine erweiterte und detaillierte Beprobungskampagne im Tonga Arc, ist aufgrund der Ergebnisse möglich geworden, und wird durch das BMBF über das Projekt MANGO in 2007-2008 (SO-192) unterstützt.

Die Entdeckung von Massivsulfiden mit hohen Edelmetallanteilen (insbesondere Gold) stellt für den Staat Tonga eine wichtige Rohstoffoption dar. Neben den wissenschaftlichen Erkenntnissen über die Bildungsmechanismen von Massivsulfidlagerstätten an submarinen Inselbogen-Vulkanen, gibt es ein internationales Interesse am Auffinden und Bergen dieser Flachwasser-Rohstoffreserven (u.a. Nautilus Ltd, Neptune Mining Ltd).

1.7 Publikationen und Konferenzbeiträge

Im Rahmen dieses Projektes sind folgende Veröffentlichungen bzw. Tagungsbeiträge erstellt worden:

- Stoffers, P., Worthington, T.J., Schwarz-Schampera, U., Hannington, M.D., Massoth, G.J., Hekinian, R., Schmidt, M., Lundsten, L.J., Evans, L.J., Vaiomo'unga, R., Kerby, T.; 2006. Submarine volcanoes and high-temperature hydrothermal venting on the Tonga arc, southwest Pacific. *Geology* 34, 453–456.
- Stoffers, P., Worthington, T.J., Hannington, M.D., Schwarz-Schampera, U., Massoth, G.J., Schmidt, M., Hekinian, R., Lundsten, L.J., Evans, L.J., Vaiomo'unga, R.; 2005.

Submarine volcanoes and high-temperature hydrothermal venting, Tonga arc, SW Pacific. AGU Fall Meeting, San Francisco, December 2005.

- Lupton, J., Butterfield, D., Lilley, M., Evans, L., Greene, R., Resing, J., Embley, R., Massoth, G., Christenson, B., de Ronde, C., Olson, E., Proskurowski, G., Nakamura, K., Schmidt, M., Stoffers, P., Worthington, T., Hannington, M.; 2005. Carbon Fluxes from Submarine Arc Volcanoes - Examples from the Mariana and Kermadec Arcs. AGU Fall Meeting, San Francisco, December 2005.

- Massoth, G.J., Arculus, R.J., Baker, E.T., Butterfield, D.A., Chadwick, W.W., Christenson, B.W., de Ronde, C.E., Embley, R.W., Evans, L.J., Faure, K., Graham, I.J., Greene, R.R., Ishibashi, J., Lebon, G.T., Lupton, J.E., Resing, J.A., Roe, K.K., Schmidt, M., Stoffers, P., Walker, S.L., Worthington, T.J., Wright, I.C., Yamanaka, T.; 2005. Plume–Vent Fluid Connections along the Tonga–Kermadec Arc. AGU Fall Meeting, San Francisco, December 2005.

Submarine volcanoes and high-temperature hydrothermal venting on the Tonga arc, southwest Pacific

Peter Stoffers

Tim J. Worthington

Institute of Geosciences, University of Kiel, Olshausenstrasse 40, 24118 Kiel, Germany

Ulrich Schwarz-Schampera Bundesanstalt für Geowissenschaften und Rohstoffe, Stilleweg 2, 30655 Hannover, Germany

Mark D. Hannington* Department of Earth Sciences, University of Ottawa, 140 Louis Pasteur, Ottawa K1N 6N5, Canada

Gary J. Massoth Institute of Geological and Nuclear Sciences, PO Box 31312, Lower Hutt, New Zealand

Roger Hekinian Keryunan, 29290 Saint Renan, France

Mark Schmidt Institute of Geosciences, University of Kiel, Olshausenstrasse 40, 24118 Kiel, Germany

Lonny J. Lundsten Monterey Bay Aquarium Research Institute, 7700 Sandholdt Road, Moss Landing, California 95039-9644, USA

Leigh J. Evans National Oceanic and Atmospheric Administration, Pacific Marine Environmental Laboratory, Hatfield Marine Center, 030 SE Marine Science Drive, Newport, Oregon 97365, USA

Rennie Vaiomo'unga Ministry of Lands, Survey and Natural Resources, Nuku'alofa, Kingdom of Tonga

Terry Kerby Hawaii Undersea Research Laboratory, University of Hawaii, 1000 Pope Road, Honolulu, Hawaii 96822, USA

ABSTRACT

Submarine hydrothermal vents and associated seafloor mineralization on the Tonga arc have been found for the first time, in the summit calderas of two shallow-water volcanoes, greatly extending the known areas and diversity of seafloor hydrothermal activity in the western Pacific region. The highest temperature vents (245–265 °C) occur at water depths of 385–540 m near the summit of one volcano at 24°S. The vents are spatially related to basaltic dike swarms exposed at a summit cone and in the caldera walls. Clusters of large (to 10 m high) barite, anhydrite, and sulfide chimneys on the summit cone are vigorously discharging clear hydrothermal fluids with temperatures on the seawater boiling curve. There is abundant evidence of phase separation, which can be seen as flame-like jets of steam (H₂O vapor) at the chimney orifices. Pyrite, marcasite, sphalerite, and chalcopyrite line the interiors of the highest temperature vents, similar to black smoker chimneys on the mid-ocean ridges.

Keywords: Tonga arc, submarine hydrothermal vents, boiling, sulfide-sulfate chimneys.

INTRODUCTION

The majority of known high-temperature hydrothermal vents in the western Pacific are found in intraoceanic backarc settings, such as the Lau Basin, the North Fiji Basin, and the Mariana Trough. Hydrothermal vents and related mineral deposits have been discovered on the submarine volcanoes at the fronts of the arcs (e.g., de Ronde et al., 2003). Many of these volcanoes are actively degassing, and there is clear evidence of magmatic volatiles being released to the seafloor. However, black smoker vents, typical of the deep mid-ocean ridges and backarc spreading centers, have been found only in the deepest calderas at water depths in excess of 1 km (e.g., Myojin Knoll on the Izu-Bonin arc at 1300 m depth, Iizasa et al., 1999; Brothers volcano on the southern Kermadec arc at 1600 m depth, de Ronde et al., 2005). In this paper we describe the first observations of high-temperature hydrothermal venting and large sulfide-sulfate chimneys on shallow submarine volcanoes of the Tonga arc.

A recent multibeam bathymetric survey

during the SO-167 cruise of the FS *Sonne* located 27 major volcanic edifices along the 650-km-long Tonga arc (Fig. 1A; Stoffers et al., 2003). Calderas occur on nine of these volcanoes. Dredging recovered mainly basaltic andesite to dacite and rhyolite, as well as intensely altered and mineralized lavas, most notably from Volcano 1 (21°09'S, 175°45'W) and Volcano 19 (24°48'S, 177°01'W) (Fig. 1B). Particle plumes and water-column chemical anomalies were detected above seven of these volcanoes during a subsequent cruise in 2003 (Massoth et al., 2003a). The strongest plumes at Volcano 1 and Volcano 19 were targeted for a 13 dive program in June 2005, using the submersibles *PISCES IV* and *PISCES V*, the remotely operated vehicle *RCV-150*, and their support ship *R/V Ka'imikai-o-Kanaloa*.

HYDROTHERMAL VENTING, MINERALIZATION, AND BIOLOGICAL COMMUNITIES: VOLCANO 19

Volcano 19 has a basal dimension of 14 × 12 km and rises from a water depth of 1400 m to 385 m (Fig. 2A). An outer caldera, 3.5

× 2.5 km, outlines the summit region. A large central cone complex with a basal diameter of 1.7 km and a height of ~300 m occurs at the center of the caldera. The upper part of this complex comprises numerous explosion craters and pits, relict scoria cones, and a prominent ridge constructed of 2–3-m-wide vertical dikes. A younger caldera, 1.9 km in diameter with 200–600-m-high inner walls, occurs on the west side of the volcano. The caldera walls expose massive lavas (flows and sills) with spectacular columnar jointing and abundant dikes that extend from the floor to near the caldera rim (180 m of vertical exposure). Analyzed lavas from Volcano 19 span a limited compositional range from basalt to basaltic andesite (51.5–54.7 wt% SiO₂; 14 analyses).

Two large hydrothermal fields occur on Volcano 19. One is situated near the summit of the central cone between 385 and 540 m water depth. A second is in the western caldera, near the base of the southern wall at a depth of 970 m (Fig. 2A). The upper part of the central cone (an area of ~800 × 800 m) is almost completely covered by Fe-oxyhydroxide crusts, as thick as 50 cm, formed from diffusely venting low-temperature fluids. Where partly eroded, the bright orange to brown Fe-oxyhydroxides are underlain by dark green clay. Chimneys as high as 1 m, composed of Fe-oxyhydroxides, have formed where the venting fluids reach temperatures of ~70 °C. More focused, high-temperature venting occurs along the narrow, NE-SW-trending ridge at the top of the cone complex. Here, clusters of large barite and anhydrite chimneys, as high as 10 m, occur along a series of vertical dikes and faults. The largest hydrothermal structure, which has a distinctive “beehive” chimney at its top (385 m depth, Fig. 3A), occurs at the shallowest point of the ridge and is surrounded by 10–12 smaller chimneys (2–3 m in height). Clear fluids venting from both the large tower and

*E-mail: mhanning@uottawa.ca.

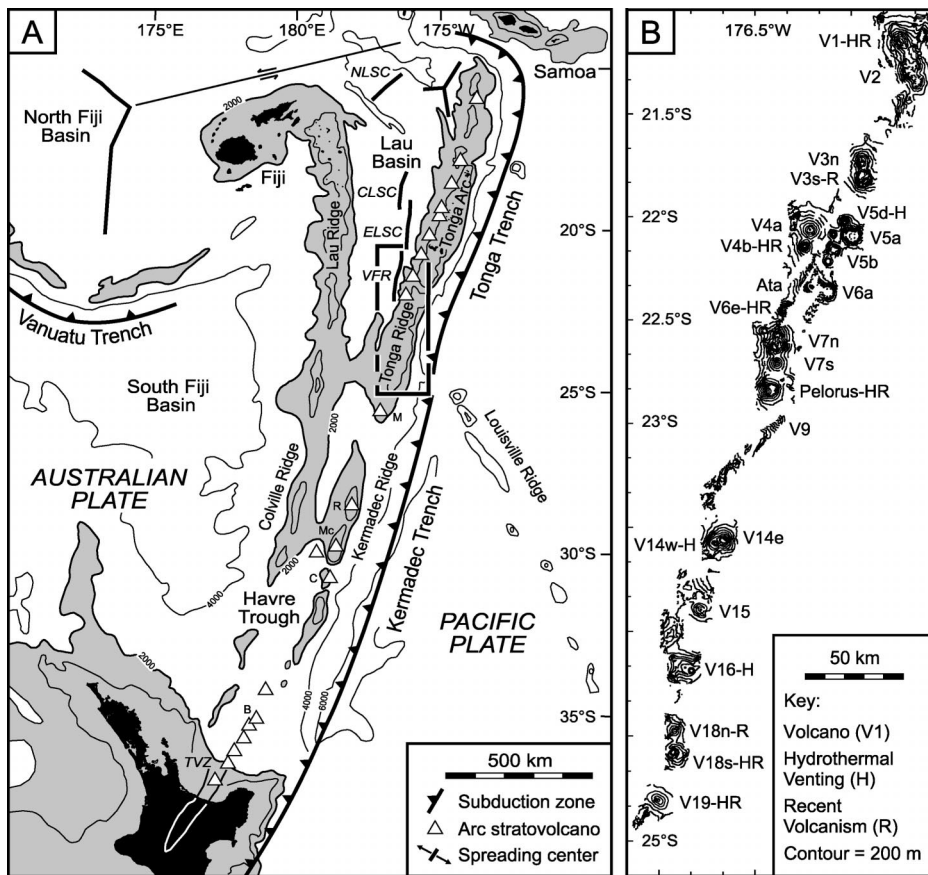


Figure 1. Regional bathymetry of Tonga arc and adjacent Lau backarc basin showing major tectonic boundaries and locations of selected arc volcanoes. Area of study is indicated by box in A. Submersible dives were carried out on Volcano 19 in south and on Volcano 1 in north (B). Abbreviations: NLSC—Northwestern Lau spreading center, CLSC—Central Lau spreading center, ELSC—Eastern Lau spreading center, VFR—Valu Fa Ridge, M—Monowai, R—Raoul, Mc—Macauley, C—Curtis, B—Brothers, TVZ—Taupo Volcanic Zone.

smaller chimneys have maximum temperatures of 245 °C. At slightly greater water depths (420–435 m) at the southern end of the ridge, other large barite and anhydrite chimneys, as tall as 7 m, have maximum vent temperatures of 253 °C, with vigorous flow including weak “black smoke.” The highest temperature chimneys (Fig. 3B) consist of anhydrite, with a lining of chalcopyrite, dark sphalerite, and wurtzite. These chimneys exhibit a distinctive “flame-like” discharge caused by phase separation (Fig. 3C). The discharge is produced by a small jet of steam (H₂O vapor) that condenses rapidly in contact with cold seawater a few centimeters above the vent orifice. An extremely vigorous two-phase vent was generated at one location where a chimney was knocked over (Fig. 3D).

Focused high-temperature venting also occurs at a water depth of 540 m in one of the shallow pit craters on the central cone. Here, small chimneys and low-relief mounds of barite and anhydrite protrude from the sediment in the pit. Clear two-phase venting at 265 °C occurs from the orifices of several chimneys. The largest chimneys (~2 m high) have thick walls of barite and anhydrite with central con-

duits filled by fine-grained pyrite, marcasite, and sphalerite. The highest temperature vents are lined by coarsely crystalline chalcopyrite.

The measured temperatures of venting fluids from Volcano 19 are directly on the boiling curve at their respective depths (385, 430, and 540 m; Fig. 4). This is consistent with the abundant visual evidence of phase separation. Similar steam vents have been observed at shallow-water boiling vents on the Mid-Atlantic Ridge near Iceland (Hannington et al., 2001), and visible phase separation has been reported at higher-temperature vents on the Juan de Fuca Ridge (Massoth et al., 1989; Butterfield et al., 1990) and East Pacific Rise (Von Damm et al., 1997). Shipboard measurements (for details, see GSA Data Repository¹) of the sampled vent fluids (pH, total alkalinity, salinity, total gas, and H₂S concentrations) indicate compositions that are generally comparable to mid-ocean ridge (MOR) vent fluids. The pH in the highest temperature vents rang-

¹GSA Data Repository item 2006114, shipboard methods, is available online at www.geosociety.org/pubs/ft2006.htm, or on request from editing@geosociety.org or Documents Secretary, GSA, P.O. Box 9140, Boulder, CO 80301, USA.

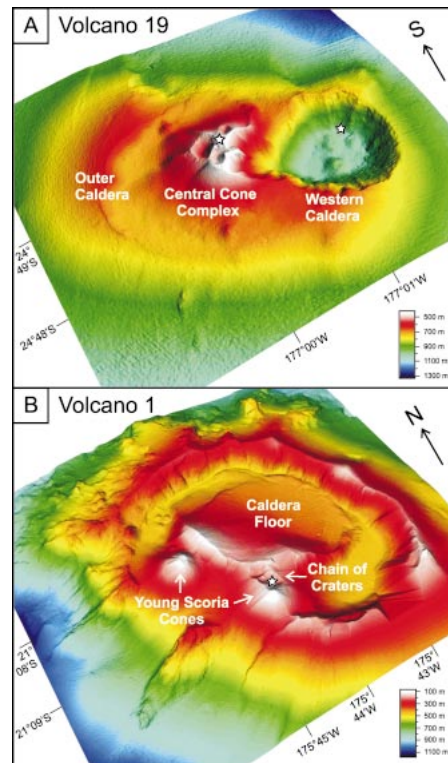


Figure 2. A: Bathymetry of Volcano 19, looking south, showing large outer caldera, central cone complex, and western caldera. High-temperature vents (245–265 °C) and large barite-anhydrite chimneys are located on central cone complex (385–540 m). Fe-oxyhydroxide chimneys, amorphous silica, and barite chimneys and crusts, and low-temperature vents (to 112 °C) occur in western caldera. B: Bathymetry of Volcano 1, looking north. Widespread diffuse venting (30–70 °C), vigorous gas discharge, sulfur deposits, and live mussel beds occur in chain of craters. Maximum measured temperatures at 200 m water depth were 112 °C. Bathymetric data are from Stoffers et al. (2003). Stars indicate locations of main venting areas.

es from 4.6 to 6.1, and total gas concentrations in samples from gas-tight bottles range from 3.1 to 15 mM. These gas concentrations are within the range of MOR vents and insufficient to have caused a significant depression of the boiling point. The low gas contents support the interpretation that the gas phase in the discharge is mainly steam (H₂O vapor).

A diverse fauna occurs in the vent fields, although the abundance of animals is low compared to MOR vents. Vent crabs (Bythograeidae), vent shrimp (unknown species), and rare polychaete worms (Alvinellidae) occur at the highest temperature vents. Clumps of vent worms (Siboglinidae) and two types of vent-associated mussels (live *Bathymodiolus* and shells of *Gigantidas*) were found in the shallow pit crater, together with abundant sea stars (Asteroidea) that were foraging among the shell beds.

A second, large area of low-temperature

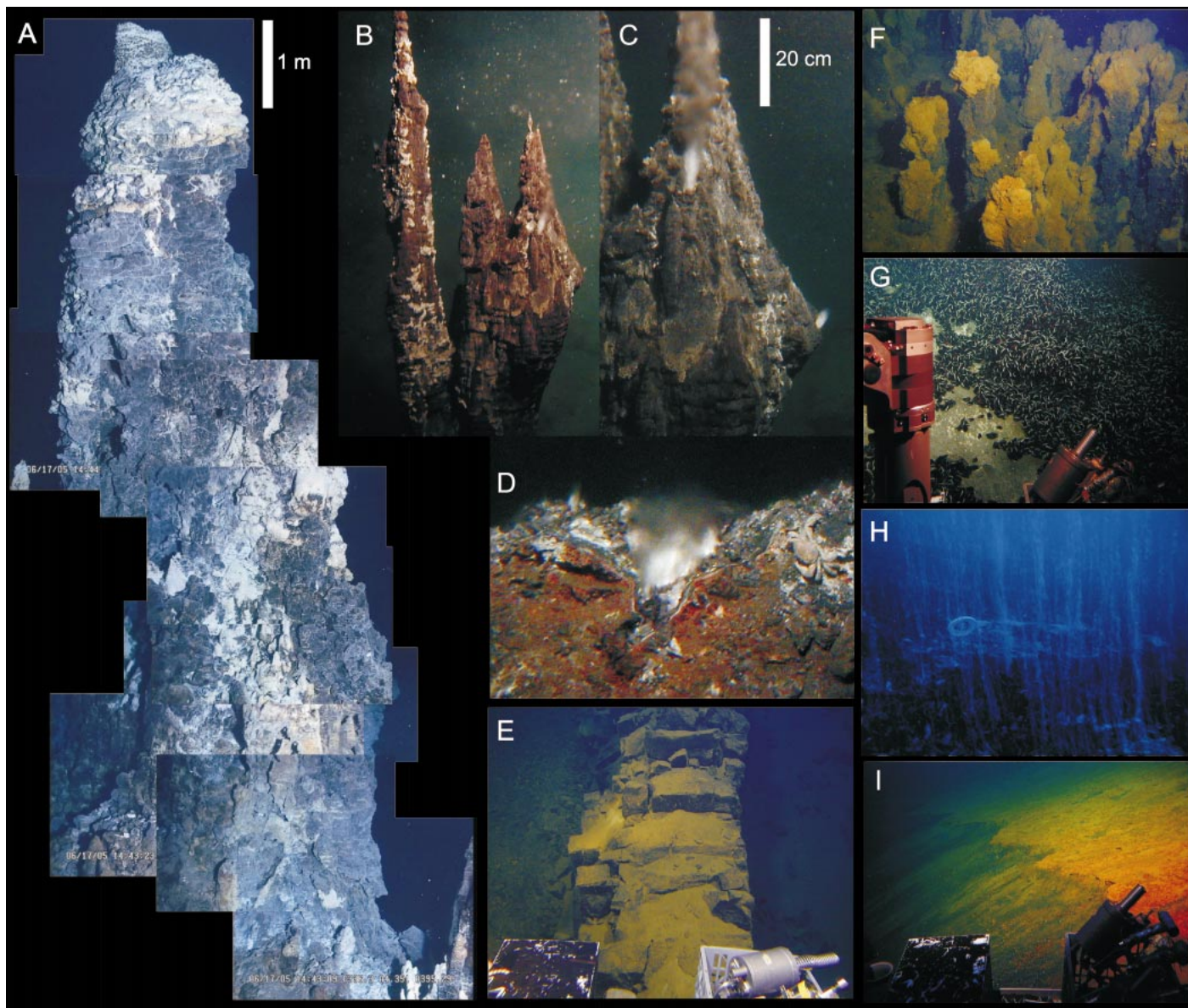


Figure 3. Bottom photographs from *PISCES IV* and *PISCES V* submersibles. **A:** Large, 10-m-tall barite chimney at summit of Volcano 19. This tower is surrounded by numerous smaller barite-anhydrite-sulfide chimneys, 1–3 m tall. Image is composite; lowermost photograph was taken at depth of 395 m. Small beehive-like feature at top of chimney is at 385 m depth. **B:** Anhydrite spires (2 m tall) at high-temperature (265 °C) vents in pit crater (540 m depth) on central cone complex of Volcano 19. Clear, two-phase venting can be seen at several orifices. **C:** Close-up of “flame-like” jets of steam (H₂O vapor) on anhydrite spires in **B**. **D:** Vigorous two-phase venting from 20-cm-diameter orifice at base of anhydrite spires in **B**, created by knocking over chimneys. Orifice is lined by chalcopyrite. **E:** Vertical dike in wall of western caldera, Volcano 19. Swarms of these dikes are closely associated with areas of active venting. **F:** Field of Fe-oxyhydroxide and amorphous silica chimneys (1–2 m tall) along south wall of western caldera, Volcano 19. **G:** Densely populated mussels (*Bathymodiolus*) around gas-rich, sulfurous vents in chain of craters on Volcano 1. White areas are patches of native sulfur with vent temperatures as high as 152 °C. **H:** Streams of gas bubbles (mainly CO₂) discharging from seafloor within mussel fields. Photograph was taken in ambient light with submersible lights turned off. **I:** Extensive deposits of amorphous Fe-oxides surrounding explosion craters at Volcano 1.

venting occurs among a swarm of dikes in the south wall of the western caldera (Fig. 2A). Here, Fe-oxyhydroxide crusts extend for more than 900 m along the base of the caldera wall and over a depth range of 985–850 m. Diffuse venting of warm fluids (up to 30 °C) and mats of Fe-stained filamentous bacteria occur throughout this field. At the center of the field (985 m water depth), large clusters of 1–2-m-high Fe-oxyhydroxide and silica chimneys cover an area of 200 × 300 m (Fig. 3F). The

largest chimneys include 4–5-m-high spires surrounded by crusts of barite and silica. Measured vent temperatures in this area reach 112 °C. Vent-associated fauna are less abundant than on the central cone complex, although vent crabs, vent shrimp, and polychaete worms were found near the hottest vents.

VOLCANO 1

Volcano 1 has a basal diameter of ~28 km and rises from a water depth of 1800 m to a

summit at 65 m below sea level (Fig. 2B). A large oval caldera, 7 × 4.5 km, and two well-preserved scoria cones dominate the volcano summit. Analyzed lavas from Volcano 1 are mainly basaltic andesite to andesite (56–58 wt% SiO₂; 25 analyses).

A chain of explosion craters, as deep as 100 m, occurs on the flank of one of the scoria cones, and thick deposits of scoria and ash blanket the caldera floor in this area. Widespread diffuse hydrothermal venting, vigorous

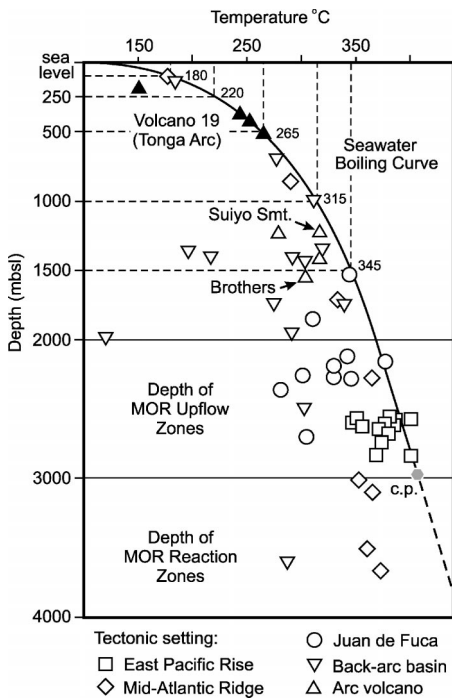


Figure 4. Boiling curve for seawater showing maximum measured temperatures of submarine hydrothermal vents in different volcanic and tectonic settings (modified after Hannington et al., 2005). Hydrothermal vents on Volcano 19 (filled triangles) were found at depths of 540 m (265 °C), 433 m (253 °C), and 385 m (245 °C). Temperatures at all three sites are on boiling curve, and visible phase separation (steam) was found at 540 m and 430 m depth. Shallow-water venting on Volcano 1 (filled triangle at 200 m depth) is characterized mainly by gas discharge (dominantly CO₂) at maximum temperature of 152 °C. Temperatures of vents on Suiyo Seamount (Izu-Bonin arc) and Brothers volcano (Kermadec arc) are shown for comparison. MOR—mid-ocean ridge; mbsl—meters below sea level.

gas discharge, and thick beds of sulfur-cemented ash occur at water depths of 160–210 m in and around the explosion craters. A densely populated field of mussels (200 × 400 m) almost completely covers the seafloor in this area (Fig. 3G). The mussels (*Bathymodiolus*) occur where temperatures in the ash substrate are 30–70 °C, but patches with higher temperatures (to 152 °C) occur locally. No chimneys were observed, but continuous streams of gas bubbles emanate from small holes and cracks in the sulfur-rich crusts (Fig. 3H). The water column throughout this area is clouded with white particles, most likely elemental sulfur from the vigorously discharging gas vents. The pH of the clear venting fluids is between 3.2 and 5.8, and the total gas content is ~130 mM (significantly higher than at Volcano 19). Concentrations of H₂S measured in the vent water (as high as 3 mM) are within the range of MOR vents, and the streams of rising gas bubbles are most likely dominated by CO₂.

Surrounding the chain of craters and on the nearby southern cone, the seafloor is almost completely covered by “snowy” white fields of filamentous bacteria. These areas are underlain by extensive Fe-oxyhydroxide crusts (Fig. 3I).

DISCUSSION

The hydrothermal fields on Volcano 19 are closely associated with intrusive dike swarms that are well exposed on the central cone and in the walls of the western caldera. The dikes are manifestations of the underlying magmatic system ultimately responsible for the hydrothermal venting. Such prominent dike swarms are rarely seen on active submarine volcanoes, partly because they are covered by the products of explosive eruptions, and it is uncommon to observe such a clear relationship between intrusive magma and seafloor hydrothermal activity.

High-temperature venting at such shallow water depths also has not been widely observed. On submarine volcanoes shallower than ~1000 m, most vent fluids will have cooled significantly from their end-member temperatures before reaching the seafloor. A zone of boiling beneath the vents on Volcano 19 may extend well below the volcano summit. For example, fluids originating as much as 1 km below the seafloor would cool by as much as 100 °C as they rise along the seawater boiling curve before venting at ~400 m water depth (cf. Fig. 4), resulting in subseafloor deposition of metals. This may explain the lack of “smoke” emitted by the highest temperature vents on Volcano 19, in contrast to the vigorous black smokers found at deeper volcanoes (e.g., Brothers volcano on the southern Kermadec arc). The venting of steam also contrasts with the more typical voluminous discharge of gas bubbles observed on other shallow-water volcanoes (such as Volcano 1), which are characterized mainly by CO₂ gas rather than steam (e.g., de Ronde et al., 2003; Massoth et al., 2003b).

The high-temperature vents on the Tonga arc differ from sites of hydrothermal activity in the adjacent backarc basins in being at shallow depths and associated directly with the volcanic arc. These findings extend the depth range and geographical distribution of known high-temperature venting in this setting and indicate a strong likelihood of similar activity on other submarine volcanoes along the ~650 km of the arc (Fig. 1B).

ACKNOWLEDGMENTS

We thank Captain Ross Barnes, the crew of the R/V *Ka'imikai-o-Kanaloa*, and the Hawaii Undersea Research Laboratory teams operating the *PISCES* submersibles (T. Kerby, M. Cremer, S. Price, C. Wollerman, D. Bloedorn) and the RCV-150 (D. Green, P. Townsend). We also thank the Kingdom of Tonga for permission to work within Tongan waters. Principal funding for this research was provided by Bundesministerium für Bildung und Forschung grant 03G0632A and Deutsche Forschungsgemeinschaft grant STO 110/42-1.

REFERENCES CITED

- Butterfield, D.A., Massoth, G.J., McDuff, R.E., Lupton, J.E., and Lilley, M.D., 1990. Geochemistry of hydrothermal fluids from ASHES vent field, Juan de Fuca Ridge: Subseafloor boiling and subsequent fluid-rock interaction: *Journal of Geophysical Research*, v. 95, p. 12,895–12,921.
- de Ronde, C.E.J., Massoth, G.J., Baker, E.T., and Lupton, J.E., 2003. Submarine hydrothermal venting related to volcanic arcs, in Simmons, S.F., and Graham, I.J., eds., *Giggenbach Memorial Volume: Volcanic, geothermal and ore-forming fluids: Rulers and witnesses of processes within the Earth: Society of Economic Geologists Special Publication 10*, p. 91–109.
- de Ronde, C.E.J., Hannington, M.D., Stoffers, P., Wright, I.C., Ditchburn, R.G., Reyes, A.G., Baker, E.T., Massoth, G.J., Lupton, J.L., Walker, S.L., Greene, R.R., Soong, R., Ishibashi, J., Lebon, G., Bray, C.J., and Resing, J.A., 2005. Evolution of a submarine magmatic-hydrothermal system: Brothers volcano, Southern Kermadec arc: *Economic Geology and the Bulletin of the Society of Economic Geologists*, v. 100, p. 1097–1134.
- Hannington, M.D., de Ronde, C.E.J., and Petersen, S., 2005. Sea-floor tectonics and submarine hydrothermal systems, in Hedenquist, J., et al., eds., *100th Anniversary Volume of Economic Geology: Littleton, Colorado, Society of Economic Geologists*, p. 111–141.
- Hannington, M.D., Herzog, P., Stoffers, P., Scholten, J., Garbe-Schonberg, D., Jonasson, I.R., Roest, W., and Shipboard Scientific Party, 2001. First high-temperature submarine hydrothermal vents and massive anhydrite deposits off the north coast of Iceland: *Marine Geology*, v. 177, p. 199–220.
- Iizasa, K., Fiske, R.S., Ishizuka, O., Yuasa, M., Hashimoto, J., Ishibashi, J., Naka, J., Horii, Y., Fujiwara, Y., Imai, A., and Koyama, S.A., 1999. A kuroko-type polymetallic sulfide deposit in a submarine silicic caldera: *Science*, v. 283, p. 975–977, doi: 10.1126/science.283.5404.975.
- Massoth, G.J., Butterfield, D.A., Lupton, J.E., McDuff, R.E., Lilley, M.D., and Jonasson, I.R., 1989. Submarine venting of phase-separated hydrothermal fluids at Axial Volcano, Juan de Fuca Ridge: *Nature*, v. 340, p. 702–705, doi: 10.1038/340702a0.
- Massoth, G.J., Baker, E.T., de Ronde, C.E.J., Arculus, R.J., Lupton, J.E., Ishibashi, J.-I., Resing, J.A., Martinez, F., Stoffers, P., and Worthington, T., 2003a. Back-arc neighbors, arc-like fluid sources: *Geological Society of America Abstracts with Programs*, v. 35, no. 6, p. 13.
- Massoth, G.J., de Ronde, C.E.J., Lupton, J.E., Feely, R.A., Baker, E.T., Lebon, G.T., and Maenner, S.M., 2003b. Chemically rich and diverse submarine hydrothermal plumes of the southern Kermadec volcanic arc (New Zealand), in Larter, R., and Leat, P., eds., *Intra-oceanic subduction systems: Tectonic and magmatic processes: Geological Society [London] Special Publication 219*, p. 119–139.
- Stoffers, P., Worthington, T., and the Shipboard Scientific Party, 2003. Cruise Report SONNE 167, Louisville Ridge: Dynamics and magmatism of a mantle plume and its influence on the Tonga-Kermadec subduction system: Reports of the Institut für Geowissenschaften, Universität Kiel, no. 20, 276 p.
- Von Damm, K.L., Buttermore, L.G., Oosting, S.E., Bray, A.M., Fornari, D.J., Lilley, M.D., and Shanks, W.C., III, 1997. Direct observation of the evolution of a seafloor “black smoker” from vapor to brine: *Earth and Planetary Science Letters*, v. 149, p. 101–111, doi: 10.1016/S0012-821X(97)00059-9.

Manuscript received 19 October 2005
 Revised manuscript received 5 January 2006
 Manuscript accepted 20 January 2006

Printed in USA

GSA Data Repository Item, Vent Fluid Sampling and Shipboard Analyses

G22227 – Stoffers *et al.*

Submarine volcanoes and high-temperature hydrothermal venting on the Tonga arc, SW Pacific

Methods

Samples of vent fluids were collected separately for liquid and gas phases: liquids in 750 mL capacity Major Sampler syringes constructed of titanium with teflon seals (Von Damm *et al.*, 1985) and gases in pre-evacuated, 150 mL capacity gas-tight bottles, also constructed of titanium (Edmond *et al.*, 1992). Both samplers were configured with titanium intake snorkels, which were positioned using *PISCES* manipulator arms directly within focused flowstreams where maximum temperatures had been previously measured.

Hydrogen sulphide and silica were determined colorimetrically in batch mode using the methylene blue (nominal precision: 4%) and silicomolybdate (nominal precision: 1%) methods, respectively. Potentiometry was used to assess pH (nominal precision: 0.3%) at room temperature relative to NBS buffers and to measure alkalinity (nominal precision: 0.5%) by the Gran method. Total gas concentrations were determined using manometric and gravimetric procedures (nominal precision: 2%).

Values reported in the text are from samples with “purest” hydrothermal components, which ranged: 16% at Volcano 19 pit site, 19% at Volcano 1, and 96% at Volcano 19 summit, based on preliminary laboratory determinations of Mg compared to ambient seawater values. A comprehensive suite of determinations of the aqueous ionic and gaseous components is presently underway in Germany, New Zealand, and the United States and is intended for publication in the peer literature.

Edmond, J.M., Massoth, G.J., and Lilley, M., 1992, Submersible-deployed samplers for axial vent waters: RIDGE Events Newsletter, Spring/Summer 1992, p. 23-26.

Von Damm, K.L., Edmond, J.M., Grant, B., Measures, C.I., Walden, B., and Weiss, R.F., 1985, Chemistry of submarine hydrothermal solutions at 21°N, East Pacific Rise: *Geochimica et Cosmochimica Acta*, v. 49, p. 2197-2220.

SUBMARINE VOLCANOES AND HIGH-TEMPERATURE HYDROTHERMAL VENTING, TONGA ARC, SW PACIFIC

Peter Stoffers¹, Tim Worthington¹, Mark Hannington², Uli Schwarz-Schampera³, Gary Massoth⁴, Mark Schmidt¹, Roger Hekinian¹, Lonny Lundsten⁵, Leigh Evans⁶, Rennie Vaiomo'unga⁷



¹ Inst. fuer Geowissenschaften, Universitaet Kiel, Germany (tw@gpi.uni-kiel.de)

² Dept. of Earth Sciences, University of Ottawa, Canada

³ Bundesanstalt fuer Geowissenschaften und Rohstoffe, Hannover, Germany

⁴ Inst. Geological and Nuclear Sciences, Lower Hutt, New Zealand

⁵ Monterey Bay Aquarium Research Institute, Moss Landing, USA

⁶ Hatfield Marine Science Center, PMEL / NOAA, Newport, USA

⁷ Ministry of Lands, Survey and Natural Resources, Nuku'alofa, Kingdom of Tonga



Presented at the AGU Fall Meeting, San Francisco, December 2005

OBJECTIVES

What is the fluid flux (and heat flow) through a volcanic arc?

Relationship to magma flux and components of the slab?

Fluid sources: arc magma vs seawater vs crust?

Fluid evolution: degassing vs phase separation vs wall reactions?

Submarine arc mineralization vs subaerial epithermal systems?

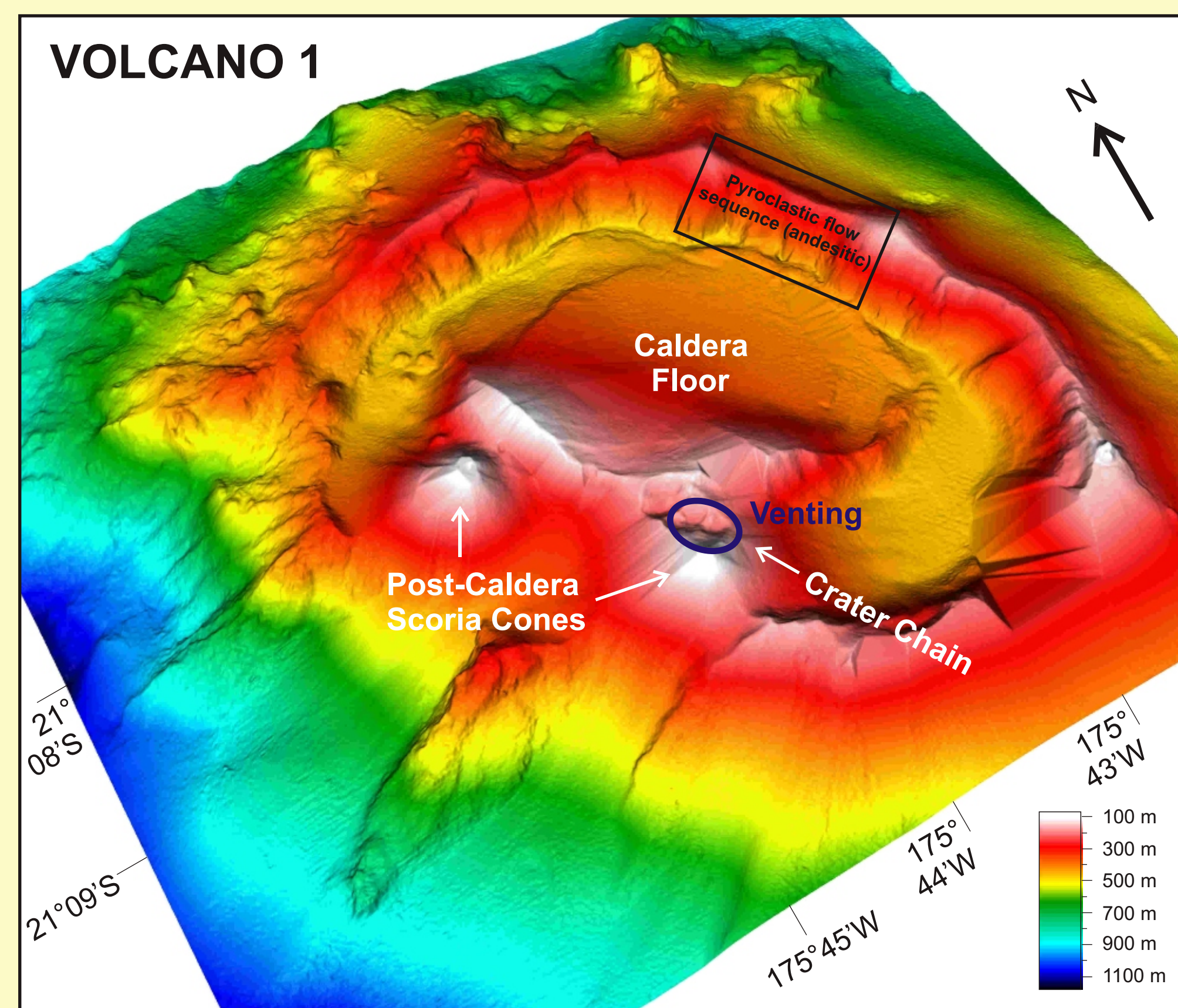
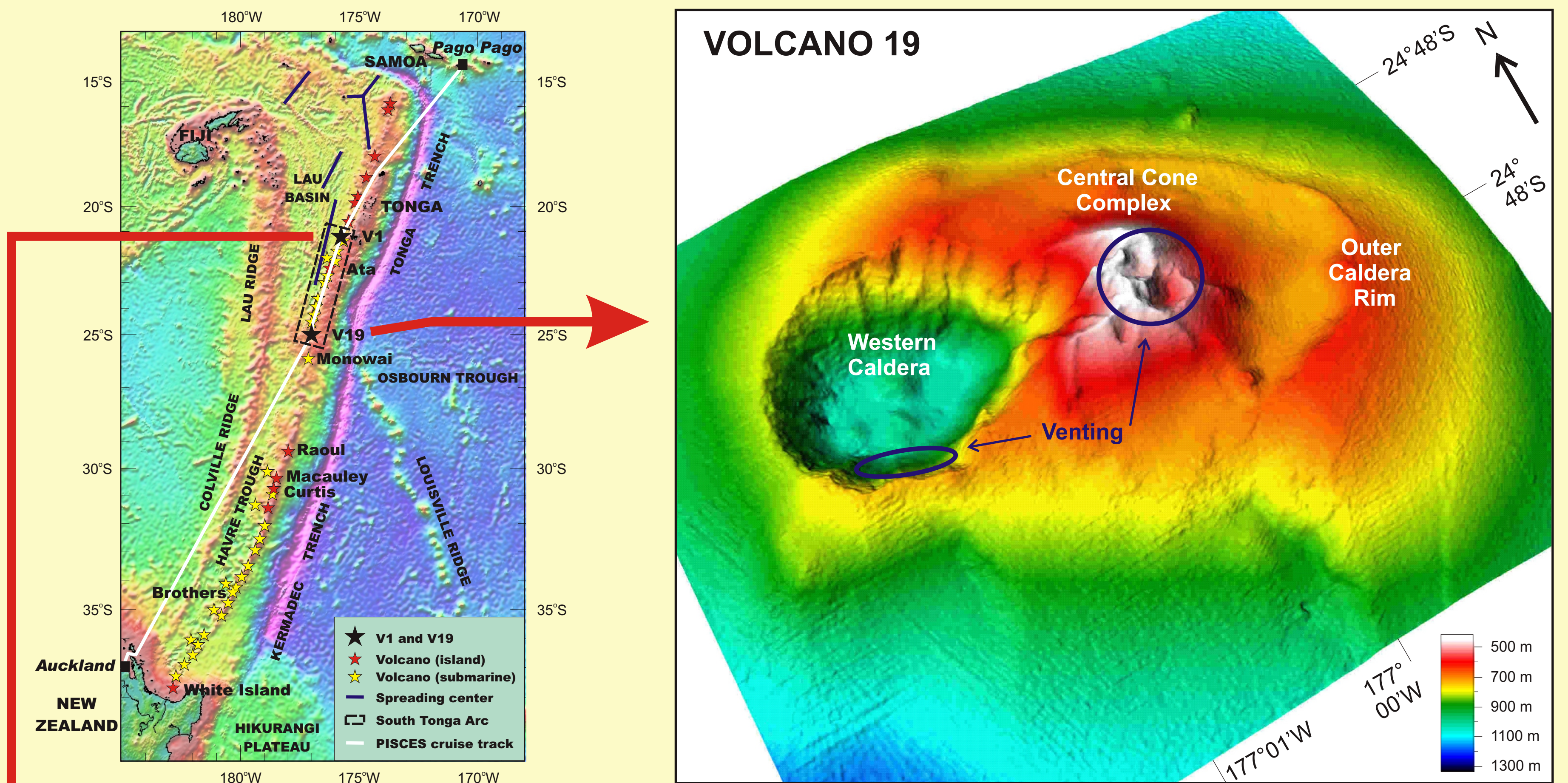
Differences between arc, back-arc and mid-ocean ridge systems?

Magmatic volatiles before vs after caldera-forming eruptions?

Vent fauna migration between arcs and back-arc basins?

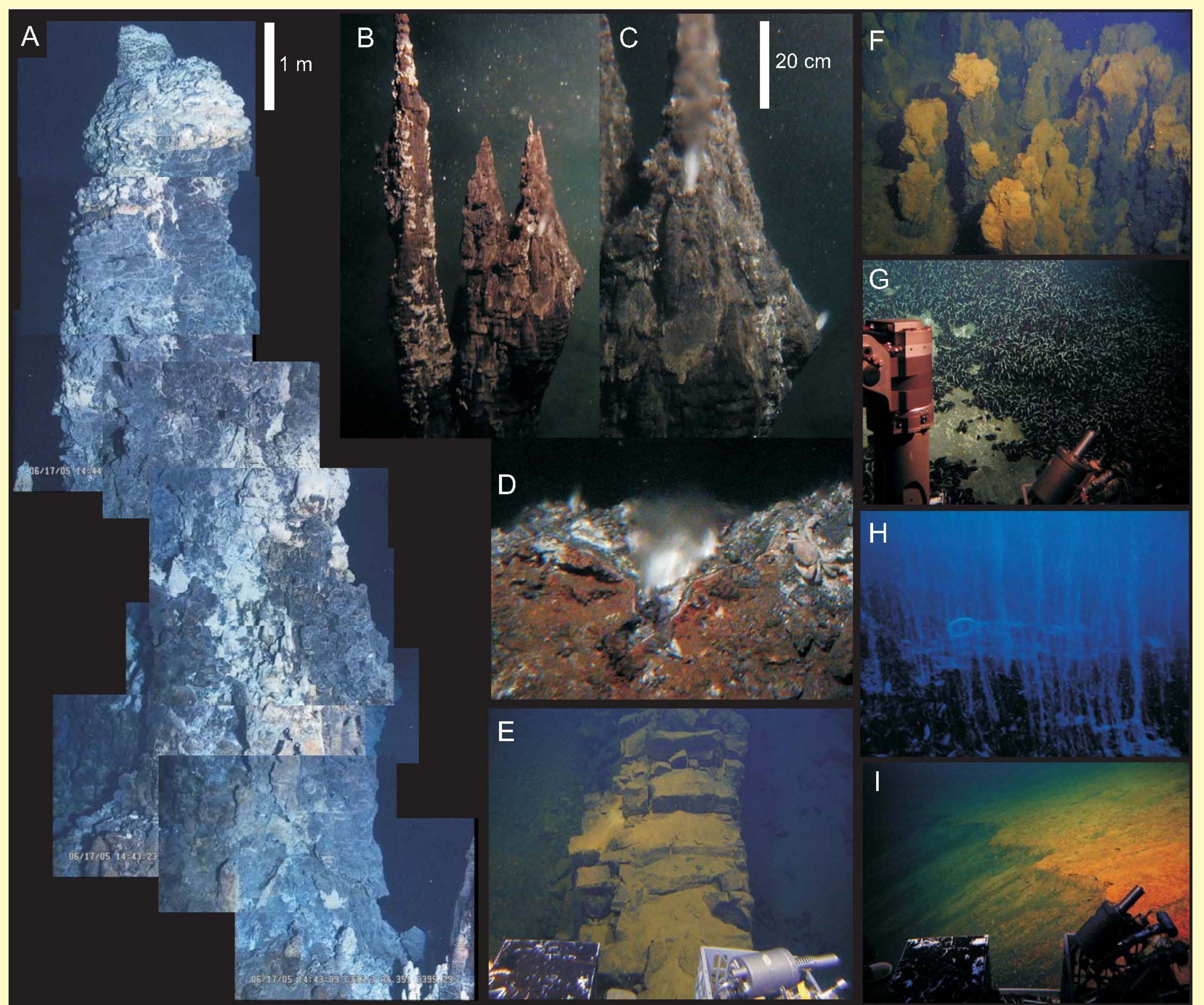
To address these objectives we returned to the South Tonga Arc, where fluid venting and mineralization were detected at 9 of 27 volcanoes during the SONNE-167 and TELVE cruises (2002-2003).

Our 13-dive PISCES submersible program collected venting fluids and gases, mineralization, lavas and faunas at Volcano 1 and Volcano 19.

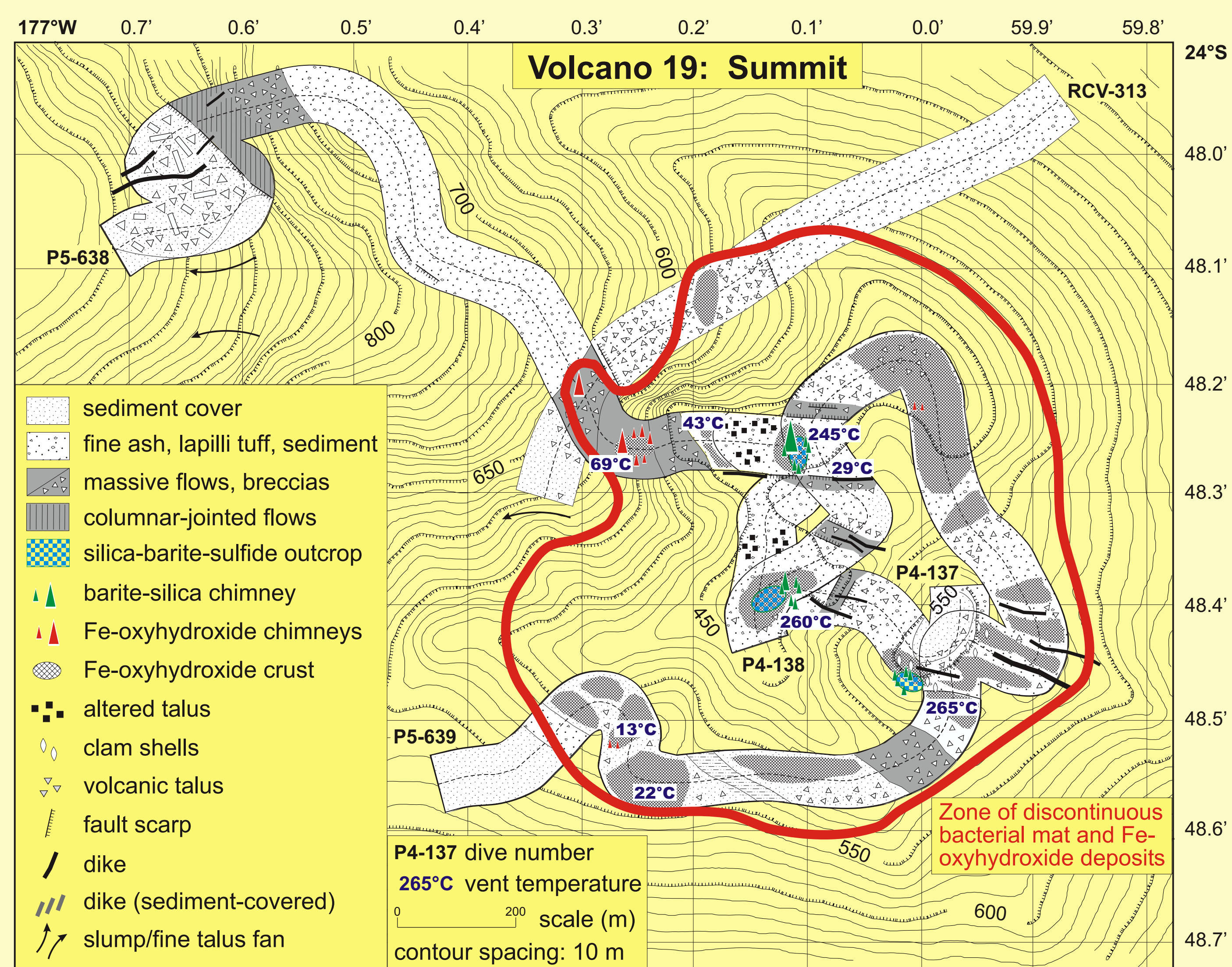
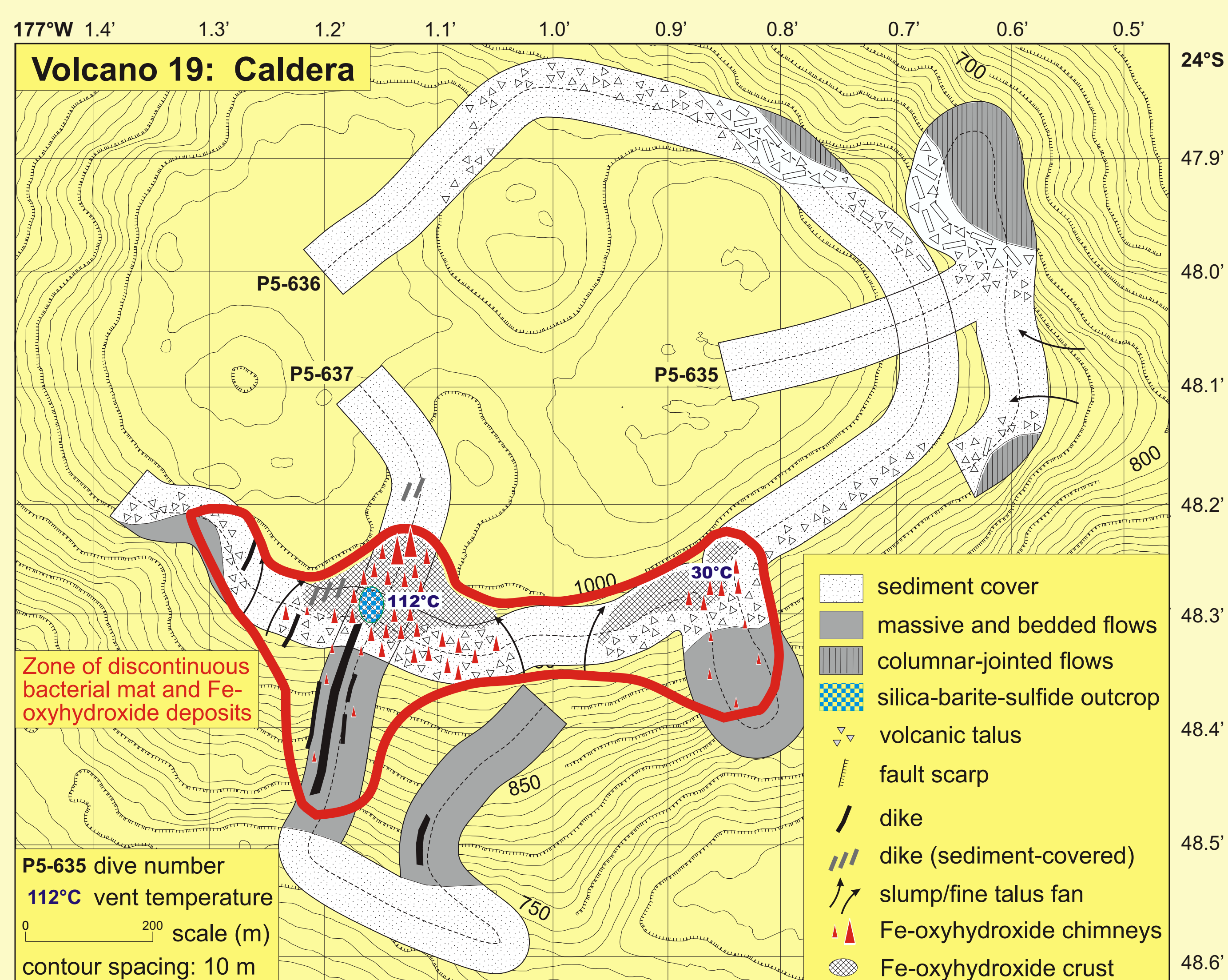


VOLCANO 1

- Large stratovolcano with summit caldera 7 x 4.5 km; resurgent volcanism at the western caldera wall has built two scoria cones together with a prominent "crater chain" of explosion pits.
- Pre- and post-caldera lavas are mostly andesite (56-58 wt.% SiO₂); the caldera-forming eruption comprises andesitic pyroclastic flows.
- Widespread diffuse venting covers 400 x 600 m, including the 2 largest explosion pits and part of the SW scoria cone (210-160 mbsl).
- The adjacent face of the scoria cone to 75 mbsl is largely covered by white filamentous bacteria underlain by Fe-oxyhydroxide-silica crust.
- Sulfur mounds and sulfur-cemented ash cover much of the field, with continuous streaming of gas bubbles from substrate cracks at 30-70°C.
- Blocks of solidified molten sulfur have embedded fresh ash and glass fragments on their basal surfaces; eruptions of molten sulfur may have occurred.
- Disseminated pyrite and marcasite are common within the altered and sulfur-cemented ash beds.
- Temperatures to 152°C were recorded in localized patches, but chimneys were not observed.
- Venting fluids are clear and have pH = 3.2-5.8 with high gas contents (130 mM; CO₂ and minor H₂S).
- Water within the caldera is extensively clouded by white sulfur particles that impart low visibility.
- Dense mussel beds (Bathymodiolus) cover much of the low-temperature field; limpets (living on the mussels), Brachyuran crabs and several species of polychaete worms were also observed.



- A 10 m-high barite-anhydrite-sulfide chimney (395-385 mbsl) venting clear fluid at 245°C from the summit beehive; V19 summit.
- B 2 m-high anhydrite spires (540 mbsl) with 2-phase venting of clear fluid at 265°C from several orifices; V19 summit (pit crater).
- C Close-up of 2-phase venting seen in B; the "flame" features are H₂O steam jets.
- D Vigorous 2-phase venting from a chalcopyrite-lined orifice 20 cm in diameter at the base of chimneys seen in B. A 30 cm-high anhydrite chimney grew at this site in the following 24 hours.
- E Vertical basalt dike; further along strike this dike controls the most vigorous venting on the inner southern wall, V19 caldera.
- F Field of 1-2 m-high Fe-oxyhydroxide-silica chimneys on the inner southern wall, V19 caldera.
- G Dense mussel field (Bathymodiolus) around gas-rich sulfurous vents (30-70°C) with white patches of native sulfur (152°C); V1.
- H Gas bubble streams (CO₂, minor H₂S) discharging from vents within the mussel field on V1. Photo in ambient light at 160 mbsl.
- I Extensive deposits of Fe-oxyhydroxide-silica crust surrounding the vent field in the "crater chain"; V1.



VOLCANO 19

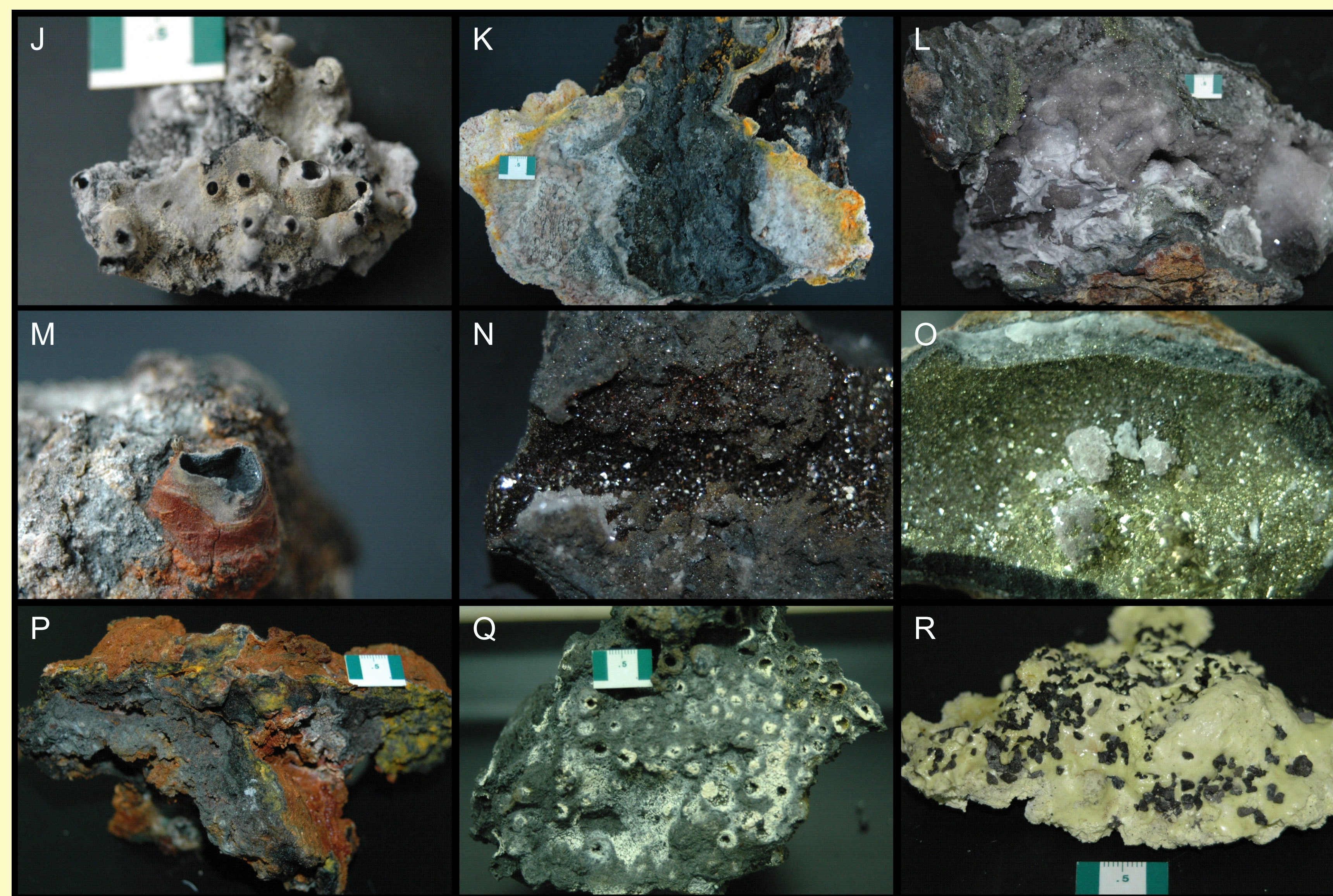
- Large stratovolcano with a largely infilled outer summit caldera (3.5 x 2.5 km), central cone complex and circular western caldera 1.9 km in diameter.
- Youngest flows are from the SE crater of the summit cone complex; all lavas are basalt-basaltic andesite (51.5-54.7 wt.% SiO₂).

Western Caldera Field

- Diffuse venting (mostly 30°C) occurs through Fe-oxyhydroxide-silica crusts and Fe-stained filamentous bacteria for >900 m along the inner south caldera wall at 985-850 mbsl.
- Developed in thick basaltic lavas and talus; spatially associated with a major NNE-SSW trending dike swarm.
- Central 200 x 300 m features large clusters of 1-2 m-high Fe-oxyhydroxide-silica chimneys.
- Largest chimneys are 5 m-high spires surrounded by barite-silica crusts with pyrite; vent temperatures reach 112°C.
- Vent fauna of crabs, shrimps and polychaete worms near the hottest vents.

Summit Cone Complex Field

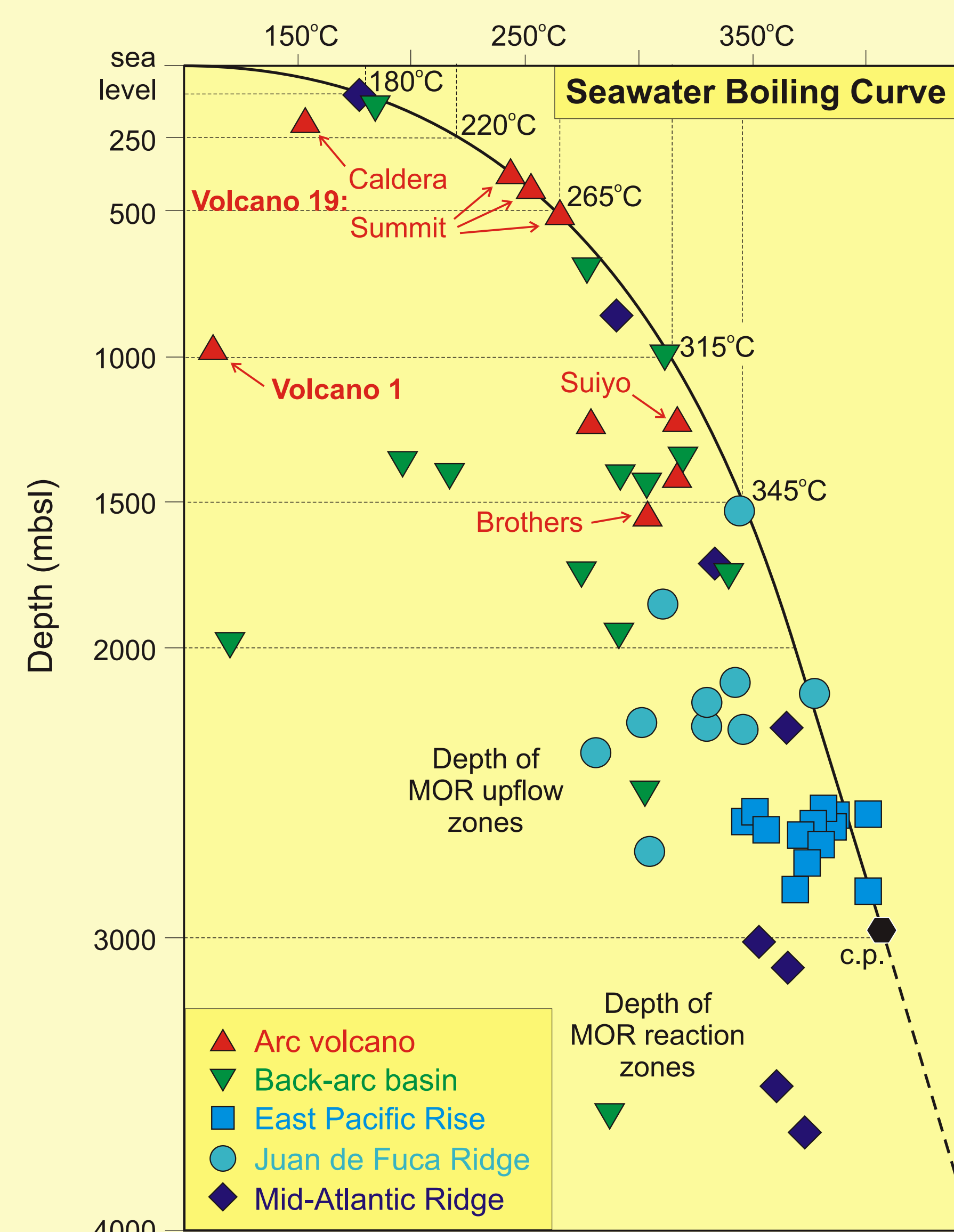
- Widespread diffuse venting occurs throughout an area of 800 x 800 m at the summit cone complex (540-385 mbsl); Fe-oxyhydroxide-silica crusts typically 0.5 m-thick cover most of this area.
- Developed in basaltic scoria, ash and talus both within and surrounding recently active craters; spatially associated with an ESE-WNW trending dike swarm.
- Fe-oxyhydroxide-silica chimneys up to 1 m-high occur where venting fluids exceed 70°C.
- Focused 2-phase venting of clear to slightly dark fluid and gas (H₂O vapor) occurs along the NE-SW summit ridge and in the SE pit crater from barite-anhydrite chimneys up to 10 m-high; vent temperatures reach 265°C.
- 2-phase venting chimneys consist of thick barite-anhydrite walls with central conduits filled by chalcopyrite-sphalerite-wurtzite-pyrite-marcasite.
- Vent fluids have pH = 4.6-6.1 and low gas contents (3.1-15 mM), comparable to MOR vent fluids.
- Diverse vent fauna: crabs (Bythograeidae), shrimps, polychaete and vent worms (Alvinellidae, Siboglinidae), mussels (Bathymodiolus, Gigantidas) and abundant sea stars (Asteroidea).
- The abundance of vent fauna is low relative to mid-ocean ridge vent fields.



- J 3-5 mm-wide 2-phase vents (245°C) consisting of barite with an inner lining of fine-grained sphalerite; V19 summit
 K Cross-section of 2-phase venting barite-anhydrite chimney with porous sphalerite-pyrite-marcasite conduit; V19 summit
 L Coarse-grained massive anhydrite with minor chalcopyrite-sphalerite-wurtzite at spire with 2-phase venting; V19 summit
 M 3 mm-wide 2-phase vent lined by sphalerite-pyrite-marcasite on a 30 cm-high barite-anhydrite chimney; V19 summit
 N Sphalerite-wurtzite lining the central conduit (1 cm-wide) of a high-temperature anhydrite chimney; V19 summit
 O Fine-grained chalcopyrite from a large spire with 2-phase venting; V19 summit
 P Massive silica-barite crust with minor pyrite-marcasite and an Fe-oxyhydroxide coating; V19 caldera at 112°C vents
 Q Altered ash block with sulfur-coated gas vents (also minor pyrite and barite); V1 at 152°C vents
 R Solidified sulfur flow with embedded fragments of fresh volcanic glass; V1

CONCLUSIONS

- Hydrothermal venting and seafloor mineralization were discovered and sampled using the *PISCES* submersibles near the summits of 2 shallow-water volcanoes in the South Tonga Arc.
- At Volcano 1, Fe-oxyhydroxide-silica crusts and bacteria-mussel fields cover a 400 x 600 m area where voluminous gas streaming (CO₂ bubbles) occurs through sulfur-cemented ash.
- At Volcano 19, vigorous 2-phase venting of clear fluid at 245-265°C occurs from tall barite-anhydrite chimneys with chalcopyrite-sphalerite-wurtzite-pyrite-marcasite lined conduits at the summit cone complex. A second lower temperature field occurs within the western caldera.
- The 2-phase vents, on the seawater boiling curve for their depth, most likely overlie an extensive field of sub-seafloor metal deposition.



- Venting fluids from the V19 summit field plot on the seawater boiling curve for their depth, confirming the observation of 2-phase venting.
- Though 2-phase venting of H₂O occurs in MOR settings (observed at the MAR, JdFR and EPR), gas discharge at most shallow-water volcanoes elsewhere (and at V1) is instead characterized by CO₂ (phase separation).
- Our evidence for sub-seafloor boiling beneath the V19 summit field suggests deposition of metals and development of extensive vein mineralization in a deep stockwork zone.
- Sub-seafloor boiling and mineralization may also explain the lack of "black smoke" (relative to mid-ocean ridge systems) at the high-temperature vents within the V19 summit field.

Acknowledgements

We are indebted to:

- the *PISCES* and *RCV-150* crews (T. Kerby, S. Price, M. Cremer, C. Wollerman, D. Greeson, P. Townsend) for their expertise and efforts
- the Captain and crew of the RV *KA'IMIKAI-O-KANALOA*
- A. Malahoff, J. Wiltshire, J. Smith and C. Komenaka at the HURL office for their foresight in enabling this cruise and logistical assistance
- the Kingdom of Tonga for permission to work in their territorial waters.

Primary funding for this project was provided by the Bundesministerium für Bildung und Forschung (BMBF) supplemented by a grant from the Deutsche Forschungsgemeinschaft (DFG).

Carbon Fluxes from Submarine Arc Volcanoes - Examples from the Mariana and Kermadec Arcs

Lupton, J., Butterfield, D., Lilley, M., Evans, L., Greene, R., Resing, J., Embley, R., Massoth, G., Christenson, B., de Ronde, C., Olson, E., Proskurowski, G., Nakamura, K., Schmidt, M., Stoffers, P., Worthington, T., Hannington, M.

Recent investigations of volcanic arcs have revealed unusually high fluxes of CO₂ from several submarine arc volcanoes. In 2004 the ROPOS ROV was used to map and sample ~10 active volcanoes along the Mariana arc, and in 2005 a similar study of volcanoes along the Kermadec arc was conducted using the HURL *Pisces* submersible. Of particular interest are 3 volcanoes that, in addition to discharging hot vent fluid, were found to be venting a separate CO₂-rich phase in the form of gas bubbles or, in one case, droplets of liquid CO₂. The Champagne hydrothermal site situated at ~1600-m depth near the summit of NW Eifuku volcano (21.49°N, 144.04°E) in the northern Mariana Arc, was discovered in 2004 during NOAAs Submarine Ring of Fire (SROF) project. This unusual site was discharging two distinct fluids from the same vent field: a 103 °C gas-rich hydrothermal fluid, and cold (4 °C) droplets of liquid CO₂. The hot fluid contained ~2.2 moles/kg CO₂, the highest ever reported for submarine hydrothermal fluids and about twice the saturation value at that p,T. The carbon flux from this site was estimated to be ~23 moles CO₂/sec, about 0.1% of the global MOR carbon flux. Two similar but much shallower CO₂-rich systems were discovered on the Kermadec arc. *Pisces* dives on Giggenbach volcano (30.04°S, 178.71°W) in the Kermadec arc discovered a mixture of gas bubbles and 203 °C fluid discharging at 164-m depth. The fluid contained 250 – 500 mM/kg total gas. At Volcano 1 (21.15°S, 175.75°W), *Pisces* found streams of gas bubbles rising from the seafloor at ~100 m depth. This vent area had areas of diffuse discharge (30 to 150 °C) with gas contents up to 130 mM/kg. Although analyses are still in progress for these two sites, the gas bubbles are assumed to be mainly CO₂. It is notable that discharges of pure CO₂ have never been reported for MOR hydrothermal systems, and only one other submarine occurrence of liquid CO₂ has been reported (in the Okinawa Trough, a back-arc system). This suggests that such CO₂-rich systems occur much more frequently in subduction zone systems compared to MOR systems, probably due to the supply of subducted marine carbonates and organic matter. It seems likely that the high CO₂ levels arise from direct degassing from a magma chamber and/or de-volatilization of the subducting slab. The apparent high carbon flux from these sites suggests that submarine arc volcanoes may play a larger role in oceanic carbon cycling than previously realized.

Plume–Vent Fluid Connections along the Tonga–Kermadec Arc

Massoth, G.J., Arculus, R.J., Baker, E.T., Butterfield, D.A., Chadwick, W.W., Christenson, B.W., de Ronde, C.E., Embley, R.W., Evans, L.J., Faure, K., Graham, I.J., Greene, R.R., Ishibashi, J., Lebon, G.T., Lupton, J.E., Resing, J.A., Roe, K.K., Schmidt, M., Stoffers, P., Walker, S.L., Worthington, T.J., Wright, I.C., Yamanaka, T.

The full extent of the 2530 km-long Tonga–Kermadec intra-oceanic arc was systematically surveyed for hydrothermal plume emissions during 5 expeditions between 1999 and 2005: NZAPLUME I, II and III covered the Kermadec arc using the New Zealand RV *TANGAROA* and the TELVE and NoToVE cruises surveyed the Tonga arc aboard the Australian RV *SOUTHERN SURVEYOR* after preliminary swath mapping by the German RV *SONNE*. At least 71 volcanic centers comprise the arc front, with about 75% of these first mapped or newly discovered during the expeditions. Hydrothermal plumes were detected as light scattering and chemical anomalies over more than half (36) of the volcanoes surveyed. Forty submersible dives were made on one-third (12) of the hydrothermally active volcanoes during the past year: 4 inaugural dives by the Japanese submersible *SHINKAI 6500* on Brothers volcano, and 36 dives using the NOAA/HURL submersibles *PISCES IV* and *V* on Brothers and an additional 11 volcanoes spread along the arc front. At least 25 venting sites were observed, and most were sampled for gaseous and liquid hydrothermal fluid emanations. We will summarize the pre-dive plume detection results with emphasis on the variability in the magnitude and character of the chemical signals over the active sites and compare/test predictions of the nature of seafloor sources at dive sites with what was actually observed. While most chemical determinations for the seafloor samples are pending, analyses conducted shipboard confirm that simple extension of plume results to the seafloor can be misleading and in contrast to the MOR experience.

2 SUMMARY

The first multi-beam bathymetry and dredge sampling of the 650 km-long intra-oceanic South Tonga volcanic arc was completed during the SO-167 "LOUISVILLE" cruise of the FS *SONNE* in late 2002 (Stoffers et al., 2003). Intensely altered and mineralized lavas were recovered from several volcanoes (in addition to fresh lavas), most notably from Volcano 1 (21.2°S) and Volcano 19 (24.8°S) (Schwarz-Schampera et al., 2003). Particle plumes and water-column chemical anomalies were detected above seven of the South Tonga arc volcanoes during the subsequent "TELVE" cruise with the Australian ship RV *SOUTHERN SURVEYOR* in 2003 (Massoth et al., 2004). The strongest plumes were also found at Volcano 1 and Volcano 19, and interpreted to represent magmatic degassing and/or high-temperature hydrothermal venting.

A series of research proposals by German, New Zealand, and USA geologists were approved during 2004 with the intention of using the *PISCES-IV* and *PISCES-V* submersibles, the remotely operated *RCV-150*, and their support ship RV *KA'IMIKAI-O-KANALOA* to systematically sample hydrothermal venting along the Tonga–Kermadec arc. Together with a similar program using the remotely operated *ROPOS* and *JASON II* submersibles in the Mariana arc (Embley et al., 2004; later April–May 2006 cruise at <http://www.oceanexplorer.noaa.gov/explorations/06fire>), they represent the first serious attempt to constrain hydrothermal venting at volcanic arcs. The SITKAP proposal, led by the Institute for Geosciences at the University of Kiel and the Economic Geology Research Unit of the BGR (Hannover), called for a minimum 10-dive program targeting the most prospective hydrothermal fields on Volcano 1, Volcano 18s and Volcano 19 (Figs. 2.1, 2.2). This cruise took place from 6–29 June 2005, running from Auckland (New Zealand) to Pago Pago (American Samoa) as the RV *KA'IMIKAI-O-KANALOA* returned towards its base in Hawaii. Close collaboration exists between members of the SITKAP Shipboard Scientific Party and their New Zealand and USA colleagues who participated in the earlier cruise legs visiting volcanoes on the Kermadec arc.

The SITKAP cruise was highly successful. Sea conditions allowed 13 *PISCES* dives (79 hours of on-bottom survey time) and ten deployments of the *RCV-150* (Table 2.1). Shallow-water high-temperature hydrothermal venting and associated seafloor mineralization were discovered and documented at both Volcano 1 and Volcano 19 (Figs. 2.2, 2.3, 2.4). In addition, weaker venting was investigated on the eastern flank cone of Volcano 18s. A total of 58 mineralised or hydrothermally altered samples, 14 gas samples and 13 vent fluid samples were collected from these fields for analytical work, together with 99 biological samples of the associated vent fauna. A further 73 rock samples, many of which represent fresh youthful lavas sampled in situ, were recovered to constrain the geochemical and magmatic evolution of the volcanoes and to provide the unaltered endmember composition of the lavas hosting the active hydrothermal vent fields.

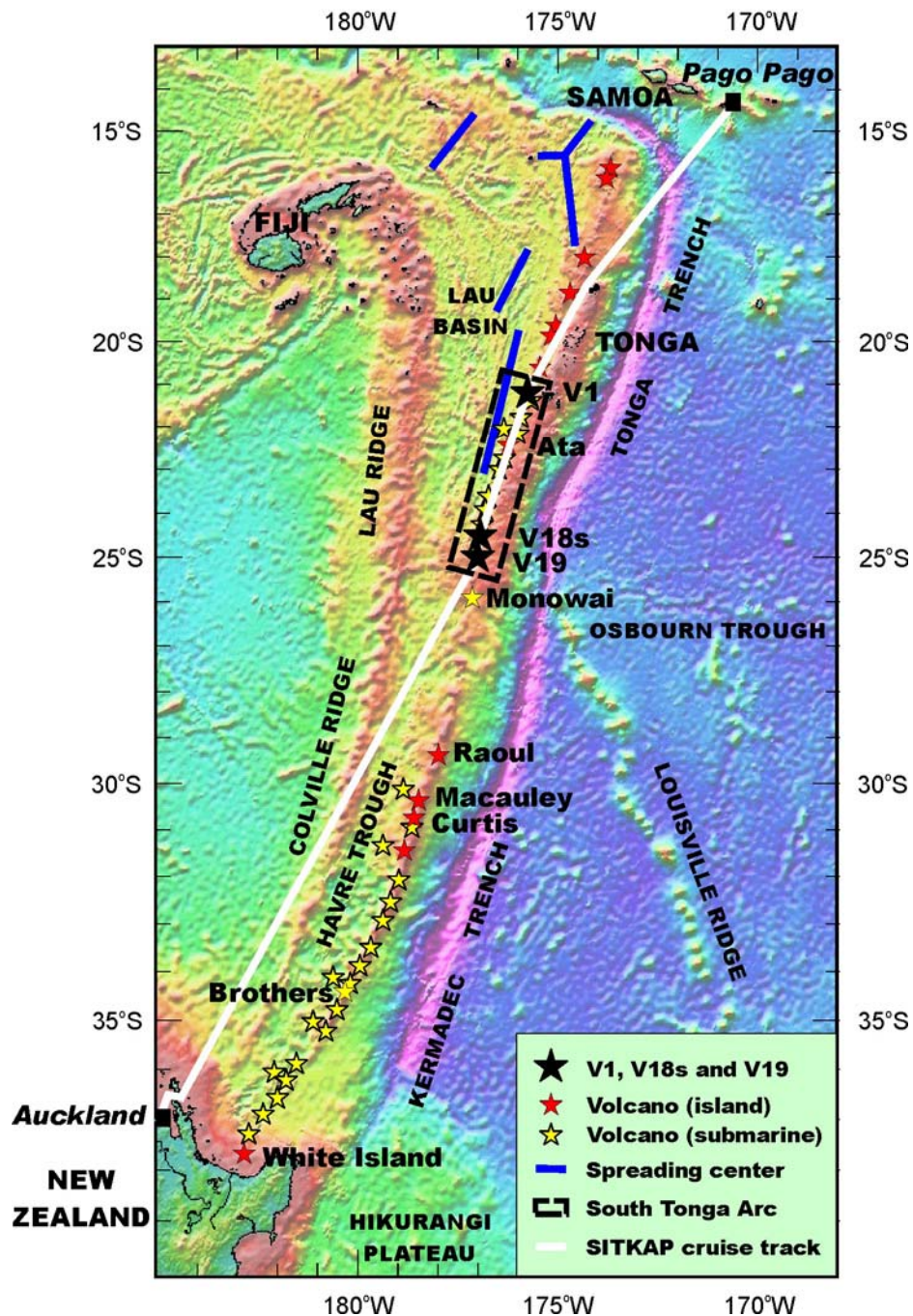


Fig. 2.1: Overview of the Tonga–Kermadec subduction system, SW Pacific. The SITKAP cruise track from Auckland (New Zealand) to Pago Pago (American Samoa) is in white. The three explored volcanoes (Volcano 1, Volcano 18s, Volcano 19) on the South Tonga arc are shown as black triangles.

Two spatially distinct active hydrothermal fields were found on Volcano 19, located at the summit of the central cone complex and within the western caldera respectively (Fig. 2.2). The highest temperature vents (245–265 °C) occur at water-depths of 385–540 mbsl in the summit field (Fig. 2.3). They comprise clusters of large barite and anhydrite chimneys up to 10 m-high, and are surrounded by extensive deposits of Fe-oxyhydroxides

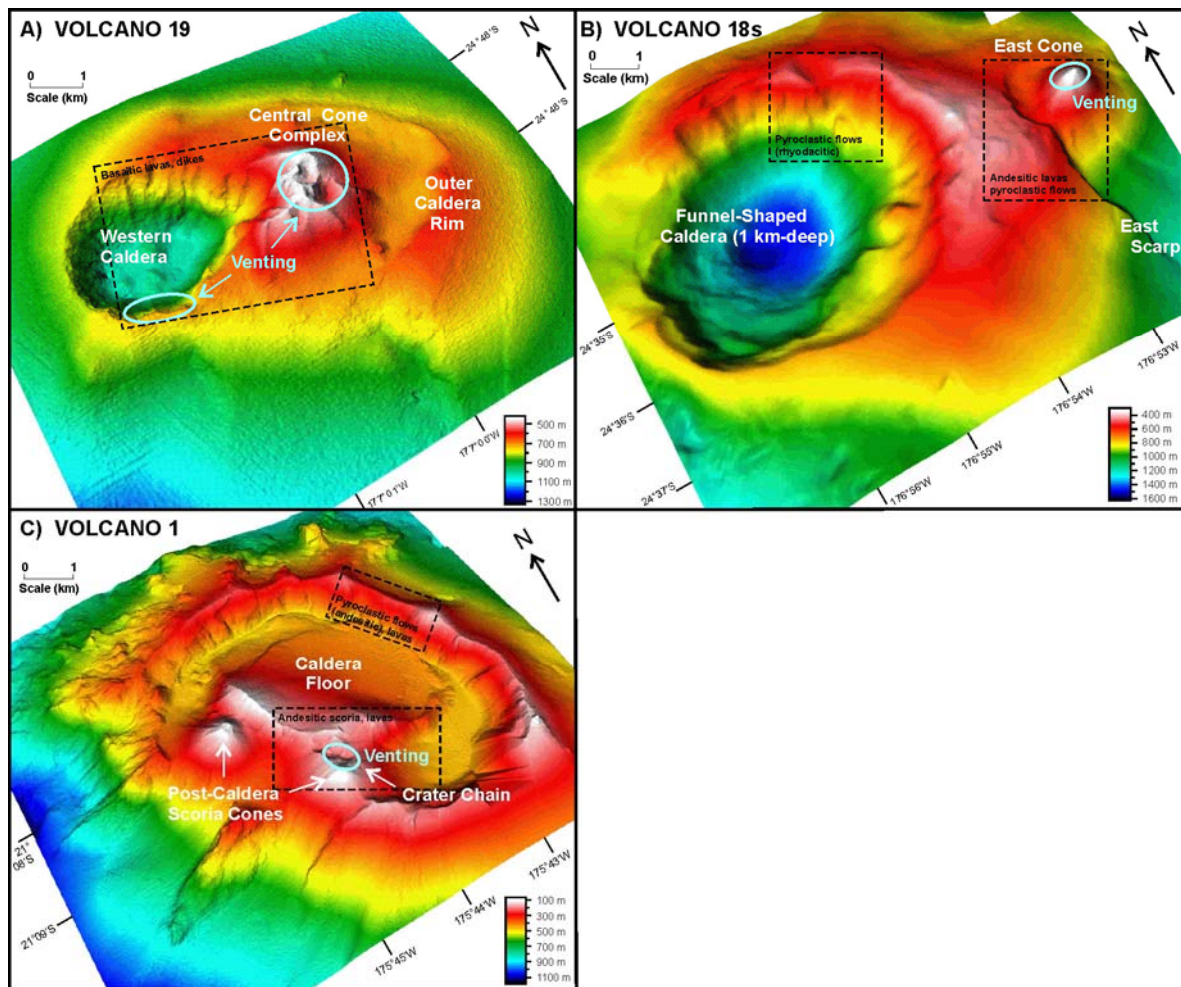


Fig. 2.2: Bathymetric images of Volcano 1, Volcano 18s and Volcano 19. Active hydrothermal fields (pale blue ellipses) and areas visited during SITKAP (black rectangles) are shown. Each volcano is viewed looking towards 030° and from 60° elevation.

formed from more diffuse hydrothermal venting over an area of 800 x 800 m. The chimneys are characterized by vigorous venting of clear fluids with temperatures on the seawater boiling curve, pH of 4.6–6.1, and low gas contents (3.1–15 mM). Evidence of phase separation abounds, and it can be seen as flame-like jets of steam (H₂O vapor) discharging from the chimney orifices. Pyrite, marcasite, sphalerite, and chalcopyrite line the interiors of the highest temperature vents (Fig. 2.4), similar to the black smoker chimneys at mid-ocean ridge hydrothermal fields. Venting in the second field within the western caldera is more diffuse, at lower temperature (up to 112 °C), and in deeper water (850–985 mbsl). This field covers an area of >900 m along strike near the base of the inner south caldera wall and features large clusters of Fe-oxyhydroxide and silica chimneys at its core. Both vent fields on Volcano 19 are spatially related to basaltic dike swarms and are hosted by basaltic lavas and scoria. Outcrops of silicic lava and/or pumiceous ash were not found even within (and around) the caldera, confirming the mafic character of this volcano. A diverse vent fauna of crabs (Bythograeidia), shrimps, polychaete and vent worms

Table 2.1: Summary of PISCES and RCV-150 Dives

<u>P4/5 Dive</u>	<u>Scientist</u>	<u>Pilot</u>	<u>Co-Pilot</u>	<u>Date</u>	<u>Surv</u>	<u>DVD</u>	<u>Photos</u>	<u>Rock</u>	<u>Min</u>	<u>Gas</u>	<u>Water</u>	<u>Bio</u>	<u>Location</u>
P5-635	Massoth	Kerby	Price	12.06.05	1:35	1	3301-3329	1	-	-	-	-	V19, NE caldera and base of shute
P5-636	Hannington	Kerby	Cremer	13.06.05	5:23	3	3330-3386	1	4	-	-	1	V19, eastern half of caldera
P5-637	Schwarz	Kerby	Wollerman	14.06.05	6:18	3	3387-3447	2	5	2	2	6	V19, inner southern caldera wall
P5-638	Massoth	Kerby	Price	16.06.05	7:01	4	3448-3530	1	4	2	3	3	V19, shute to summit vents
P5-639	Hekinian	Kerby	Cremer	17.06.05	6:53	4	3531-3622	16	12	-	-	16	V19, summit
P5-640	Worthington	Kerby	Wollerman	18.06.05	7:08	4	3623-3679	14	4	-	-	8	V18s, eastern scarp and flank cone
P5-641	Worthington	Kerby	Price	19.06.05	6:34	4	3680-3719	17	2	-	-	10	V18s, inner north caldera wall
P4-137	Hannington	Kerby	Cremer	20.06.05	3:15	2	3720-3765	-	3	2	2	6	V19, eastern summit vents
P4-138	Lundsten	Kerby	Wollerman	21.06.05	7:30	4	3766-3842	-	5	2	2	4	V19, eastern summit vents
P4-139	Schwarz	Kerby	Price	23.06.05	7:05	4	3843-3875	-	4	-	-	26	V1, crater valley and ridge
P4-140	Schmidt	Kerby	Cremer	24.06.05	0:20	-	-	-	-	-	-	-	V1, electrical malfunction - aborted
P4-141	Stoffers	Kerby	Cremer	24.06.05	5:00	3	3876-3911	-	6	3	2	10	V1, south and central craters
P4-142	Vaiomo'unga	Kerby	Price	25.06.05	8:13	4	3912-3969	1	6	3	2	9	V1, ridge and crater valley
P4-143	Hekinian	Kerby	Cremer	26.06.05	6:47	4	3970-4046	20	3	-	-	-	V1, inner east caldera wall
Totals:	Successful dives = 13	Aborted dives = 1			79:02	44	746	73	58	14	13	99	

<u>RCV Dive</u>	<u>Date</u>	<u>Time</u>	<u>Surv</u>	<u>DVD</u>	<u>Location and Purpose</u>
RCV-313	20.06.05	19:51-20:36	0:45	1	V19, traverse across the north summit to delineate extent of the vent field
RCV-314	22.06.05	18:33-20:58	2:25	2	V1, traverse along crater valley to check hazards (cables) and locate any venting
RCV-315	23.06.05	19:12-19:45	0:33	1	V1, traverse across crater valley to determine whether venting was focussed on the north or south side
RCV-316	23.06.05	20:40-21:22	0:42	1	V1, traverse across crater valley to determine whether venting was focussed on the north or south side
RCV-317	24.06.05	19:57-20:15	0:18	1	V1, central traverse across north crater valley to delineate extent of the vent field
RCV-318	24.06.05	20:59-21:28	0:29	1	V1, traverse north of north crater valley to delineate extent of the vent field
RCV-319	24.06.05	22:13-22:31	0:18	1	V1, traverse south of north crater valley to delineate extent of the vent field
RCV-320	25.06.05	19:09-19:44	0:35	1	V1, traverse up inner NE caldera wall to check hazards
RCV-321	25.06.05	20:35-20:59	0:24	1	V1, traverse up inner eastern caldera wall to check hazards
Totals:	Successful dives = 9		6:29	10	

Date, Time and Surv (= survey time on-bottom) are ship time in hours and minutes. DVD and Photos are the number of DVDs and digital stills taken during each dive; note that the full filename of each still photo is preceded by the month and date (e.g. 6123301 for the first photo of P5-635). Rock, Min, Gas, Water and Bio are the number of rock, mineralised or altered, gas tight, vent fluid, and biological samples collected respectively (11 samples belong to both the Rock and Min categories).

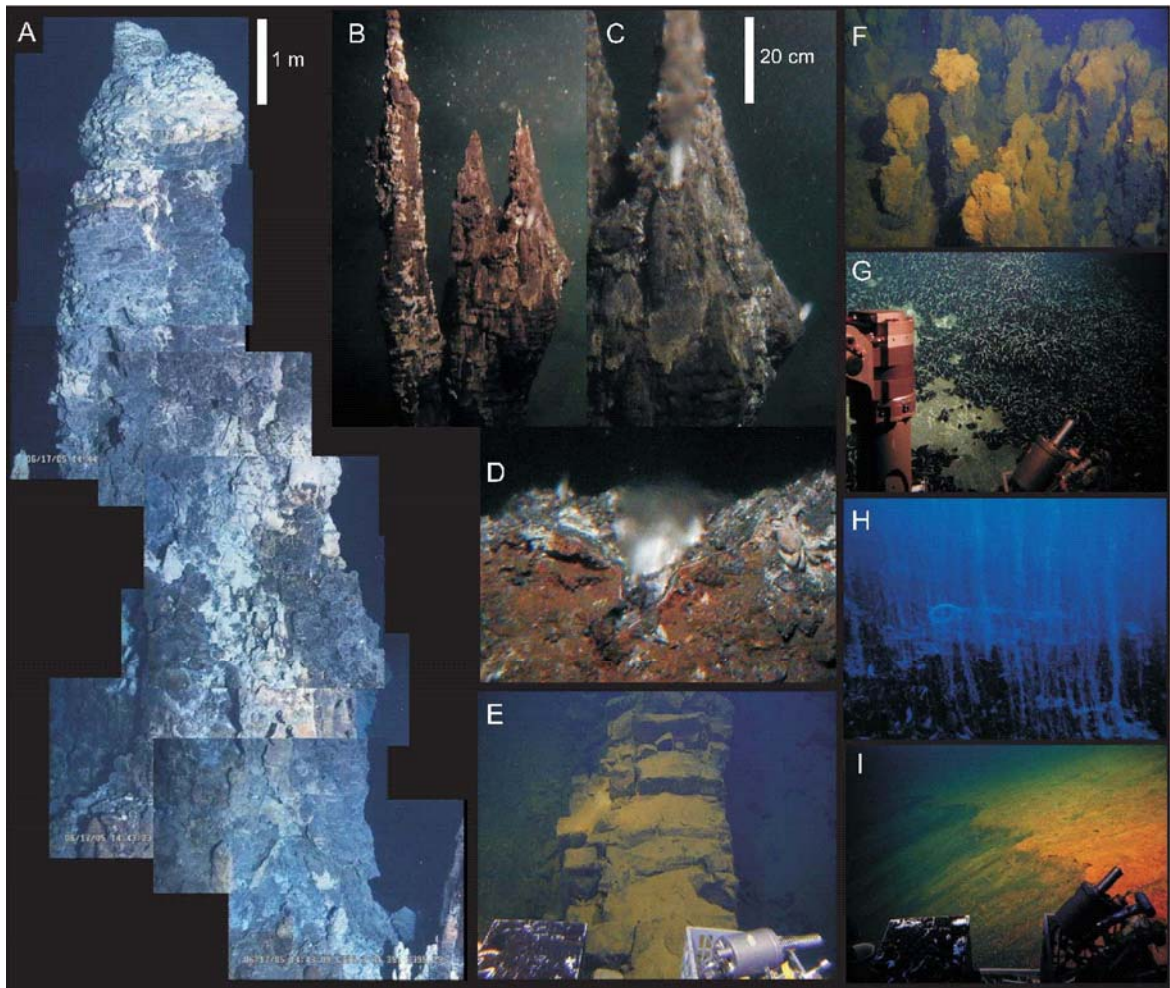


Fig. 2.3: Composite of key hydrothermal and geological observations –

- A) 10 m-high barite-anhydrite-sulfide chimney (385–395 mbsl) venting clear fluid at 245 °C from its summit beehive; Volcano 19 summit field*
- B) 2 m-high anhydrite spires (540 mbsl) with 2-phase venting of clear fluid at 265 °C from several orifices; Volcano 19 summit field (SE pit crater)*
- C) Close-up of 2-phase venting seen in B); the "flame" features are H₂O steam jets*
- D) Vigorous 2-phase venting from a chalcopyrite-lined orifice 20 cm in diameter at the base of chimneys seen in B); a 30 cm-high anhydrite chimney grew at this site in the following 24 hours*
- E) Vertical basalt dike; further along strike this dike controls the most vigorous venting on the inner southern wall of the Volcano 19 caldera*
- F) Field of 1–2 m-high Fe-oxyhydroxide-silica chimneys on the inner southern caldera wall of Volcano 19*
- G) Dense mussel field (*Bathymodiolus*) around gas-rich sulfurous vents (30–70 °C) with white patches of native sulfur (152 °C); crater chain field of Volcano 1*
- H) Gas bubble streams (CO₂, minor H₂S) discharging from vents within the mussel beds at the crater chain field on Volcano 1; photo is in ambient light at 160 mbsl*
- I) Extensive deposits of Fe-oxyhydroxide-silica crust surrounding the crater chain vent field of Volcano 1.*

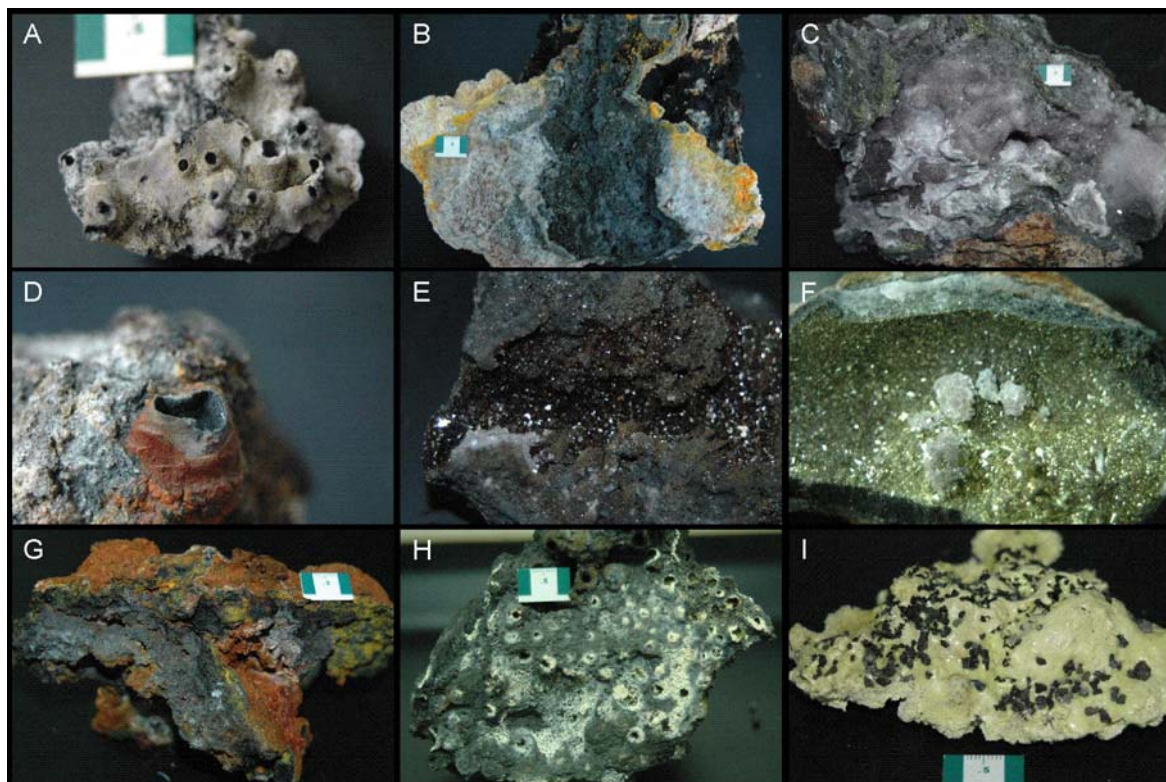


Fig. 2.4: Composite of key hydrothermal (mineralized) samples (white scale unit is 1 cm wide) –

- A) 3–5 mm-wide 2-phase vents (245 °C) consisting of barite with an inner lining of fine-grained sphalerite; Volcano 19 summit field
- B) Cross-section of 2-phase venting barite-anhydrite chimney with porous sphalerite-pyrite-marcasite conduit; Volcano 19 summit field
- C) Coarse-grained massive anhydrite with minor chalcopyrite-sphalerite-wurtzite at spire with 2-phase venting; Volcano 19 summit field
- D) 3 mm-wide 2-phase vent lined by sphalerite-pyrite-marcasite on a 30 cm-high barite-anhydrite chimney; Volcano 19 summit field
- E) Sphalerite-wurtzite lining the central conduit (1 cm-wide) of a high-temperature anhydrite chimney; Volcano 19 summit field
- F) Fine-grained chalcopyrite from a large spire with 2-phase venting; Volcano 19 summit field
- G) Massive silica-barite crust with minor pyrite-marcasite and an Fe-oxyhydroxide coating; Volcano 19 caldera field at 112 °C vents
- H) Altered ash block with sulfur-coated gas vents (also minor pyrite and barite); Volcano 1 field at 152 °C vents
- I) Solidified sulfur flow with embedded fragments of fresh volcanic glass; Volcano 1 field.

(Alvinellidae, Siboglinidae), mussels (Bathymodiolus, Gigantidas) and sea stars (Asteroidea) populate the summit field but are less abundant in the western caldera.

At Volcano 18s, the prime focus was gaining new insights into the origin of the 1.1 km-deep funnel-shaped caldera and post-caldera volcanism at the eastern flank cone (Fig. 2.2). Stratigraphically controlled samples were collected from pyroclastic flow sequences

exposed at the 150 m-high east scarp and over a 750 m-thick interval on the inner north caldera wall (500–1250 mbsl). Three distinct pyroclastic formations were identified; the caldera may be a product of multiple large eruptions rather than a single gigantic blast. Quenched basaltic clasts and alternating dacitic pumice and black scoria beds in the upper sections of the pyroclastic sequences indicate the eruptions were triggered by repeated influxes of hot basaltic magma into a large dacitic magma chamber. The post-caldera eastern flank cone consists of stacked basaltic andesite flows and intervening breccia beds. A large area of Fe-oxyhydroxide and silica crust with bacterial mats (250 x 600 m) covers the upper western part of the cone from 440 mbsl to its summit at 270 mbsl. Diffuse very low-temperature venting (up to 2 °C above ambient) occurs throughout this field.

At Volcano 1, low to medium-temperature venting (up to 152 °C; typically 30–70 °C) was found within two craters of the post-caldera "crater chain" and on the adjacent flanks of the SW post-caldera scoria cone (Fig. 2.2). The venting is most intense in water-depths of 160–210 mbsl, where much of the water within the caldera is clouded by white sulfur particles. Large fields of densely populated mussels (*Bathymodiolus*), white filamentous bacteria, limpets, Brachyuran crabs and several species of polychaete worms cover Fe-oxyhydroxide-silica crusts and sulfur-cemented ash in and around the craters over an area of 400 x 600 m (Fig. 2.3). Venting of clear fluids with pH of 3.2–5.8 and high gas contents (130 mM) is associated with voluminous gas streaming (most likely CO₂ bubbles) through cracks in the sulfur-cemented ash. Blocks of formerly molten sulfur with fresh volcanic glass embedded in their lower surfaces are common, and disseminated pyrite and marcasite occur within the sulfur-cemented and altered ash beds (Fig. 2.4). A series of pillow andesite lavas interbedded with volcanoclastic sediments and numerous thin ash beds is intruded by dikes and exposed along the inner NE caldera wall. The absence of pyroclastic flow deposits combined with volcano bathymetry and geochemistry favours a caldera origin by sector collapse and not a single voluminous eruption.

References

- Embley, R.W., Baker, E.T., Chadwick, W.W., Lupton, J.E., Resing, J.A., Massoth, G.J., Nakamura, K.; 2004. Exploration of Mariana arc volcanoes reveal new hydrothermal systems. *EOS Trans. AGU*, 85, 37–40.
- Massoth, G.J., Baker, E.T., Lupton, J.E., de Ronde, C.E.J., Walker, S.L., Ishibashi, J.-I., Worthington, T.J., Arculus, R.J., Resing, J.A., Greene, R.R., Lebon, G.T., Nakamura, K.-I., Stoffers, P.; 2004. A systematic reconnaissance of submarine hydrothermal venting along the south Tonga (Tofua) intra-oceanic arc. *AGU Fall Meeting, San Francisco, December 2004*.
- Stoffers, P., Worthington, T.J., Schwarz-Schampera, U., et al.; 2003. *Cruise Report SONNE 167: Louisville. Ber.- Rep., Inst. für Geowiss., Universität Kiel, 20, 276 pp.*
- Schwarz-Schampera, U., Herzig, P.M., Gibson, H., Stoffers, P.; 2003. Auriferous pyrite mineralization in the Tonga island arc, SW-Pacific: first evidence for shallow submarine hydrothermal activity. *SGA Conference, Athens*.

3 ACKNOWLEDGEMENTS

We are indebted to Terry Kerby and the *PISCES* team for their outstanding efforts, both in keeping the submersibles operational with minimal down-time and in safely navigating through the overhanging walls, pinnacles and other hazards encountered on the irregular upper flanks of active volcanoes. These are feats requiring exceptional levels of skill and concentration. Their highly professional attitude, stamina and maintenance skills came to the fore during the main dive series, when sea conditions had improved sufficiently to allow six consecutive and highly successful dive days.

Thanks are also due to Dan Greeson and Pete Townsend, who never flinched from the difficult job of repairing and maintaining the *RCV-150* after sea-water penetrated the main power unit during the early stages of the cruise and again later when a leak developed in the electronics box. Their persistence allowed eight *RCV-150* dives on Volcano 1 during the latter part of the cruise, including the key task of establishing whether the shallow summit targets were safe from abandoned fishing nets and cables.

Captain Ross Barnes, his officers and the crew onboard the RV *KA'IMIKAI-O-KANALOA* are thanked for their hospitality and efforts in the launching and retrieving the submersibles. Sea and wind conditions were difficult throughout the first phase of the diving campaign, and we much appreciated their willingness and endeavours to do everything possible without compromising safety.

We thank the Kingdom of Tonga for permission to work within their territorial waters along the arc, and are certain our results will be of much interest and benefit to Tonga.

Principal funding for the SITKAP project, covering the charter cost of the *PISCES-IV* and *PISCES-V*, the *RCV-150* and the RV *KA'IMIKAI-O-KANALOA*, was provided by the Bundesministerium für Bildung und Forschung (BMBF) through grant 03G0632A. Additional funding for travel expenses was provided by the Deutsche Forschungsgemeinschaft (DFG) through grant STO 110/42-1.

The SITKAP cruise was one of four *PISCES* cruises along the Tonga–Kermadec Arc during March–June 2005. Although visiting different parts of the arc, these four cruises constitute only the second time any volcanic arc has been similarly explored (the other being the Marianas with the unmanned *ROPOS* in 2004). Close collaboration exists between many of the working groups on these four cruises. We thank Alex Malahoff, John Wiltshire, John Smith and others at HURL for their foresight in facilitating, co-ordinating and encouraging these four cruises.

Last, but not least, we are truly indebted to Cheryl Komenaka in the HURL office for her sterling efforts in helping us get our samples out of Pago Pago and safely to Germany despite the remarkable inertia of two American Samoa-based freight companies.

4 PARTICIPANTS

SITKAP is a multidisciplinary international project utilising the twin submersibles *PISCES-IV* and *PISCES-V*, the remote controlled *RCV-150*, and their support ship RV *KA'IMIKAI-O-KANALOA* to obtain samples of venting fluids and gases, associated mineralisation and vent faunas, and stratigraphically controlled lavas from three volcanoes in the south Tonga arc. SITKAP is led by the Institute for Geosciences at the University of Kiel and the Economic Geology Research Unit of the BGR (Hannover). Other participating research groups include the Ministry of Lands, Survey and Natural Resources (Kingdom of Tonga), the University of Ottawa (Canada), the Institute of Geological and Nuclear Sciences (New Zealand), the Monterey Bay Aquarium Research Institute (United States), and the Pacific Marine Environmental Laboratory (PMEL) of NOAA (United States). The ten members of the Shipboard Scientific Party have diverse interests spanning the fields of petrology, geochemistry, mineralisation, fluid and gas chemistry, and biology. Their full contact details are listed in Appendix 1.

Shipboard Scientific Party:

Stoffers, Prof. Dr. Peter	Chief Scientist, PI	IfG-Kiel	Geology/Petrology
Evans, Leigh		NOAA/PMEL	Gas chemistry
Hannington, Prof. Dr. Mark		Uni Ottawa	Mineralisation/Geology
Hekinian, Dr. Roger		IfG-Kiel	Petrology/Geology
Lundsten, Lonny		MBARI	Biology
Massoth, Dr. Gary		GNS	Fluid chemistry
Schmidt, Dr. Mark		IfG-Kiel	Gas chemistry
Schwarz-Schampera, Dr. Uli		BGR	Mineralisation/Geology
Vaiomo'unga, Rennie		Min Lands Surv	Geology
Worthington, Dr. Tim		IfG-Kiel	Petrology/Geochemistry

PISCES-IV, *PISCES-V* and *RCV-150* Operations:

Kerby, Terry	Ops Director/Chief Pilot		
Price, Steve	PISCES	Cremer, Max	PISCES
Wollerman, Colin	PISCES	Bloedorn, Doug	PISCES
Greeson, Dan	RCV/PISCES	Townsend, Pete	RCV/PISCES

Officers and Crew of the RV *KA'IMIKAI-O-KANALOA*:

Barnes, Ross	Captain		
Gutzeit, Clary	First Mate	Furlong, Dan	Chief Engineer
Gall, John	Second Mate	Carlin, John	First Engineer
Dubois, Dave	Electronics Technician	Reyes, William	Oiler
Sobolewski, Jan	Chief Cook	Williamson, Mario	Oiler
Ramos, Paul	Cook	Atienza, Deren	Wiper
Ano, Josh	Seaman	Dussault, Todd	Seaman
Hodge, Mike	Seaman		

5 CRUISE NARRATIVE

The Shipboard Scientific Party (SSP) boarded the RV *KA'IMIKAI-O-KANALOA (KOK)* in Auckland at 09:30 on 6 June. The ship had come out of a 3 week dry-dock a few days earlier and spent the morning bunkering and taking on supplies. At 11:00 the SSP held an introductory meeting during which the participants were introduced to the *PISCES* and *RCV-150* teams. Various members of the SSP then presented a synopsis of the Tonga–Kermadec Arc, previous work (especially the SO-167 LOUISVILLE and TELVE cruises), the results of the March–May *PISCES* dives on Kermadec volcanoes undertaken by New Zealand and US colleagues, and an overview of the SITKAP cruise plan and prime targets (Monowai, Volcano 19, Volcano 18s and Volcano 1). A provisional decision was taken to head for Volcano 19, leaving open the option to back-track to Monowai (an overnight 8 hour transit) if Volcano 19 failed to live up to expectations. Members of the SSP then unpacked and familiarised themselves with the ship and submersibles. The *KOK* sailed from Devonport Wharf in Auckland a few minutes earlier than scheduled at 15:55, assisted by a stern tow from a tug boat. Despite severe winter weather over much of New Zealand, sea conditions remained moderate throughout the night and during 7 June. The ship made steady progress at 9.5 knots in open seas throughout this period, travelling with a 2–3 m southerly swell.

Strong to gale force SE winds affected much of the Tonga–Kermadec region over the next few days. These were generated by an intense high pressure system that became stuck over Auckland. Sea conditions for the *KOK* deteriorated rapidly on 8 June, with 4–5 m waves hitting the ship beam-on and inducing a heavy roll that threatened the stability of the *PISCES-V* on the open aft deck. In consequence, the *KOK* was forced to reduce speed to 4–6 knots and the scheduled 3.5 day transit to Volcano 19 eventually took nearly 5 days. Throughout this period several SSP meetings were held, dive plans for Volcano 19 were formulated, and the labs were prepared. Attempts to get the detailed bathymetry of the target volcanoes (generated using Surfer v8) into the onboard ArcGIS software proved unsuccessful. Eventually a series of hard copy maps for each target volcano were prepared by exporting the Surfer files to CorelDraw using the dxf format and also through GMT; the incompatibility of Surfer and ArcGIS proved to be only a minor inconvenience. The *KOK* changed to Samoan time on 8 June and repeated the day (NB: the International Dateline actually deflects eastward around Tonga from 180° longitude and Tonga keeps the same day as NZ; nevertheless, the *KOK* elected to adopt Samoan time as though the dateline remained centred on 180° longitude- all dates and times in this report are ship time).

The weather improved briefly on 10 June and the *KOK* reached Volcano 19 at 10:00. However, sea conditions were deemed too severe and changeable for submersible operations. Within a few hours the weather deteriorated again, and during 11 June the *KOK* briefly left station to answer a mayday from a yacht in distress near Minerva Reef (several

yachts and small boats in the general Tonga–Kermadec area were in difficulties during this period, though all eventually found safe refuge).

On 12 June conditions had eased to marginal, with 3 m swells. The *PISCES-V* was launched at 09:30 to explore the inner NE caldera wall of Volcano 19 and proceed up the shute (P5-635; Gary Massoth). Cloudy water and other evidence of nearby hydrothermal venting was observed, though the vent sites remained elusive. By late morning an increase in wind speed caused the Captain to abort the dive in the interests of a safe recovery (the dive was aborted before the mid-shute target area was reached). The recovery proved extremely difficult with a rolling aft deck due to the confused sea state (4 m-high waves from several directions) and high gusting winds. Despite the weather, the evening SSP meeting took place in an atmosphere of considerable optimism with expectations that the next dive would find active venting.

Conditions were much improved on 13 June, with 2–3 m swells easing throughout the day. A full *PISCES* dive was achieved; Fe-oxyhydroxide chimneys together with low temperature (30 °C) venting were discovered along part of the inner southern caldera wall near 950 mbsl (P5-636; Mark Hannington). Spectacular geology, including a series of NNE-trending dykes concentrated along the south caldera wall and columnar jointed basalt flows, was also observed. An unwelcome find was that sea-water had penetrated the main ship-mounted power supply to the *RCV-150* during the stormy weather. The major task of carefully cleaning and drying the power supply began in earnest but, hampered by further spells of inclement weather, the *RCV-150* was to remain out of commission until 18 June.

On 14 June similar sea conditions permitted another full dive that focussed on the south caldera wall (P5-637; Uli Schwarz-Schampera). Iron-silica chimneys venting medium-temperature (up to 113 °C) fluids were discovered below the area of the previous dive. Although encouraged by these discoveries, it was felt that attention should now shift to the shute and summit areas of the volcano in an attempt to find more vigorous venting. Stormy conditions on 15 June precluded any launch attempts and the aft deck was often awash. The *KOK* was on stand-by to assist a small boat in difficulties throughout much of the day, although fortunately no action was required (the boat was ~350 km distant).

By dawn on 16 June the seas had settled to 2 m-high waves. The dive program on Volcano 19 resumed with the *PISCES-V* traversing the shute from its base to the three summit peaks (P5-638; Gary Massoth). High-standing anhydrite-barite chimneys with venting at up to 245 °C were discovered throughout an area encompassing both the central and south summits. The following dive on 17 June concentrated on geological mapping and rock sampling of the summit area, further delineating the high-temperature vent field (P5-639; Roger Hekinian). After considerable discussion it was felt that both the caldera and summit vent fields of Volcano 19 were now well mapped and that, while further dives on both would be beneficial, it was time to proceed to Volcano 18s. The 2 hour transit then began and the *KOK* was on station at Volcano 18s before day break.

Calm conditions over Volcano 18s permitted two full dives. On 18 June the 150 m-high eastern scarp and youthful eastern satellite cone were visited (P5-640; Tim Worthington). A cross-section through a major pyroclastic flow sequence was exposed along the sub-vertical scarp, including a series of basal fallout beds, sub-welded pyroclastic flows, and upper fallout beds containing quenched basaltic clasts in addition to the predominant dacitic pumice. Massive aa flows of basaltic andesite on the eastern satellite cone were also sampled, and a field of diffuse very low temperature venting (up to 2 °C above ambient) with iron-silica chimneys and bacterial mats was traversed on the upper part of the cone. Although cloudy water limited visibility in this region, focussed venting was not observed. An evening attempt to deploy the *RCV-150* in the cloudy water over the eastern satellite cone aborted when the cable shorted out. On 19 June the steep inner north caldera wall of Volcano 18s between 1250 and 500 mbsl was mapped (P5-641; Tim Worthington). Vertical walls and pinnacles exposed a sequence through 3 major pyroclastic flow sequences of various ages, with the middle sequence being equivalent to that seen on the eastern scarp during the previous dive. These findings demonstrate that the large caldera of Volcano 18s is a product of several eruptions rather than one gigantic blast. Pods of alteration and veining occurred locally within the lowermost of the pyroclastic flow sequences, but outcrops of the chlorite-clay rock recovered from this vicinity during SO-167 proved elusive. A highlight of the dive was following the gouged trail of dredge 96-DR from SO-167 for ~200 m.

The hard rock objectives at Volcano 18s having now been achieved, considerable discussion ensued as to the relative merits of tracking down possible venting within the large caldera of Volcano 18s, further investigating the cloudy water and weak venting on the eastern satellite cone to locate more focussed venting, returning to Volcano 19 to sample the high-temperature venting fluids in more detail, or proceeding to the highly prospective Volcano 1. A consensus was reached that diving on either Volcano 19 or Volcano 1 represented a better use of time than tracking down the less dramatic venting at Volcano 18s. The *KOK* then completed an overnight transit back to Volcano 19.

On 20 June the Titan arm of the *PISCES-V* failed to respond during launch preparations. The morning was spent readying the *PISCES-IV* and rotating the positions of the two submersibles on the aft deck, a task made easier by the now flat seas. Following a thorough and trouble-free checkout, the *PISCES-IV* was launched in the early afternoon to explore the eastern summit crater of Volcano 19 (P4-137; Mark Hannington). This was a highly successful dive, locating two-phase venting at up to 265 °C from tall anhydrite chimneys cored by pyrite-chalcopyrite-sphalerite. A traverse over the north summit by the *RCV-150* that evening revealed no venting, thus closing off the field in this direction (#313). The *RCV-150* traverse had accomplished its prime objectives when sea-water infiltrated the electronics box and the dive had to be terminated. Cleaning and drying of the exposed circuit boards and re-sealing of the electronics box put the *RCV-150* out of commission until 22 June. The final dive at Volcano 19 took place on 21 June (P4-138; Lonny

Lundsten). This dive re-visited the high-temperature vents on the central summit and eastern crater to thoroughly sample venting fluids and gases, together with collecting vent fauna and further chimney samples.

All necessary samples from the high-temperature vent field on Volcano 19 having now been obtained, the 25-hour transit to Volcano 1 commenced. The *KOK* reached Volcano 1 at 18:00 on 22 June, with concern building about the possibility of abandoned fishing nets and cables on the shallow summit (~100–200 mbsl) in close proximity (55 km) to Tongatapu. The *RCV-150* was deployed and functioned flawlessly (#314). No cables or nets were seen, but thick plumes of cloudy water and a widespread bacterial mat field over iron-silica crust were observed in the crater valley regarded as the prime hydrothermal target.

The first dive on Volcano 1 took place on 23 June and followed the northern side of the crater valley (P4-139; Uli Schwarz-Schampera). Contrary to expectations, the dive had limited success until entering a mussel field in the central crater late in the day. At this stage a hydraulic failure on the *PISCES-IV* caused the dive to be aborted about 30 minutes early. Two *RCV-150* deployments in the evening found dense mussel fields covering much of the central and south craters, concentrated along the southern side of the crater valley (#315, #316). A further hydraulic failure of the *PISCES-IV* on reaching the seafloor caused the immediate abandonment of the next dive on 24 June (P4-140; Mark Schmidt). The *PISCES-IV* was repaired and re-launched after lunch (P4-141; Peter Stoffers). This dive concentrated on the central and south craters and southern flank of the adjacent south cone, sampling the mussel beds and locating venting at up to 68 °C from several iron-silica chimneys. Three deployments of the *RCV-150* that evening closed off the vent field to the north and identified a few small chimneys as the source of the plumes seen on the first *RCV-150* dive (#317, #318, #319). On 25 June the next dive traversed the semi-circular ridge north of the crater valley, which was believed to be prospective for venting (P4-142; Rennie Vaiomo'unga). No venting was found, and most of the dive was instead spent sampling vent fluids, crusts and mussels from the central and south craters.

Two evening *RCV-150* deployments investigated the sub-vertical 100–150 m-high NE and eastern inner caldera walls, recording spectacular outcrops of stacked lava sequences cut by occasional dykes at the former and volcanoclastic sediments at the latter (#320, #321). These sites were followed by the *PISCES-IV* dive of 26 June, which recovered a wide variety of in situ lavas, breccias and sediments (P4-143; Roger Hekinian). Some evidence of diffuse low-temperature venting was also found along the base of the inner eastern caldera wall. Deteriorating seas and increasing winds then led to the cancellation of the final *RCV-150* deployment, and the *KOK* commenced its transit to Pago Pago at 17:00.

Conditions further deteriorated throughout 27 June, with seas rising to 4–5 m waves beam-on to the ship in squally conditions. This was caused by a slow-moving trough (low pressure convergence zone) developing almost directly over Volcano 1. The *KOK* was forced to reduce speed to 4–6 knots, which closely matched the velocity of the slow

moving trough. Consequently, the trough remained overhead and conditions were difficult throughout the transit. The *KOK* berthed at 14:00 on 29 June in Pago Pago, accompanied by unseasonal heavy showers and minor flooding of the town. The SSP packed up their samples and cleaned the labs during the latter stages of the transit, disembarking from the *KOK* at 16:00 on 29 June. Thus terminated a most successful cruise that discovered and intensively sampled two major hydrothermal fields together with providing new insights into the evolution and geochemistry of three volcanoes.

6 SMOKER MINERALIZATION AND HYDROTHERMAL PRECIPITATES

6.1 Introduction

Four active hydrothermal fields were discovered during the SITKAP cruise (Fig. 2.2). Two of these occur on Volcano 19, being a high-temperature field located at the summit of the central cone complex (Fig. 6.1) and a moderate-temperature field at greater depth within the western caldera (Fig. 6.2). The remaining two fields are located within the Volcano 1 caldera and on the upper western flank and summit of the eastern cone at Volcano 18s. Our observations and direct measurements made using the PISCES submersibles at the Volcano 19 and Volcano 1 fields are summarized in the attached publication (Stoffers et al., 2006). Here, we provide further data obtained by lab work on samples from the high-temperature summit field on Volcano 19.

The first high-temperature submarine hydrothermal vents and associated seafloor mineralization on the Tonga arc have been found near the summit caldera of Volcano 19 in relatively shallow water. The highest temperature vents (245–265 °C) occur at water depths of 385–540 mbsl in the central cone complex. The vents comprise clusters of large (2–10 m-high) barite, anhydrite, and sulfide chimneys surrounded by extensive deposits of Fe-oxyhydroxides, and the vent field is about 800 m in diameter. The chimneys are characterized by vigorous venting of clear fluids with temperatures on the seawater boiling curve (Fig. 6.3). There is abundant evidence of phase separation, which can be seen as flame-like jets of steam (H₂O vapor) discharging from the chimney orifices. The chimneys have grown on top of prominent sulfide mounds consisting of chimney debris and thick sulfide crusts, as well as on strongly altered and mineralized volcanoclastic sediments.

Preliminary studies on the mineralogical and geochemical composition of sulfide and sulfate precipitates from a two-phase venting chimney were undertaken in order to characterize the mineralization processes and to evaluate the effects of phase separation on base and precious metal precipitation.

6.2 Chimney Mineralogy

The chimneys consist of coarse-grained sulfide and sulfate precipitates, predominantly pyrite, sphalerite and wurtzite together with minor marcasite, galena and chalcopyrite growing within a porous network of anhydrite and barite. The interiors of the highest temperature chimneys are lined by a dense intergrowth of wurtzite, pyrite, galena, and minor chalcopyrite (Fig. 6.4).

Wurtzite is almost always euhedral in shape and coarse-grained, most likely as a consequence of ideal conditions for crystallization close to fluid saturation with respect to

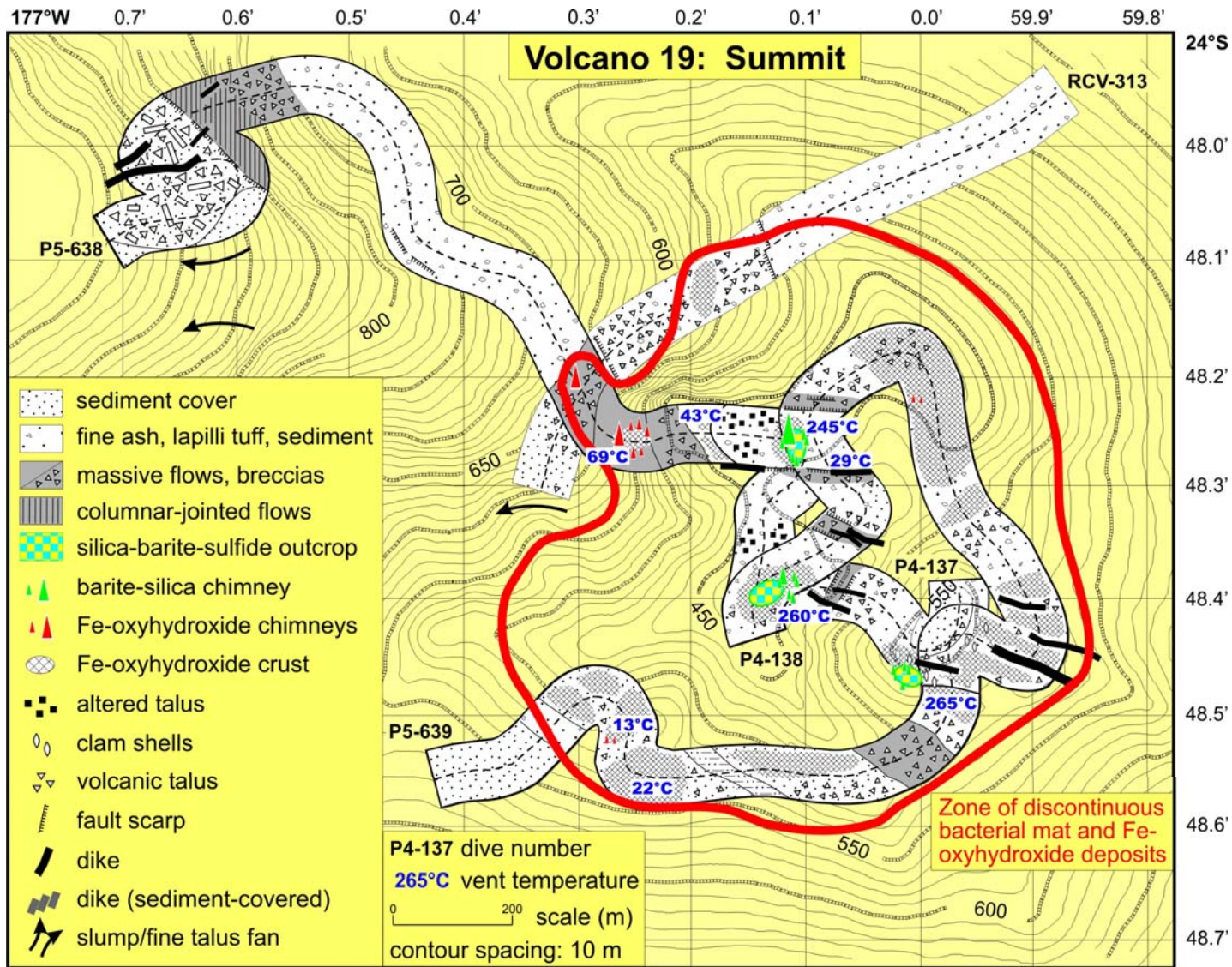


Fig. 6.1: Map of the active hydrothermal field at the summit of Volcano 19.

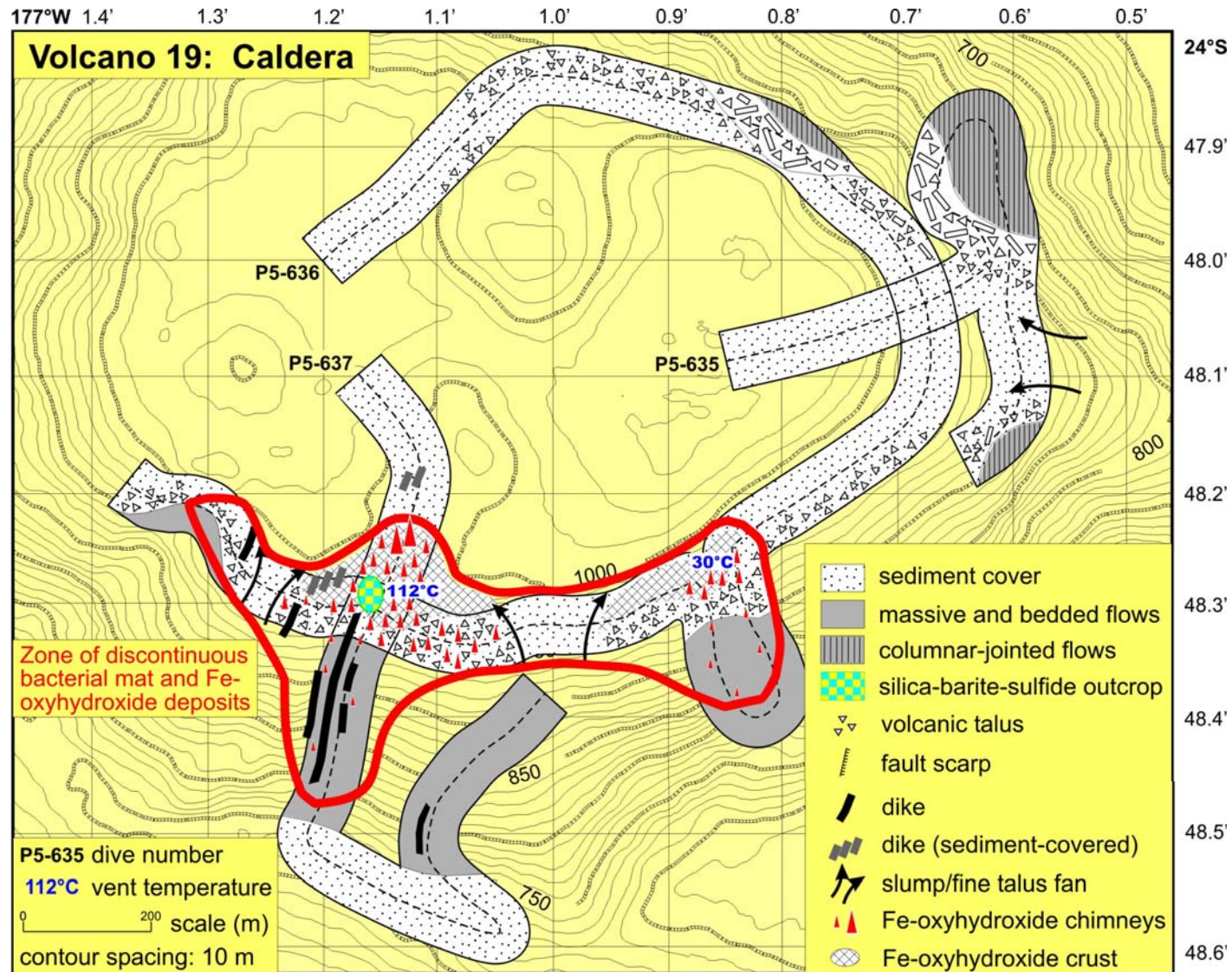


Fig. 6.2: Map of the active hydrothermal field in the western caldera of Volcano 19.

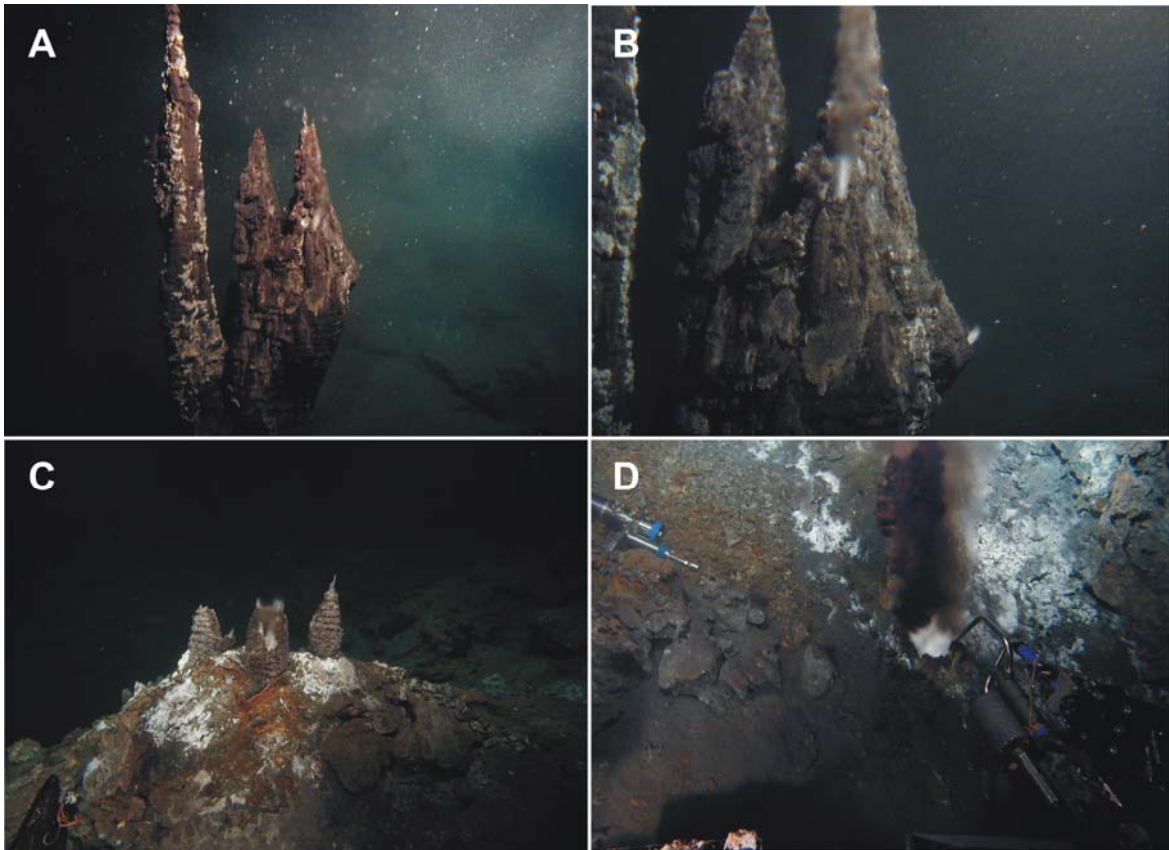


Fig. 6.3: Two-phase venting at 265 °C in a pit crater at the summit of Volcano 19 (540 mbsl) -
A+B) 2 m-high anhydrite spires venting clear and phase-separated fluids from several orifices. Steam jets probably consist of H₂O and dissolve into the seawater shortly after venting, as can be seen from streams of shimmering water.
C) The same chimney complex, which was demolished for fluid sampling. Returning after ~24 hours, three new chimney structures with vigorous two-phase venting had grown about 30 cm high.
D) Black metalliferous smoke venting after removal of the chimney.

sphalerite–wurtzite. The predominance of wurtzite over sphalerite is likely related to elevated formation temperatures. There is microscopic evidence that the wurtzite contains rather low Fe contents, indicating a high-sulfidation state for the sulfide mineralization.

Pyrite occurs mainly as collomorphic aggregates and less often as euhedral crystals. Pyrite overgrowths on wurtzite indicate a later crystallization from the mineralizing fluid. Galena forms a wide variety of crystal shapes, including euhedral cubes, elongated grains, rosette-like crystals and platy aggregates. Galena is always intergrown with wurtzite and anhydrite. Chalcopyrite is less abundant and is closely associated with the more fine-grained, pyrite-rich, parts of the chimneys. Where it occurs, it is much more coarse-grained than the pyrite and often euhedral in shape. Marcasite is always intergrown with pyrite and anhydrite, forming inclusions as well as rims around larger aggregates. From the existing thin sections, there is no evidence for the occurrence of visible gold or other sulfide minerals.

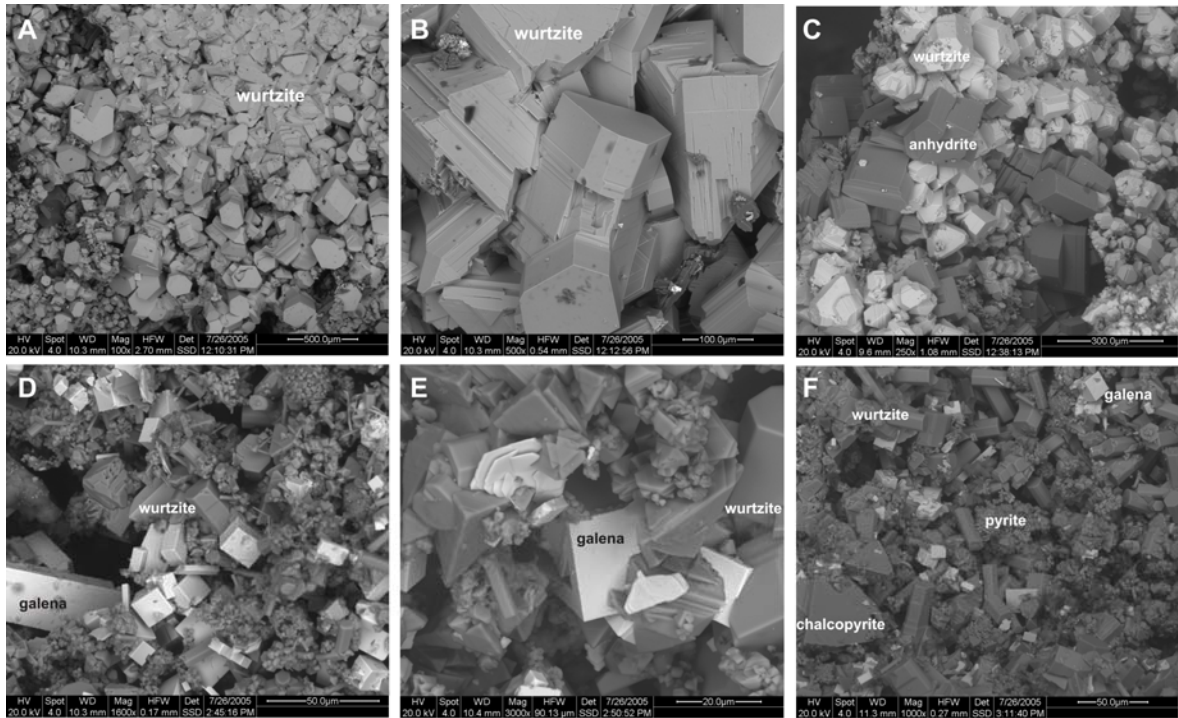


Fig. 6.4: Sulfide mineralization from a two-phase venting (265 °C) chimney -

- A) Predominantly wurtzite mineralization in a matrix of anhydrite.
- B) Close-up of coarse-grained, euhedral wurtzite crystals showing their characteristic hexagonal shape.
- C) Close intergrowth of hexagonal wurtzite and anhydrite.
- D) Intergrowth of euhedral wurtzite and galena, overgrown by collomorphic pyrite.
- E) Close-up of a wurtzite–galena intergrowth. Galena forms euhedral cubes as well as rosette-like crystals.
- F) Fine-grained intergrowth of euhedral wurtzite, chalcopyrite and galena, associated with collomorphic pyrite.

The outer rim of the chimneys generally consists of a dense intergrowth and porous network of barite and/or euhedral anhydrite crystals, typically overgrown by a thin crust of marcasite or Fe-oxyhydroxides. The sulfates often form dendritic aggregates up to 1 cm in size, chiefly dominated by laths of anhydrite with barite dendrites and blades in the interstices. The sulfides and sulfates mostly show concentric growth. Their grain size, as well as textural evidence and intergrowths, likely reflect oversaturation in the fluid and precipitation as a consequence of phase separation.

At their base, some chimneys include strongly altered and hydrothermally indurated scoria as well as fragments from former, now collapsed, chimneys (Fig. 6.5). These volcanoclastic sediments show evidence of intense argillic alteration with the formation of illite–kaolinite, other as yet unidentified mixed-layer clay minerals, and beads and needle-like aggregates of amorphous silica. The alteration extends into the volcanoclastic components, but generally decreases towards the interior of single fragments. Fragment cores (up to 1 cm in size) can be largely unaffected and represent weakly-altered, nearly



Fig 6.5: Hydrothermal induration and argillic alteration of volcaniclastic sediment -

Left: Chimney-type channelway through formerly unconsolidated volcaniclastic sediment, indurated by the formation of clay minerals and the precipitation of barite and marcasite-pyrite. The central channel is composed of a dense intergrowth of sphalerite and barite.

Right: Scoriaceous sediment showing intense argillic alteration and induration by amorphous silica, native sulfur, rims of marcasite-pyrite intergrowths and Fe-oxyhydroxides.

pristine, vesicular basalt. However, scoria clasts are rimmed and indurated by pyrite, barite and anhydrite precipitates. There is increasing sulfide mineralization towards the lower surface of the crusts, which may point to enhanced sulfide precipitation at depth. It seems obvious that the boiling process immediately on or below the sea floor results in extensive and widespread mineralization coupled with replacement of the rock/sediment substrate.

6.3 Chimney Geochemistry

The composition of the chimneys is variable due to the heterogeneous mix of sulfide and sulfate precipitation. The base metal sulfides are mainly associated with the inner portions of the chimney edifices, whereas sulfates build up the porous chimney walls. As a consequence, the base and precious metal contents are quite variable but generally grade in composition towards the centre and other fluid channels. Sample P4-137-2 provides an example of this complexity, and is not characterized by a single central channel but rather by a multichannel network through a massive block of sulfate and sulfide precipitates. Different portions of this chimney, including massive sulfide precipitates from the center, massive sulfate from the top (mainly anhydrite), massive sulfate from the base (mainly barite), and samples consisting of various mixes of these components were analyzed for their major and minor element composition in our preliminary study.

Table 6.1: Composition of the P4-137-2 two-phase chimney ^a

<u>Element</u>	<u>Unit</u>	<u>Average</u>	<u>Min.</u>	<u>Max.</u>
SiO ₂	wt.%	0.74	0.24	1.12
CaO	wt.%	23.24	5.60	39.43
Ba	wt.%	5.49	0.03	18.50
Fe	wt.%	2.17	0.19	12.80
Zn	wt.%	6.77	0.58	22.00
Pb	wt.%	1.18	0.05	2.08
Cu	wt.%	0.37	0.05	0.64
Au	ppm	3.9	0.3	12
Ag	ppm	91	7	210
As	ppm	75	6	158
Sb	ppm	40	4	145

^a Analyses by standard XRF and INAA techniques, $n = 10$.

The chimney is characterized by significant zinc (to 22.0 wt.% Zn, average 6.77 wt.% Zn) and iron (to 12.8 wt.% Fe, average 2.17 wt.% Fe), with more moderate copper (to 0.64 wt.% Cu, average 0.37 wt.% Cu) and lead (to 2.08 wt.% Pb, average 1.18 wt.% Pb) concentrations (Table 6.1). Notable enrichments exist for the element suite Au–Ag–Sb–As, which is typical of epithermal-style ore deposits. Gold is generally above the detection limit and ranges between 0.3 and 12 ppm (average 3.9 ppm Au), with silver in the range 7 to 210 ppm (average 91 ppm Ag). Arsenic (to 158 ppm, average 75 ppm As) and antimony (to 145 ppm Sb, average 40 ppm Sb) are slightly enriched, but do not attain the high concentrations found in many other shallow-water hydrothermal systems.

Significant concentrations exist for CaO (average 23.24 wt.% CaO) and Ba (average 5.49 wt.% Ba), reflecting the presence of anhydrite and less frequent barite in the chimney. Low silica contents are a consequence of amorphous silica precipitation in the porous chimney walls.

6.4 Conclusions

The preliminary results from the recovered venting chimneys attest to precipitation processes influenced by phase separation processes. Two-phase venting from the orifices was observed prior to sampling. The temperature of the hydrothermal fluid was measured as 265 °C. It is suggested that the fluid evolved along the two-phase stability boundary of seawater during its ascent to the ocean floor. A certain proportion of the possible primary copper content may be lost during the ascent and precipitated close to the ocean floor. However, the saturation point for the formation and co-precipitation of wurtzite, pyrite, chalcopyrite and galena was reached within the chimneys. In consequence, the majority of the metals were precipitated within the chimney edifices and the sulfide mounds

immediately underneath. Precipitation due to fluid saturation likely occurred as a consequence of boiling and phase separation from the hydrothermal fluids. Oversaturation with respect to zinc and calcium sulphate is suggested by the very coarse-grained crystals of hexagonal wurtzite and anhydrite. The highest gold contents are associated with the highest zinc values, and there is some evidence for co-precipitation. However, gold has the capacity for enhanced solubility following the boiling process. The presence of elevated (HS)⁻ ligands may result in the complexation of gold and its transportation at lower fluid temperatures. The ongoing analyses focus on the mineralogical and geochemical distribution of gold and on the element and isotope fractionation generated as a consequence of fluid boiling.

Our findings indicate that active subduction systems, such as the south Tonga volcanic arc, represent a favorable tectonic setting for the generation of shallow seawater epithermal-style deposits. The style of magmatism and associated hydrothermal activity at the arc volcanoes suggests mobilization and enrichment of volatiles at the interface between the subducting slab and overlying mantle wedge, and their subsequent recycling into the crust via arc magmas. In such systems, partial melting at elevated oxygen fugacities and the enrichment in fluid-mobile elements lead potentially to elevated contents of chalcophile elements in the arc magmas and, thereby, the associated hydrothermal fluids and precipitates. The south Tonga arc also features subduction of the intensely altered aseismic Louisville Ridge (a hotspot chain), which may play a key role in enhancing mass transfer and the oxygen fugacity of the sub-arc melting zone. To date, our sampling of the south Tonga arc indicates a high potential for Au and Cu–Zn–Pb mineralization.

7 VENT FLUID ANALYSES

7.1 Sampling and *In Situ* Analyses

Vent fluids (mixtures of liquids and gases) moderate and are moderated by the geological substrate and organisms (macro- and micro-) that border their seafloor pathways. Observations of the physico-chemical state of vent fluids provide important clues about processes occurring within the sub-seafloor and at its ocean interface where prolific communities of macro- and micro-organisms derive life and mineral assemblages derive form from these same fluids. In the complex subduction setting, where the subducted slab, overlying sediments, and mantle wedge may variably contribute to fluid flux, resolution of fluid provenance by geochemical inference based on composition is critical to understanding elemental cycling. The character and magnitude of fluid flux from submarine arcs remains poorly constrained, even though intra-oceanic arcs border much of the convergent edge of the Pacific Plate where fluid discharge may be of global significance. Thus, the collection and study of vent fluids during these "early days" of submarine arc exploration carries the promise of exciting and important new insights that justify the significant effort required to sample fluids *in situ* and determine their various components at sea and ashore.

During the SITKAP expedition a total of 27 vent fluid samples were collected (Table 7.1). Of these, 13 were liquid-phase samples for determination of aqueous ionic chemical species abundances and isotopic fractions, and 14 were gas-phase samples for determination of gaseous components and isotopic signatures. Liquid samples were collected *in situ* using 750 ml titanium piston syringes (Major Samplers, designated as MS on sample lists). Gas-phase samples were collected in 150 mL gas-tight bottles (Lupton bottles, designated as GT on sample lists). Both Major and Gas-Tight Samplers were equipped with intake snorkels, which were placed directly into the sample flow stream using the submersible's manipulator arm. Particular effort was expended to capture phase separated gas bubble emissions discharging at the summits of Volcanoes 1 and 19. Fluid temperatures were determined immediately prior to discrete sample collections by Major and Gas-Tight samplers.

Onboard determinations included pH, alkalinity, hydrogen sulphide, silica and total gas concentration. Hydrogen sulphide and silica were determined colorimetrically in batch mode using the methylene blue (nominal precision: 4%) and silicomolybdate (nominal precision: 1%) methods, respectively. Aliquots used for determinations of hydrogen sulphide were fixed within minutes of sampler opening and sub-samples for Si were diluted to preclude polymerization-induced artifacts. Potentiometry was used to assess pH (nominal precision: 0.3%) at room temperature relative to NBS buffers and to measure

Table 7.1: Water and Gas Samples (*In Situ* and Shipboard Measurements)

A: Water (Major) Samples

Location	Dive	Sample	Longitude °W	Latitude °S	Depth mbsl	pH	Temp. °C	Alk meq	S ‰	H ₂ S mmol	Si mmol
Volc 19	P5-637	MS-blue	177°01.145'	24°48.297'	985	5.84	31.3	2.65	36	21.6	707
		MS-white	177°01.145'	24°48.297'	984	5.4	112.9	2.36	36.5	35.9	2140
Volc 19	P5-638	MS-yellow	177°00.108'	24°48.250'	385	5.41	245	1.47	35	920	1576
		MS-blue	177°00.108'	24°48.250'	385	4.98	245	1.87	33.5	2900	1897
		MS-white	177°00.262'	24°48.262'	504	5.8	79.2	2.91	34.5	10.8	1509
Volc 19	P4-137	MS-blue	176°59.952'	24°48.488'	542	5.65	boiling	1	36	1416	4435
		MS-yellow	176°59.952'	24°48.488'	542	6.12	boiling	1.68	35.5	744	1840
Volc 19	P4-138	MS-white	177°00.114'	24°48.251'	393	5.55	113	1.44	37.5	575	4718
		MS-blue	177°00.167'	24°48.389'	433	4.65	boiling	0.11	44.5	850	8764
Volc 1	P4-141	MS-yellow	175°44.662'	21°09.201'	195	5.12	50?	3.29	34.7	3000	3500
		MS-white	175°44.702'	21°09.270'	199	5.37	68?	-	35.5	1480	1390
Volc 1	P4-142	MS-yellow	175°44.676'	21°09.292'	197	3.17	152	-1.21	29.5	1245	5550
		MS-blue	175°44.676'	21°09.292'	197	5.76	152	1.56	35	274	5530

B: Gas Samples ^a

Location	Dive	Sample	Longitude °W	Latitude °S	Depth mbsl	Total gas mmol/kg	Gas vol. ml	Gas press. torr	Gas vol. ml	Gas press. torr	Gas vol. ml	Gas press. torr
Volc 19	P5-637	GT-6-blue	177°01.145'	24°48.297'	985	9.1	3	310.6	35	177.5		
		GT-12-yellow	177°01.145'	24°48.297'	984	8.5	3	192.4	35	187.9		
Volc 19	P5-638	GT-10-red	177°00.108'	24°48.250'	385	15	3	533.5	35	321.5		
		GT-2-green	177°00.262'	24°48.262'	504	3.1	3	113.6	35	63.6		
Seawater		GT-12-yellow	176°55'	24°35'	0	2.7	3	102.8	35	57.5		
Volc 19	P4-137	GT-10-red	176°59.952'	24°48.488'	542	13.0	3	215.9	35	210.9		
		GT-12-yellow	176°59.952'	24°48.488'	542	4.2	3	159.4	35	90.3		
Volc 19	P4-138	GT-6-blue	177°00.114'	24°48.251'	385	5.01	3	194.3	35	109.4		
		GT-2-green	177°00.167'	24°48.389'	433	8.92	3	282.3	35	166.4		
Volc 1	P4-141	GT-10-red	175°44.702'	21°09.270'	199	137	3	710.5	35	710.7	35	636.2
		GT-12-yellow	175°44.662'	21°09.201'	196	120	3	683.3	35	718.1		
		bubble scoop	175°44.702'	21°09.270'	199	n.a.	3	259.3	35	283	50	760
Volc 1	P4-142						3	242.9	35	301.5		
		GT-2-green	175°44.676'	21°09.292'	197	5.3	3	110.5	35	130.3		
		bubble scoop	175°44.676'	21°09.292'	197	n.a.	3	251.3	35	292.2		
								3	245.3	35	285.7	
		GT-6-blue	175°44.706'	21°09.252'	200	5.9	3	131.4	35	154.7		

C: Notes on Gas Sampling Locations

Dive	Sample	Notes
P5-637	GT-6-blue	Top of smoker in venting fluid at 31 °C
	GT-12-yellow	Base of smoker in venting fluid at 112 °C
P5-638	GT-10-red	10 cm hole at base of a 14 m-high smoker, 245 °C
	GT-2-green	Small crack at base of smoker mound, 69.3 °C
P4-137	GT-10-red	Base of smoker with boiling, ~270 °C
	GT-12-yellow	
P4-138	GT-6-blue	Large chimney, 113 °C
	GT-2-green	Black smoker with boiling
P4-141	GT-10-red	Bubbles in the vent and mussel field, 68 °C
	GT-12-yellow	Vent field but no bubbles, ~50 °C
P4-142	Bubble scoop	Bubbles in the vent and mussel field, 68 °C
	GT-2-green	"Mussel bowl", strong flow with some bubbles, 152 °C
	Bubble scoop	"Mussel bowl", strong flow with some bubbles, 152 °C
	GT-6-blue	Bubble site, 51 °C

^a The extra "Gas vol." and "Gas press." columns give details for multiple gas samples collected from each sample site.

alkalinity (nominal precision: 0.5%) by the Gran method. Total gas concentrations were determined using manometric and gravimetric procedures (nominal precision: 2%).

7.2 Post-Cruise Fluid Analyses

Sample splits were separated and selectively preserved at sea for shore-based determinations of major and trace dissolved ionic species abundances (Li, B, NO₃⁻+NO₂⁻, NH₃, Mg, Al, SO₄²⁻, Si, PO₄³⁻, Cl, K, Ca, Mn, Fe, Cu, Zn, Se, Br, Rb, Sr, Mo, Ag, Te, I, Cs, Ba, Hg, Pb, Bi, and U, etc.). These ongoing determinations are being conducted under the direction of David Butterfield at NOAA/PMEL and the University of Washington in Seattle, Washington, USA. Methodologies include high-precision titrations, color spectrophotometry, ion chromatography, flame and graphite furnace atomic absorption (+ hydride generation in some cases), ICP-MS, and ICP-OES. The liquid fractions of selected Gas-Tight samples are also being analysed for elemental composition.

Shore-based determinations of gas abundances are being overseen by John Lupton (He and other noble gases) at NOAA/PMEL in Newport, Oregon, USA, and by Mark Schmidt (CO₂, H₂, N₂, H₂S, CH₄, and other C-species) at the Institut für Geowissenschaften, Kiel University, in Kiel, Germany. A full inventory of archived gas samples resides with John Lupton in Newport.

Isotopic determinations of $\delta^{34}\text{S}$, $\delta^2\text{H}$, $\delta^{18}\text{O}$, DIC- $\delta^{13}\text{C}$ in liquid phase samples have been completed in New Zealand, coordinated by Gary Massoth of GNS. Lead and Sr isotope determinations will be performed later in the USA by Dave Butterfield. A collaborative agreement with Lui-Heung Chan of Louisiana State University has been established for determination of Li isotopes. Gas phase determinations of He isotopes were determined under the direction of John Lupton in Newport, OR, USA. Isotopic abundances for major gas components will be performed at the University of Kiel pending approval of funding.

Table 7.2: Vent Fluid Analyses

	<u>Volc 1 Summit</u>	<u>Volc 19 Summit</u>	<u>Volc 19 Caldera</u>
<i>In Situ</i>			
MS Number	4	7	2
GT Number	4	8	2
Depth (m)	195-200	385-542	984-985
Temperature (°C)	62-152	79-265	31-113
<i>Shipboard Determinations</i>			
pH _{NBS}	3.2-5.8	4.7-5.8	5.4-5.8
Alkalinity (meq/kg)	-1.2-3.2	0.1-2.6	2.3-2.6
H ₂ S _{LIQUID} (mol/kg)	265-2925	10-2610	20-35
Si (μmol/kg)	590-5180	1415-7535	710-2060
Total Gas (mmol/kg)	5.3-137	3.0-15.3	8.4-8.9
<i>Shore-based Determinations</i>			
Cl (mmol/kg)	515-537	515-699	539
Mg (mmol/kg)	43.7-52.2	2.3-50.9	43.5-48.8
Li (μmol/kg)	27.2-32.1	27.4-473	61.5-138
Na (mmol/kg)	446-462	383-462	454-464
K (mmol/kg)	9.3-10.2	11.7-27.1	13.0-17.4
Ca (mmol/kg)	6.6-12.9	14.4-107	14.0-24.8
Fe (μmol/kg)	1.6-3.8	4.4-210	22-62
Mn (μmol/kg)	15-48	76-1012	17-145
Fe/Mn (mol/mol)	0.07-0.11	0.05-1.6	0.4-1.3
Br (μmol/kg)	860-875	840-1150	1038
SO ₄ (mmol/kg)	27.9-59.4	5.9-23.5	24.9
Rb (μmol/kg)		5.7-10.2	
Cs (μmol/kg)		0.16-0.41	
Ba (μmol/kg)		0.85-3.2	
U (μmol/kg)		6.2-11.6	
Tl (nmol/kg)		1.2-8.2	
Co (nmol/kg)		15-43	
Zn (nmol/kg)		543	
Pb (nmol/kg)		4	
Au (nmol/kg)		249	
δD-H ₂ O (‰)	-0.6 to 3.3	-2.8 to 2.4	-1.1 to -1.7
δ ¹⁸ O-H ₂ O (‰)	0.58 to 0.81	0.06 to 0.95	-0.18 to 0.13
δ ¹³ C-DIC (‰)	7.35 to 9.38	2.95 to 9.15	8.72 to 8.77
δ ³⁴ S (‰)	-4.0 to 4.2	1.1 to 14.4	16.1 to 16.2
³ He (pmol/kg)	0.7-4.4	0.2-5.6	0.5-0.6
⁴ He (nmol/kg)	76-481	20-587	53-63
R/R _a	6.6-6.9	6.9	7.0
Ne (nmol/kg)	2.0-8.9	3.3-13.8	9.4-10.6
CO ₂ (mmol/kg)	3.6-121	5.8	
H ₂ S _{GAS} (μmol/kg)	5400-7810	1650	
N ₂ (μmol/kg)	1640-7810	1470	
CH ₄ (μmol/kg)	0.56-43.3	11.5	
C ₂ H ₆ (μmol/kg)		0.054	

Table 7.2 provides a preliminary listing of the ranges of concentrations determined so far within samples collected from the three primary sampling regions (Volcano 1 summit, Volcano 19 summit, and Volcano 19 caldera). Missing values indicate determinations that are in progress, and therefore the concentration ranges should not be taken as final.

7.3 Conclusions

The preliminary findings of the vent fluid analytical program are summarized below:

- 1) Chemical results support our physical observations of phase separation (sub-critical boiling) of fluids discharging at the summits of Volcanoes 1 and 19. Trends in the concentration of Cl compared to Mg (where "zero Mg" is inferred to represent the pure hydrothermal endmember fluid) suggest a mixing line between seawater and pure water (i.e., a completely separated phase of boiled seawater) at the summit of Volcano 1. At Volcano 19 summit, conjugate phase separated and segregated fluid phases appear to have been sampled, with the Cl-depleted endmember trend having about 400 mmol/kg Cl at zero Mg concentration, and the Cl-enriched endmember being in excess of 700 mmol/kg Cl.
- 2) Clear evidence for high-temperature water-rock reaction is evidenced at Volcano 19 summit by the very high concentrations of Li observed there (projected endmember about 500 $\mu\text{mol/kg}$ compared to ~ 26 $\mu\text{mol/kg}$ of Li in seawater). Endmember dilution trends for other major elements support this contention (e.g., K, Ca and Si).
- 3) The concentration of Ca venting at Volcano 19 summit is the highest so far observed anywhere along the Tonga–Kermadec arc (D. Butterfield and G. Massoth, pers. comm., 2006), and has an estimated endmember concentration (~ 110 mmol/kg). This is matched within other submarine venting systems only where more extreme brine-like fluids discharge. Dissolution of buried calcium carbonate in contact with the sub-seafloor hydrothermal flowpaths is one possible explanation for the high Ca values uniquely observed at Volcano 19.
- 4) Concentrations of Fe (and other metals) are low compared to observations of fluids venting at similar temperatures along MORs, suggesting that sub-seafloor precipitation of metals from parent vent fluids is extensive within the venting systems we have sampled along the Tonga arc. Observed Fe/Mn values are commonly an order-of-magnitude lower than experienced at most MOR venting sites.
- 5) Extremely high concentrations of gases, predominantly as CO_2 , discharge from the summit of Volcano 1. The $\text{CO}_2/{}^3\text{He}$ ratio (as high as $\sim 30 \times 10^9$) is accordingly high compared to the rather uniform value for this ratio at MORs ($\sim 2 \times 10^9$), consistent with the notion that submarine arcs may be important contributors to the oceanic CO_2 budget.

8 VOLCANO EVOLUTION AND CALDERA DEVELOPMENT

8.1 Caldera Formation

Volcanic calderas can form by a variety of different mechanisms. In subduction settings, the most common origin is by voluminous eruptions ($>10 \text{ km}^3$ of magma) that evacuate much of the underlying magma chamber and thereby lead to collapse of the overlying, now unsupported, edifice. The vast majority of such eruptions feature volatile-rich dacitic or rhyolitic magma, which is deposited as thick sequences of pyroclastic flows and pumiceous ash (e.g., Taupo 186, Krakatau 1886, Pinatubo 1991). Post-caldera activity may involve the extrusion of volatile-poor dacitic–rhyolitic domes, or a change in style to effusive cone-building eruptions of basalt or basaltic andesite (generally inferred to be the parental magma of the dacite–rhyolite). At many arc volcanoes this sequence becomes repetitive, and caldera-forming dacitic eruptions are followed by re-building of a large basaltic andesite stratovolcano, then followed by a further caldera-forming eruption, etc. Krakatau is a good example of this process, with the dacitic 1886 caldera-forming eruption being followed by the re-building of "Anak Krakatau" composed of basaltic andesite, and at least two pre-1886 cycles have been recognized. Calderas can also form by sector collapse with or without an accompanying eruption (St. Helens 1980), by incremental growth during repeated small-scale eruptions (Rumble 2 west), or by large flank eruptions of mafic lava that remove support for the volcanic edifice ($37^\circ 42' \text{S}$ seamount of the Foundation chain, SO-157). Furthermore, large caldera-forming eruptions are not always dacitic or rhyolitic, and can feature volatile-rich basaltic andesite (e.g., Tofua in the central Tonga arc at $\sim 5 \text{ ka}$).

The precipitous inner walls of calderas offer an opportunity to obtain stratigraphically controlled samples from both the pre-caldera sequence and during the caldera-forming eruption itself. On land, these walls are seldom accessible on account of their instability and, particularly for pyroclastic flow sequences, the unconsolidated nature of the beds. Those that are more stable are rapidly overgrown by dense vegetation. These problems are far less severe for submarine calderas. Eight calderas were discovered on the 27 major volcanoes of the south Tonga arc during SO-167. Either by coincidence or due to fracturing induced by caldera formation, all three volcanoes investigated for hydrothermal activity by *PISCES* during the SITKAP cruise feature calderas. The aim of the hard rock program during SITKAP was to map the inner walls of two large calderas (Volcano 1, Volcano 18s) and obtain stratigraphically-controlled samples. These two calderas differ fundamentally; that at Volcano 1 is "normal" in form, whereas the Volcano 18s caldera is exceptionally deep ($>1 \text{ km}$) and funnel-shaped, resembling a diatrema. We seek to address the question of how these calderas formed and to examine changes in magma composition,

especially with regard to volatile elements, before, during and after the caldera-forming eruption(s).

8.2 Volcano 1: Progressive Volcano Growth and a Sector Collapse

Volcano 1 has a basal diameter of ~28 km, reducing to ~18 km at the summit caldera, and rises from 1800 mbsl to the highest point on the caldera rim at 150 mbsl. The summit consists of a large oval caldera, 7 km-long by 4.5 km-wide, whose long axis trends NW–SE (Fig. 2.2). Most of the caldera rim is between 150 mbsl and 250 mbsl, although a large segment of the western rim has collapsed to the SW. A series of young, post-caldera, scoria cones and explosion craters have developed along the western side of the caldera. These generate a NE-dipping slope from the summit of the cones at ~100 mbsl down to the moat beneath the caldera walls at ~450 mbsl. Hydrothermal venting within the caldera is focussed on two explosion craters and the northern flank of the SW post-caldera scoria cone in the western part of the caldera. Outcrops in that region are exclusively of andesitic scoria, and no lava flows were observed. The main hard rock target for the *PISCES* dives was the 250 m-high inner NE caldera wall, where it was anticipated that a stacked succession of pre-caldera lavas together with a section through the caldera-forming pyroclastic flow sequence would be exposed.

Dive P4-143 encountered a complex stratigraphic sequence (Fig. 8.2). The lowermost part of the caldera wall (430–460 mbsl) and much of the middle section (375–415 mbsl) is dominated by massive pillow andesite flows, commonly 5–10 m-thick. The pillows attain "giant" size, ~3 m in diameter, probably reflecting the relatively silicic (viscous) composition of the lava (in comparison to pillow basalt elsewhere) and possibly also a rapid extrusion rate. In contrast, volcanoclastic sediments are widespread throughout the lower central and upper central parts of the wall (405–440 mbsl and <350–360 mbsl). These sediments also occur between some of the pillow flows. Numerous 1–3 m-wide subvertical dykes intrude both the pillow flows and the volcanoclastic sediments. The upper part of the caldera wall (150–350 mbsl) is mostly covered by talus, but small outcrops of volcanoclastic sediment are also present.

Contrary to expectations, the volcanoclastic sediments do not represent a simple pyroclastic flow sequence that can be linked to a caldera-forming event. Instead, the predominant sediment-type consists of finely bedded (10–20 cm-thick) white fine ash and clay beds alternating with darker coarse ash beds (e.g., Fig. 8.2B). These successions are interpreted as periods of quiescent background sedimentation (fine ash and clay) punctuated by small-scale eruptions of coarse ash-lapilli. Less commonly, the sequence is broken by 0.5–2.0 m-thick beds comprising angular lithic blocks of various lithologies (fresh andesite, altered andesite, scoria, plutonic blocks) set in a coarse ash-lapilli matrix

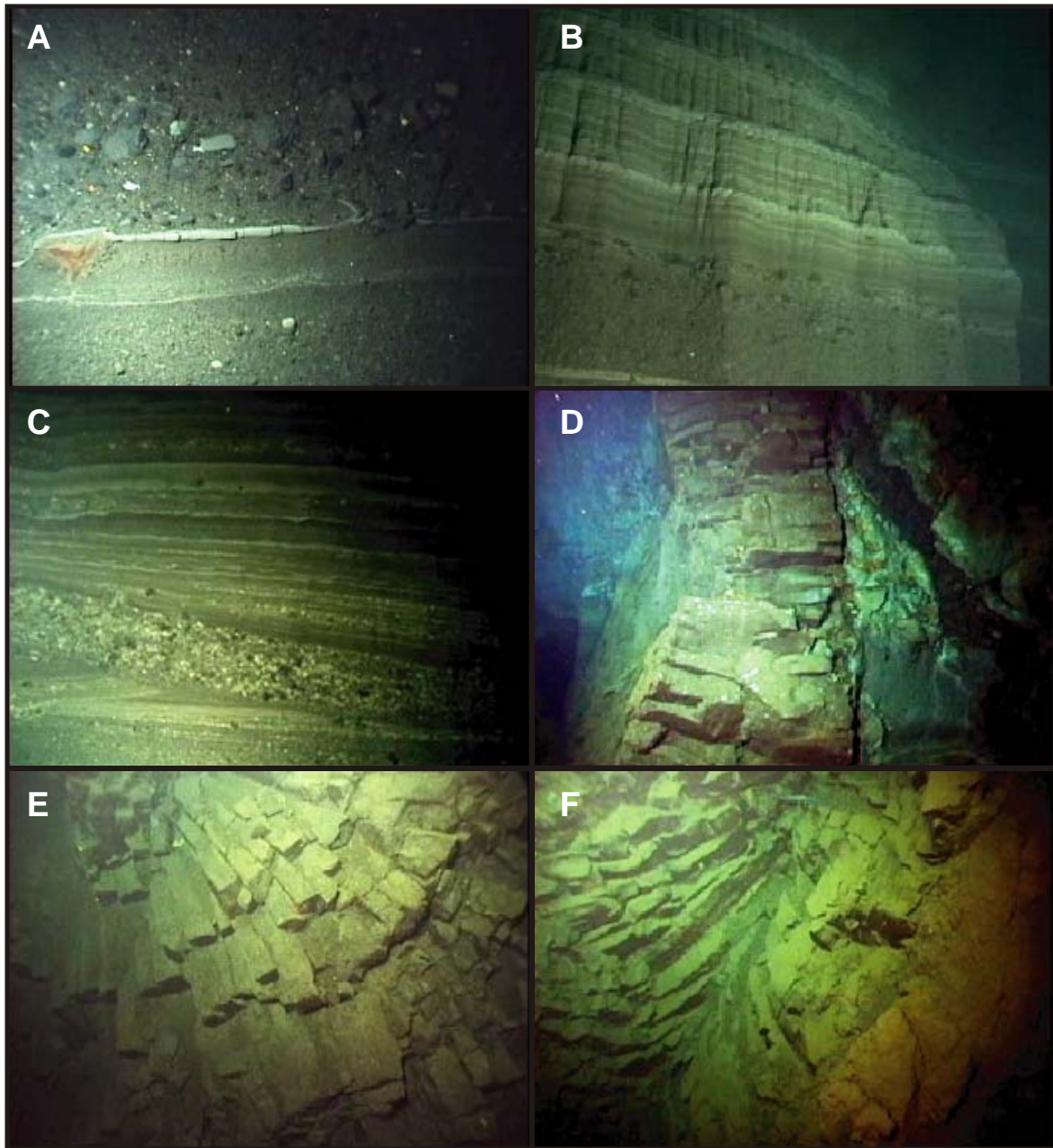


Fig. 8.1: Key stratigraphic observations from the Volcano 1 caldera -

- A) Volcaniclastic sediments separated by fine ash beds. The uppermost unit consists of angular lithics of various lithologies and ash with reverse grading, consistent with fall-out from a nearby phreato-magmatic eruption.
- B) Well-bedded fine ash layers overlying a coarser ash-lapilli unit. Note reverse grading in the coarse ash-lapilli bed, implying it represents fall.-out from a nearby eruption. In contrast, the overlying ash is inferred to represent quiescent sedimentation punctuated by small or distal eruptions.
- C) Volcaniclastic sediments ranging from fine ash to lapilli. Angular unconformities separate some of the lower beds. The polymict and unbedded to normal-graded coarser beds are interpreted as debris flows from the unstable caldera walls.
- D) 2 m-wide sub-vertical dyke intruding gravels and volcaniclastic sediment.
- E) Cross-section through a giant pillow andesite (pillow is 3 m in diameter).
- F) Cross-section through a pillow grading to massive andesite.

and commonly exhibiting reverse grading. These beds are interpreted to represent more violent, larger, explosive eruptions (Fig. 8.2A, 8.2B). The sediment sequence also contains beds ranging from a few cm to ~1 m-thick and composed of both lapilli-sized lava fragments of various lithologies together with a subequal proportion of coral and sedimentary fragments. These beds often have erosional basal contacts (angular unconformities) and lack any significant internal stratification. We interpret them as debris flows generated by collapse of the unstable shallower volcano flanks (Fig. 8.2C).

Overall, the picture revealed by the caldera wall stratigraphy is that of an andesitic stratocone growing by numerous repeated small eruptions of scoria, occasional outpourings of pillow lavas, and undergoing minor episodes of erosion or small-scale localized collapses. A very high number of eruptions is indicated by the numerous coarse ash beds and also by the number of dykes. These imply a short interval (decades?) between eruptions. Our observations are also consistent with the most recently active vents in the western part of the caldera, where there are at least two major scoria cones and several chains of explosion craters. Clearly the normal mode of behaviour for Volcano 1 features repeated small eruptions, occasional moderate eruptions building scoria cones, and rare outpourings of massive lava. No evidence of a major pyroclastic flow sequence was found.

How, then did the caldera form? An important clue to this puzzle is the absence of the western caldera wall and the unusual "hummocky" topography on the lower west to SW flank of Volcano 1. Hummocky terrain in subaerial settings, consisting of numerous hills up to 30 m-high and several hundred metres in length and restricted to one quadrant of a volcano's base, are usually the product of debris avalanches generated by major sector collapses of the upper volcano flanks (e.g., St Helens, Shasta, Egmont). Although it has not been dredged, we suspect that the unusual hummocky terrain to the west of Volcano 1, which contrasts with the smooth lower flanks of all other quadrants, formed in the same manner. The mid to upper western flank of Volcano 1 is a valley bounded by 100–200 m-high ENE-trending walls and contains a central buttress with margins that parallel the valley walls. This is indicative of collapse controlled by either faulting or subparallel dyke swarms.

Although the sector collapse could have occurred after caldera formation as an unrelated event, we consider the striking absence of any major pyroclastic flow series in the northern caldera wall to be strong evidence that no such voluminous pyroclastic eruption ever occurred. The missing caldera volume exceeds 10 km^3 and, allowing for a realistic conical summit above the caldera walls and for significant infill of the caldera, is more likely in the range $20\text{--}40 \text{ km}^3$. An eruption of this magnitude should deposit a pyroclastic flow sequence >50 m-thick near and within the caldera. Thus, the more probable scenario is that caldera formation accompanied major sector collapse and was not due to a voluminous eruption. This event would have some similarities with the 1980 eruption of St Helens, but with a much smaller eruption (if any) accompanying the collapse. It is notable that the 1980 St Helens caldera is comparable in size and form to that of Volcano 1. The sector

collapse model is consistent with: (i) the absence of major pyroclastic deposits on and in the caldera walls, (ii) the presence of hummocky terrain on the lowermost western flank of Volcano 1, and (iii) requires no change in the behaviour of Volcano 1 from that seen in the caldera walls, which indicates numerous small-scale explosive eruptions building scoria cones and intermittent outpourings of pillow andesite.

8.3 Mineralogy and Geochemistry

Major caldera-forming eruptions generally feature dacitic to rhyolitic magma. To further investigate whether any such magmas have been erupted at Volcano 1, or any evidence of an evolution towards such compositions with time, we undertook a reconnaissance petrographic and geochemical study of stratigraphically controlled lavas sampled from the inner north caldera wall.

In keeping with previously dredged lavas from the outer flanks and young scoria cones of Volcano 1 (SO-167), all lavas collected during the *PISCES* dive on the inner NE caldera wall were porphyritic with phenocrysts of zoned plagioclase and pyroxene (Table 8.1). Close examination reveals a strong tendency for the lavas to contain plagioclase–pyroxene aggregates, and many of the apparently discrete phenocrysts were probably disaggregated from such clusters. The plagioclase phenocrysts have calcic compositions (An_{79-91}) and their internal zoning is oscillatory, with an overall normal trend that seldom exceeds 4 mol.% An (Table 8.2). Groundmass plagioclase laths have compositions that range from that of the plagioclase phenocrysts to markedly more sodic compositions, attaining An_{47} in one lava. Pyroxene phenocrysts are present in most lavas and are predominantly augites that plot near the augite–diopside join in the pyroxene quadrilateral. However, orthopyroxene phenocrysts occur in several lavas. Groundmass pyroxene granules are invariably pigeonite.

Previously dredged lavas from the outer flanks of Volcano 1 and the young scoria cones in the caldera ranged from basalt to dacite (52.1–69.4 wt.% SiO_2), with the majority straddling the basaltic andesite–andesite boundary (56–58 wt.% SiO_2). Those collected by the *PISCES* dives have comparable compositions (55.4–60.4 wt.% SiO_2 , with one talus block reporting a more silicic character 62.5 wt.% SiO_2 (Tables 8.3, 8.4). Glass analyses from lava R7 show a more silicic composition than the whole rock (60.4 wt.% SiO_2 relative to 56.6 wt.% SiO_2), reflecting dilution of the relatively silicic magma by comparatively low- SiO_2 phenocrysts. When placed in stratigraphic sequence, the lavas do not display any trend towards more silicic compositions with time. Overall, the Volcano 1 lavas are typical of other south Tonga arc lavas and can be classified as part of a low-K tholeiitic sequence exhibiting strong large ion lithophile element (e.g., Rb, Sr, Ba) enrichment and high field strength element (e.g., Nb, Ta, Zr, Hf) depletion.

Table 8.1: Petrography of Volcano 1 Lavas

Sample	Description
P4-143-R1-1	Porphyric; 2 generations of plag and minor cpx phenocrysts set in a groundmass of acicular plag, cpx and a nearly opaque devitrified matrix.
P4-143-R1-2	Porphyric; 2 generations of plag and cpx phenocrysts (first is glomeroporphyritic plag-cpx aggregates), plag weakly flow aligned. Groundmass is opaque.
P4-143-R1-3	Porphyric; 2 generations of zoned plag and cpx phenocrysts (first is glomeroporphyritic plag-cpx aggregates), both cpx and plag are weakly flow aligned. A few small vesicles in the opaque groundmass.
P4-143-R1-4	Porphyric; phenocrysts are zoned plag with many glass inclusions, cpx and magnetite (the latter equal in size to the plag and cpx phenocrysts). Groundmass is devitrified with small acicular plag and cpx granules.
P4-143-R1-5	Porphyric; 2 generations of plag and cpx phenocrysts (first is glomeroporphyritic plag-cpx aggregates). Groundmass is cpx and minor small plag crystals set in a devitrified and moderately vesicular matrix. Includes a small xenolith of highly phyric lava.
P4-143-R1-6	Highly phyric; 2 generations of cpx (commonly with glass inclusions) and a few plag phenocrysts (first is glomeroporphyritic plag-cpx aggregates). Groundmass consists of plag, cpx, magnetite, quartz and abundant pyrite in a vesicular devitrified matrix. The abundant pyrite may be due to alteration or possibly primary.
P4-143-R2	Porphyric; 2 generations of zoned plag and cpx phenocrysts (first is glomeroporphyritic plag-cpx aggregates). Well crystallized groundmass consisting of plag, cpx, magnetite and a low relief late phase (quartz or K-feldspar?).
P4-143-R6	Glomeroporphyritic, with zoned plag (inclusion-rich) and cpx phenocrysts. Groundmass is devitrified and vesicular, nearly opaque with a few small cpx granules.
P4-143-R7	Glomeroporphyritic, with zoned plag and cpx phenocrysts (both with glass inclusions). Groundmass is very glassy and vesicular with plag and cpx.
P4-143-R9	Porphyric; 2 generations of zoned plag and cpx phenocrysts (first of glomeroporphyritic plag-cpx aggregates). Groundmass includes plag and cpx set in a weakly vesicular devitrified matrix.
P4-143-R15	Weakly porphyritic; flow aligned plag and cpx phenocrysts (often forming glomeroporphyritic aggregates) are separated by thin dark weakly vesicular devitrified bands imparting a layered structure to the lava. Some bands curve and bend.
P4-143-R16	Gabbro-diorite. A coarsely crystalline plutonic rock consisting of plag, cpx, amphibole, biotite and magnetite. Late-stage fluids have led to replacement of the cpx by amphibole, and the development of biotite when in contact with magnetite.
P4-143-R17	Glomeroporphyritic; with zoned plag and cpx phenocrysts. Groundmass is abundant cpx and minor plag set in an opaque devitrified and highly vesicular matrix.

Table 8.2: Mineralogy of Volcano 1 Lavas

Lava	Plagioclase			Pyroxene		
	Pheno.	µpheno.	Gmass	Phenocryst	Microphenocryst	Groundmass
R1-1	An ₇₉₋₈₆		An ₈₁₋₈₅	En ₆₅₋₆₇ Fs ₂₁₋₂₃ Wo ₄₋₅	En ₄₂₋₄₆ Fs ₁₃₋₁₅ Wo ₃₄₋₃₇	En ₂₁₋₄₆ Fs ₂₀₋₃₃ Wo ₁₉₋₃₂
R1-2	An ₈₆₋₉₀		An ₅₄₋₈₉	En ₄₆₋₄₈ Fs ₉₋₁₁ Wo ₃₅₋₃₉	En ₄₆₋₄₇ Fs ₁₀₋₁₂ Wo ₃₄₋₃₈	En ₄₅₋₆₃ Fs ₁₆₋₁₈ Wo ₁₃₋₃₁
R1-3	An ₈₄₋₉₀		An ₆₇₋₇₀	En ₄₄₋₄₈ Fs ₉₋₁₂ Wo ₃₅₋₃₉		En ₄₈₋₆₁ Fs ₁₆₋₁₉ Wo ₁₃₋₂₂
R1-4	An ₇₉₋₈₄		An ₆₂₋₆₆	En ₃₇₋₄₀ Fs ₁₆₋₂₁ Wo ₃₂₋₃₉		En ₃₉₋₅₈ Fs ₂₆₋₃₃ Wo ₄₋₂₂
R1-5	An ₈₃₋₉₁	An ₈₉₋₉₀	An ₆₉₋₇₁	En ₄₇₋₇₁ Fs ₁₀₋₁₉ Wo ₄₋₃₆	En ₄₇₋₇₁ Fs ₁₁₋₁₉ Wo ₄₋₃₅	En ₄₃₋₄₇ Fs ₁₅₋₁₉ Wo ₂₇₋₃₄
R1-6	An ₈₆₋₉₀		An ₇₀₋₈₆	En ₄₃₋₄₆ Fs ₁₂₋₁₃ Wo ₃₅₋₃₈		En ₃₇₋₄₆ Fs ₂₄₋₂₆ Wo ₂₁₋₂₉
R2	An ₈₆₋₉₀		An ₇₁₋₇₇			En ₄₂₋₅₂ Fs ₁₅₋₂₃ Wo ₂₀₋₃₂
R6	An ₈₆	An ₈₅₋₈₈		En ₄₁₋₄₂ Fs ₁₄₋₁₅ Wo ₃₇₋₃₈	En ₄₂₋₄₃ Fs ₁₅₋₁₆ Wo ₃₅₋₃₆	
R7	An ₈₃₋₈₉		An ₆₆₋₈₈	En ₅₈₋₆₆ Fs ₂₀₋₂₂ Wo ₄₋₅		En ₄₈₋₆₁ Fs ₂₁₋₂₇ Wo ₇₋₂₃
R9	An ₈₅₋₉₃	An ₈₂₋₈₇	An ₆₄₋₈₄	En ₆₆₋₆₈ Fs ₂₀₋₂₂ Wo ₄₋₅		En ₄₀₋₅₉ Fs ₁₆₋₂₃ Wo ₉₋₃₁
R15			An ₄₇₋₆₆			En ₃₃₋₅₂ Fs ₂₆₋₃₂ Wo ₉₋₂₇
R17	An ₈₁₋₈₈		An ₇₃₋₈₆	En ₄₆₋₇₁ Fs ₁₁₋₁₈ Wo ₄₋₃₇		En ₄₆₋₅₇ Fs ₁₁₋₂₀ Wo ₁₄₋₃₆

All analyses by electron microprobe at the Institut für Geowissenschaften, Universität Kiel. The table summarizes the range in plagioclase (anorthite) and pyroxene (enstatite, ferrosilite, wollastonite) compositions found in each lava for phenocrysts, microphenocrysts, and groundmass minerals.

Table 8.3: Glass Analyses of Lava P4-143-R7

Analysis Location	43 rim	44 rim	45 rim	58 interior	59 interior	60 interior	61 vesicle	62 vesicle	63 vesicle	Average	Std Dev
SiO ₂	59.07	58.87	59.31	60.58	61.14	61.27	61.13	60.90	61.12	60.38	0.94
TiO ₂	0.96	1.05	0.98	1.04	1.05	1.10	1.03	1.17	1.08	1.05	0.06
Al ₂ O ₃	12.92	12.69	12.78	12.52	12.33	12.41	12.18	11.99	11.79	12.40	0.35
Cr ₂ O ₃	0.00	0.00	0.00	0.00	0.00	0.00	0.00	0.00	0.00	0.00	0.00
FeO	11.61	11.34	11.74	10.60	10.30	10.59	10.78	10.46	10.96	10.93	0.49
MnO	0.24	0.28	0.24	0.18	0.20	0.21	0.28	0.14	0.22	0.22	0.04
MgO	2.61	2.78	2.80	2.81	2.66	2.75	2.55	2.51	2.52	2.67	0.11
CaO	8.51	8.32	8.41	7.93	7.70	7.65	7.72	7.68	7.61	7.95	0.34
Na ₂ O	2.04	2.01	2.08	2.08	2.16	2.19	2.10	2.13	2.12	2.10	0.05
K ₂ O	0.63	0.60	0.64	0.71	0.74	0.70	0.70	0.71	0.73	0.68	0.04
P ₂ O ₅	0.29	0.14	0.29	0.22	0.27	0.24	0.22	0.21	0.24	0.24	0.04
SO ₃	0.09	0.07	0.07	0.04	0.02	0.02	0.01	0.02	0.01	0.04	0.03
BaO	0.00	0.00	0.00	0.00	0.00	0.00	0.00	0.00	0.00	0.00	0.00
Cl	0.12	0.11	0.10	0.10	0.10	0.10	0.10	0.10	0.10	0.10	0.01
Total	99.10	98.25	99.45	98.81	98.66	99.22	98.81	98.03	98.51	98.76	0.43

Analyses are reported in wt.% and were completed by electron microprobe using a defocussed beam at the Institut für Geowissenschaften, Universität Kiel. Location of the analytical point is relative to the lava block, with vesicle meaning adjacent to a vesicle.

In addition to the lavas, an unusual lithic block of gabbro–diorite was recovered from one of the volcanoclastic sediment beds at 421 mbsl interpreted as an erosional debris flow (P4-143-R16). This plutonic block consists of coarse-grained plagioclase (An₇₄₋₉₀), clinopyroxene (En₃₁₋₃₉Fs₁₃₋₂₄Wo₂₂₋₄₃), Ti-magnetite (9 wt.% TiO₂) and ilmenite. Extensive breakdown and replacement of the outer part of most clinopyroxene crystals has occurred, with the development of secondary hornblende and, where in contact with magnetite, significant traces of biotite with 9 wt.% K₂O. Stringers of quartz crystals cross the rock, demarking the former pathways of hot fluids. The block is inferred to be an altered cumulate ejected from the magma chamber as a xenolith during an explosive eruption.

Table 8.4: Geochemistry of Volcano 1 Lavas

Sample	R1-01	R1-02	R1-03	R1-04	R1-05	R1-06	R2	R6	R7	R9	R15	R16	R17
SiO ₂	57.03	56.34	56.22	62.49	56.18	55.36	55.43	58.12	56.63	55.64	59.65	56.54	56.28
TiO ₂	0.63	0.57	0.57	0.81	0.51	0.68	0.52	0.78	0.72	0.57	0.83	0.73	0.62
Al ₂ O ₃	16.48	15.04	14.96	13.69	15.77	15.75	15.58	15.14	15.57	15.30	13.08	14.42	15.58
Fe ₂ O ₃	9.53	10.28	10.20	9.37	9.96	10.00	9.97	10.46	10.30	10.58	12.74	12.46	10.15
MnO	0.14	0.16	0.16	0.16	0.16	0.14	0.16	0.16	0.16	0.17	0.18	0.19	0.15
MgO	3.04	5.12	4.80	2.04	5.06	4.39	5.44	3.02	4.23	4.65	2.77	4.12	4.34
CaO	10.24	10.29	10.17	6.97	11.11	9.69	10.84	9.12	10.15	10.89	7.90	9.01	10.65
Na ₂ O	2.07	1.77	1.83	2.61	1.66	2.02	1.74	2.17	1.84	1.69	2.32	2.08	1.85
K ₂ O	0.52	0.43	0.44	0.69	0.36	0.30	0.35	0.52	0.44	0.37	0.59	0.64	0.48
P ₂ O ₅	0.11	0.09	0.08	0.15	0.08	0.10	0.08	0.11	0.10	0.08	0.13	0.09	0.10
LOI	0.13	0.00	0.31	0.26	0.00	1.95	0.00	0.52	0.00	0.00	0.00	0.00	0.00
Total	99.92	100.09	99.74	99.24	100.85	100.38	100.11	100.12	100.14	99.94	100.19	100.28	100.20
Li	5.22	3.83	5.83	5.86	2.99	1.80	3.92	4.56	4.68	4.56	4.91	3.36	5.08
Be	0.528	0.525	0.524	0.526	0.525	0.526	0.525	0.525	0.524	0.526	0.526	0.525	0.524
Sc	36.9	45.4	40.2	34.4	42.4	40.8	43.8	37.5	39.0	46.0	43.8	43.1	39.8
V	335	338	301	251	320	385	316	381	379	340	471	402	345
Cr	21.9	49.1	52.1	0.476	71.3	71.0	64.1	19.5	65.9	75.0	0.785	8.90	42.0
Co	24.8	32.1	30.9	18.5	31.0	27.2	32.4	24.6	27.2	30.6	30.2	33.5	29.6
Ni	23.6	41.2	31.6	1.89	36.2	24.5	36.2	13.2	23.4	27.3	8.47	14.0	29.1
Cu	156	88.8	112	52.6	101	88.1	71.7	74.7	89.4	96.5	182	44.3	113
Zn	79.8	73.9	100	92.8	71.5	71.4	74.2	90.6	79.1	78.8	98.4	91.6	74.0
Ga	16.9	15.3	14.7	16.3	15.3	16.5	15.3	16.5	16.1	15.4	16.4	16.2	15.7
Rb	6.84	3.54	5.83	8.73	3.41	3.91	4.04	6.32	5.54	4.56	6.96	9.08	6.35
Sr	178	160	154	181	151	181	155	171	171	157	173	160	170
Y	19.0	17.0	17.6	28.0	14.0	18.6	15.4	22.3	18.8	16.0	23.9	22.3	17.8
Zr	32.8	27.6	31.8	49.3	21.5	27.7	25.1	37.1	31.4	23.2	38.3	33.4	30.5
Nb	0.278	0.243	0.769	0.478	0.192	0.329	0.223	0.316	0.289	0.211	0.336	0.379	0.280
Mo	0.931	0.705	1.01	1.11	0.598	0.990	0.611	1.13	0.848	0.617	0.948	0.642	0.863
Sn	0.360	0.262	0.379	0.518	0.218	0.266	0.229	0.399	0.352	0.254	0.392	0.435	0.333
Sb	0.091	0.040	0.131	0.076	0.039	0.037	0.033	0.067	0.055	0.045	0.056	0.056	0.055
Cs	0.313	0.058	0.284	0.332	0.064	0.151	0.141	0.252	0.205	0.194	0.205	0.326	0.255
Ba	164	141	146	213	125	134	123	182	145	115	197	164	151
La	1.93	1.64	4.30	2.98	1.41	1.92	1.46	2.19	1.96	1.43	2.42	2.35	1.86
Ce	5.19	4.47	5.28	8.16	3.78	5.19	3.96	6.04	5.32	3.93	6.56	6.28	5.03
Pr	0.893	0.775	0.869	1.39	0.649	0.888	0.689	1.04	0.920	0.689	1.12	1.05	0.858
Nd	4.78	4.24	4.56	7.51	3.56	4.80	3.74	5.69	4.93	3.77	6.04	5.49	4.60
Sm	1.68	1.49	1.56	2.57	1.25	1.68	1.34	2.00	1.73	1.37	2.11	1.89	1.58
Eu	0.596	0.535	0.546	0.866	0.457	0.602	0.492	0.705	0.617	0.512	0.724	0.568	0.555
Gd	2.29	2.07	2.12	3.45	1.72	2.25	1.84	2.72	2.35	1.91	2.88	2.55	2.15
Tb	0.421	0.381	0.391	0.630	0.318	0.415	0.344	0.498	0.429	0.356	0.526	0.483	0.393
Dy	2.93	2.66	2.72	4.35	2.23	2.87	2.40	3.46	2.95	2.49	3.71	3.42	2.74
Ho	0.650	0.592	0.604	0.959	0.492	0.629	0.534	0.766	0.648	0.552	0.821	0.767	0.610
Er	1.89	1.69	1.75	2.75	1.42	1.81	1.54	2.21	1.89	1.60	2.38	2.27	1.76
Tm	0.297	0.266	0.274	0.433	0.225	0.285	0.244	0.348	0.296	0.252	0.377	0.366	0.280
Yb	2.05	1.84	1.90	2.97	1.54	1.94	1.68	2.39	2.03	1.74	2.59	2.56	1.91
Lu	0.314	0.282	0.290	0.457	0.238	0.298	0.259	0.369	0.310	0.266	0.404	0.396	0.296
Hf	1.12	0.958	1.04	1.67	0.774	0.955	0.856	1.27	1.07	0.811	1.32	1.24	1.04
Ta	0.017	0.016	0.049	0.032	0.011	0.027	0.014	0.019	0.017	0.014	0.021	0.024	0.022
Tl	0.050	0.018	0.128	0.080	0.018	0.010	0.030	0.087	0.054	0.037	0.042	0.051	0.036
Pb	2.08	1.17	1.20	2.33	1.13	1.17	1.48	2.37	1.72	1.44	1.64	1.55	1.67
Th	0.199	0.170	0.247	0.293	0.136	0.161	0.136	0.207	0.183	0.129	0.233	0.221	0.179
U	0.149	0.289	0.158	0.437	0.128	0.158	0.106	0.428	0.156	0.108	0.247	0.136	0.148

Major elements analyzed by standard XRF techniques are reported in wt.%, trace elements analyzed by standard ICP-MS methods are reported in ppm. All analyses completed at the Institut für Geowissenschaften, Universität Kiel.

A key inference from the mineralogy and geochemistry of Volcano 1 lavas is that a well-developed magma chamber, complete with extensive cumulates, exists below the volcano. The limited compositional range for all sampled lavas suggests this magmatic system is well-buffered, with crystallization and loss through eruption approximately balanced by input of new mafic magma batches. There is no evidence that any significant volume of dacitic (or more silicic) magma resides in this system. Nor is there any geochemical or mineralogic evidence to suggest the magma chamber has ever been evacuated by a voluminous eruption (which should generate a discontinuity in both).

8.4 Volcano 18s: Basaltic Trigger for a Voluminous Eruption

Volcano 18s has a basal diameter of ~20 km reducing to ~14 km at 1200 mbsl, which represents the lowest closed contour, and rises from 1500 mbsl to the highest point on the caldera rim at 380 mbsl. The volcano is dominated by a funnel-shaped, diatreme-like, caldera that measures 6.9 km-long by 6.3 km-wide (Fig. 2.2). The caldera floor is at 1520 mbsl, approximately the same depth as the surrounding seafloor plain, and the height from the highest point on the caldera rim to the caldera floor is 1130 m. On the outer eastern flank of the volcano is the prominent SSE-trending Eastern Scarp, which forms a vertical wall up to 200 m-high. Immediately east of the Eastern Scarp is the Eastern Cone, a well-formed stratocone 1.7 km in diameter that rises to 273 mbsl and is associated with a moderate hydrothermal plume in the water column. Volcano 18s was primarily a hard rock target for the *PISCES* dives. The aim was to obtain stratigraphically controlled samples from: (i) the inner north wall of the main caldera, where outcrops of the pyroclastic flow sequence associated with the caldera-forming eruption were expected, (ii) the Eastern Scarp, where outcrops of either the stacked pre-caldera lavas or the pyroclastic flow sequence from the caldera-forming eruption were anticipated, and (iii) the Eastern Cone, representing young post-caldera resurgent volcanism.

Mapping of the inner northern wall of the main caldera between 1250 and 500 mbsl revealed three major pyroclastic flow sequences. The lowermost of these (below ~900 mbsl) is poorly exposed and the few outcrops are predominantly of sub-welded fine-grained massive pumice, often weakly altered and cut by occasional veins of white clay. In contrast, the middle pyroclastic flow sequence at 580–900 mbsl is more continually exposed and consists of fresh alternating beds of poorly consolidated pumice clasts (up to 50 cm in diameter) and massive fine-grained pyroclastic flows locally with sub-welding textures (Fig. 8.2A, 8.2C). Dark grey ash beds consisting of andesitic to basaltic clasts and darker, more mafic enclaves within the pyroclastic flows are increasingly common above 770 mbsl (Fig. 8.2B, 8.2D). A 3–5 m-thick series of well-bedded erosional debris flows at ~580 mbsl separates the middle and upper pyroclastic flow sequences. The upper sequence is otherwise identical to the middle sequence.

The middle and upper pyroclastic flow sequences are also exposed on the Eastern Scarp between 777 and 637 mbsl, where columnar jointing structures are well-developed in some of the thicker pyroclastic flow beds (Fig. 8.2C). Again, basaltic ash beds and irregular mafic enclaves within the pyroclastic flows were observed with increasing frequency towards the top of this sequence (Fig. 8.2D, 8.2E). Many of the mafic enclaves display cooling joints whose orientations vary rapidly over domains of a few metres (Fig. 8.2F), suggesting irregular blobs of hotter material cooling within the flow, whereas some other mafic enclaves display a scoriaceous (degassed) fabric.

Diving observations confirmed that the base of the Eastern Cone overlies the pyroclastic flow sequences and the entire cone is therefore younger. The lower flanks of the cone are

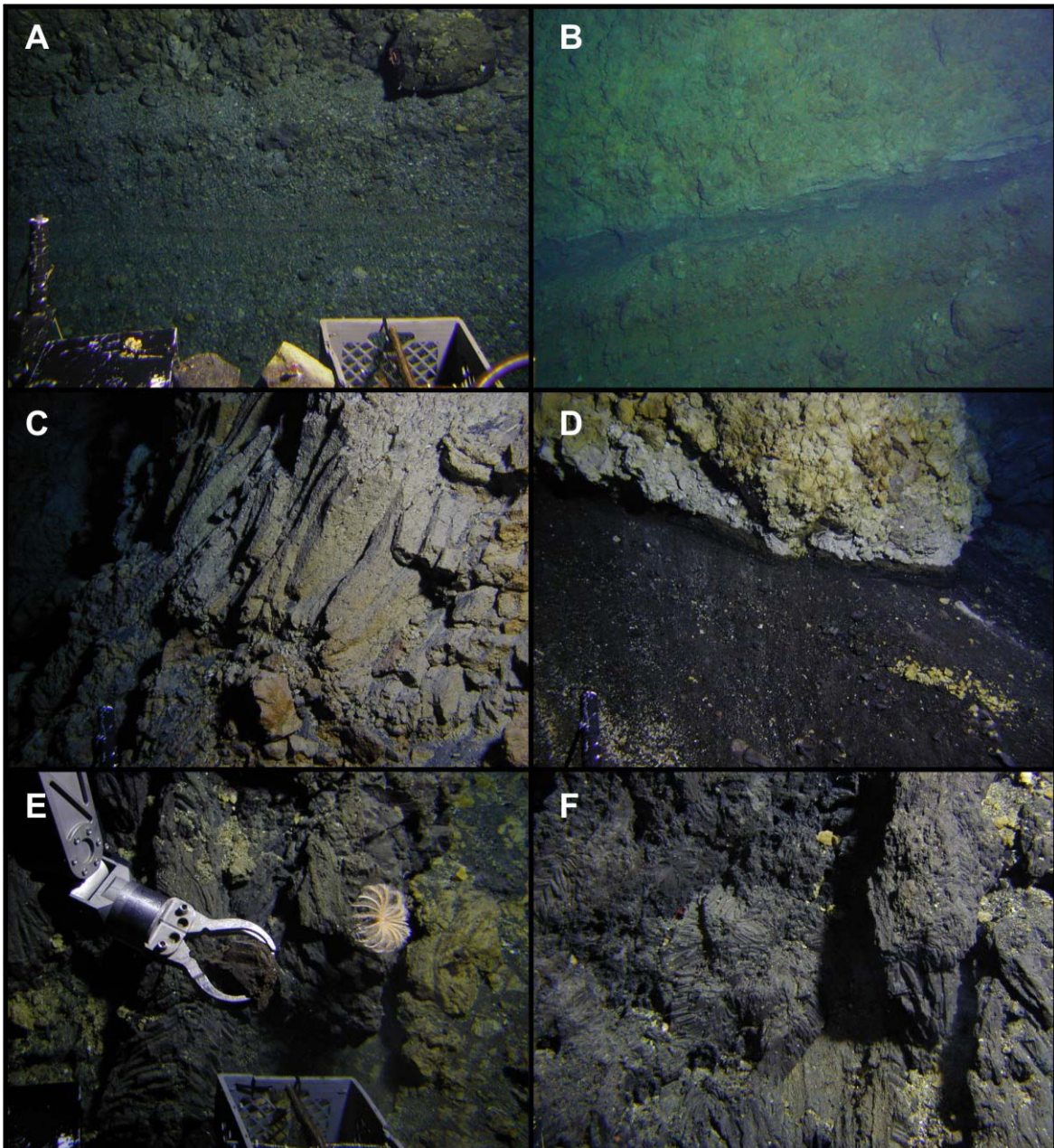


Fig. 8.2: Key stratigraphic observations from the Volcano 18s caldera -

- A) Bedded fine and coarse ash beds overlain by a massive pumice bed (pyroclastic flow).*
- B) Bedded fine and coarse ash beds separated from an overlying massive pumice bed (pyroclastic flow) by a basaltic ash layer (dark bed).*
- C) Columnar jointing indicative of slow cooling in a sub-welded massive dacitic pumice bed (pyroclastic flow).*
- D) Black basaltic coarse ash bed, easily eroded, underlying a massive dacitic pumice bed (pyroclastic flow).*
- E) Enclave of dark andesitic pumice (mixed magma) within a paler dacitic pumice bed (pyroclastic flow); the contact is sub-vertical and immediately right of the coral.*
- F) Complex enclave of dark grey to black andesitic pumice (mixed magma) within a dacitic pumice bed (pyroclastic flow). Note the irregular cooling joints, locally resembling pillow structures and suggesting the dark andesitic enclave was injected into cooler dacitic magma.*

composed of massive aa flows of basaltic andesite, typically 5–10 m-thick and separated by intervening breccia beds of comparable composition. Fall-out beds and poorly consolidated breccia dominate the mid to upper flanks, but massive aa flows with precipitous margins form the summit. A large field of diffuse, very low temperature (up to 2 °C above ambient) venting complete with iron-silica chimneys and bacterial mats occurs on the mid to upper SW flank of the cone. The size of the field, and evidence of dead or waning biota, suggest much greater hydrothermal activity in the recent past.

Overall, the >700 m-thick dacitic pyroclastic succession combined with increasing prevalence of basaltic and andesitic clasts towards the top leave little doubt that the voluminous caldera-forming eruption(s) were triggered by a basaltic intrusion into the underlying magma chamber, and that a very large part of the magma chamber was completely erupted. Poor exposure of the contact between the lower and middle pyroclastic sequences leave some doubt over the significance of this break. Potentially, the weak and intermittent alteration that characterizes the lower flow sequence could have occurred during slow cooling of this unit beneath the middle and upper flow sequences. A significant time break may have occurred, but is not required. Similarly, the better exposed break between the middle and upper flow sequences consists of debris flows that could have been generated within a few hours of the middle sequence being emplaced. Following caldera-formation, resurgent volcanism has built the Eastern Cone which is composed of basaltic andesite flows very similar in composition to the basaltic clasts within the uppermost part of the pyroclastic flow sequence.

8.5 Conclusions

Two contrasting styles of volcano evolution and caldera development are shown by Volcano 1 and Volcano 18s. At Volcano 1, no evidence of a pyroclastic flow sequence was found on the inner caldera walls. Instead, the record consists of numerous small ash eruptions coupled with occasional larger eruptions, rare outpourings of pillow andesite, and quiescent periods punctuated by small localized erosional collapses. This style of activity is similar to that seen at the youngest vents and hydrothermal field within the caldera, where explosion craters (small eruptions) and scoria cones (larger fragmental eruptions) dominate. The petrography and geochemistry of the lavas indicates a mature magmatic system whose composition varies little with time and is effectively buffered. No trace of the more silicic dacite–rhyolite magmas usually associated with voluminous caldera-forming eruptions was found. Combining these new facts with the previously obtained bathymetry for the entire volcano, we conclude that caldera formation most likely accompanied a major sector collapse of the western flank. This would have been similar to the 1980 St Helens collapse, but with a much reduced eruption component.

In contrast, the deep funnel-shaped caldera of Volcano 18s formed during one or more voluminous eruptions. Three distinct pyroclastic flow sequences are recognized on the caldera walls and nearby Eastern Scarp, but the time interval between these sequences may be negligible. All consist of dacitic pumice, and columnar jointing and subwelding textures pointing to slow cooling induced by rapid burial and complete expulsion of seawater. This, in turn, implies a very fast eruption rate. Basaltic ash beds and enclaves of basaltic to andesitic lava within the pyroclastic flows are increasingly common towards the top of both the middle and upper pyroclastic flow series. They indicate that most of the magma chamber was erupted, and imply that a basaltic intrusion triggered the eruption. Post-caldera activity has migrated east of the main caldera and constructed the Eastern Cone, which is composed of basaltic andesite and associated breccia.

Appendices

	No. of Pages
App. 1: Shipboard Scientific Party Contact Details.....	1
App. 2: Full Sample Listing.....	4
App. 3: Photologs of Recovered Samples.....	30
App. 4: Quick Look Reports.....	22

APPENDIX 1: SHIPBOARD SCIENTIFIC PARTY CONTACT DETAILS

Leigh Evans
Hatfield Marine Science Center, NOAA/PMEL
2115 S.E. OSU Drive
Newport, Oregon 97365
UNITED STATES OF AMERICA
ph: +1-541-867 0199
fax: +1-541-867 3907
e-mail: leigh.j.evans@noaa.gov

Prof. Dr. Mark Hannington
Dept of Earth Sciences
Marion Hall, University of Ottawa
140 Louis Pasteur
Ottawa, Ontario K1N 6N5, CANADA
ph: +1-613-562 5800
fax: +1-613-562 5848
e-mail: mhanning@uottawa.ca

Dr. Roger Hekinian
Keryunan
29290 Saint Renan
FRANCE
ph: +33-2-9884 9953
fax: +33-2-9884 9953
e-mail: hekinian.roger@wanadoo.fr

Lonny Lundsten
Monterey Bay Aquarium Research Institute
7700 Sandholdt Rd
Moss Landing, California 95039
UNITED STATES OF AMERICA
ph: +1-831-775 1762
fax: +1-831-775 1620
e-mail: lonny@mbari.org

Gary Massoth
Institute of Geological and Nuclear Sciences
69 Gracefield Rd
PO Box 30-368
Lower Hutt, NEW ZEALAND
ph: +64-4-570 4878
fax: +64-4-570 4657
e-mail: g.massoth@gns.cri.nz

Dr. Mark Schmidt
Institut für Geowissenschaften
Universität Kiel
Olshausenstr. 40
24098 Kiel, GERMANY
ph: +49-431-880 2874
fax: +49-431-880 4376
e-mail: mas@gpi.uni-kiel.de

Dr. Uli Schwarz-Schampera
Lagerstättenforschung
BGR
Stilleweg 2
30655 Hannover, GERMANY
ph: +49-511-643 2232
fax: +49-511-643 2304
e-mail: u.schwarz-schampera@bgr.de

Prof. Dr. Peter Stoffers
Institut für Geowissenschaften
Universität Kiel
Olshausenstr. 40
24098 Kiel, GERMANY
ph: +49-431-880 2850
fax: +49-431-880 4376
e-mail: pst@gpi.uni-kiel.de

Rennie Vaiomo'unga
Ministry of Lands, Survey and Natural Resources
PO Box 5
Nuku'alofa
KINGDOM OF TONGA
ph: +676-23 611
fax: +676-23 216
e-mail: rennie@lands.gov.to

Dr. Tim Worthington
Institut für Geowissenschaften
Universität Kiel
Olshausenstr. 40
24098 Kiel, GERMANY
ph: +49-431-880 2852
fax: +49-431-880 4376
e-mail: tw@gpi.uni-kiel.de

APPENDIX 2: FULL SAMPLE LISTING

A: Hard Rock and Mineralized Samples

<u>Sample</u>	<u>Time</u>	<u>Lat (°S)</u>	<u>Long (°W)</u>	<u>Depth</u>	<u>Comments</u>
P5-635-R1	11:04	24°48.192	177°00.642	903	Vesicular plagioclase basalt; in situ
P5-636-R1	14:09	24°48.280	177°00.929	971	Clay-altered talus; dissem. pyrite
P5-636-R2	14:35	24°48.336	177°01.089	969	Fe-oxyhydroxide crust
P5-636-R3	14:43	24°48.339	177°01.157	934	Aphyric basalt from dyke
P5-636-Sc#1	11:57	24°48.29	177°00.91	972	Fe-oxyhydroxide floc
P5-636-Sc#5	13:39	24°48.280	177°00.929	971	Clay-altered ash; dissem. pyrite
P5-637-R1	11:33	24°48.23	177°01.13	985	Fe-oxyhydroxide chimney
P5-637-R2	12:40	24°48.297	177°01.145	969	Barite-silica-pyrite crust; 112°C vent
P5-637-R3	14:05	24°48.501	177°01.215	725	Gabbro; talus
P5-637-Sc#1	10:41	24°48.110	177°01.173	1010	Soft sediment (lost during ascent)
P5-637-Sc#2	12:25	24°48.297	177°01.145	985	Fe-oxyhydroxide, bacterial mat
P5-637-Sc#3	15:03	24°48.519	177°01.107	781	Fe-oxyhydroxide, altered lapilli
P5-637-Sc#4	14:30	24°48.577	177°01.065	698	Friable crystal cumulates (dom. plag)
P5-638-R1	09:46	24°48.017	177°00.626	890	Plagioclase basalt; talus
P5-638-R2	13:35	24°48.260	177°00.189	425	Fe-oxyhydroxide; 69°C
P5-638-R3	14:08	24°48.269	177°00.108	399	Small barite chimney with sphalerite
P5-638-R4	16:00	24°48.40	177°00.16	414	Barite-silica crust; Fe-oxyhydroxide
P5-638-Sc#5	14:08	24°48.269	177°00.108	385	Barite chimney, gas outlets; 245°C
P5-639-R1	10:37	24°48.563	177°00.053	481	Plagioclase basalt; summit talus
P5-639-R2	10:37	24°48.563	177°00.053	481	Plagioclase basalt; summit talus
P5-639-R3	10:58	24°48.563	177°00.053	478	Plagioclase basalt; 2 pieces in situ
P5-639-R4	11:20	24°48.481	176°59.998	528	Aphyric basalt; in situ
P5-639-R5	14:43	24°48.258	177°00.092	540	Alt. plag basalt; dissem. pyrite; in situ
P5-639-R6	11:52	24°48.431	176°59.937	514	Plagioclase-olivine basalt from dyke
P5-639-R7	12:20	24°48.414	176°59.965	563	Plag basalt; altered surface; in situ
P5-639-R8	12:33	24°48.461	176°59.897	485	Fe-oxyhydrox. cemented scoria, ash
P5-639-R9	13:19	24°48.269	177°00.100	405	Glassy plagioclase basalt; in situ
P5-639-R10	13:34	24°48.261	177°00.090	438	Altered ash; dissem. pyrite
P5-639-R11	13:34	24°48.261	177°00.090	438	Altered ash; dissem. pyrite
P5-639-R12	13:34	24°48.261	177°00.090	438	Plagioclase basalt; in situ
P5-639-R13	14:00	24°48.24	177°00.10	384	Plag basalt; dissem. pyrite; in situ
P5-639-R14	14:15	24°48.24	177°00.10	384	Alt. plag basalt; dissem. pyrite; in situ
P5-639-R15	14:36	24°48.250	177°00.108	396	Plagioclase basalt; 2 pieces in situ
P5-639-R16	14:36	24°48.250	177°00.108	396	Plagioclase andesite; in situ
P5-639-R17	15:10	24°48.350	177°00.051	480	Alt. plag basalt; dissem. pyrite; in situ
P5-639-R18	15:46	24°48.402	177°00.165	426	Altered ash with Fe-oxyhydr. coating
P5-639-R19	15:46	24°48.402	177°00.165	426	Altered ash with pyrite, Fe-oxyhy. crust
P5-639-R20	15:46	24°48.402	177°00.165	426	Barite-pyrite cemented breccia
P5-639-R21	15:46	24°48.402	177°00.165	426	Fe-oxy. cemented lapilli; dissem. pyrite
P5-639-R22	15:46	24°48.402	177°00.165	426	Fe-oxy. cemented lapilli; dissem. pyrite
P5-639-Sc#1	09:33	24°48.555	177°00.426	557	Gravel and sand
P5-639-Sc#2	09:33	24°48.555	177°00.426	557	Gravel and sand
P5-639-Sc#3	14:36	24°48.378	177°00.147	412	Altered gravel and sand
P5-640-R1	09:28	24°35.772	176°52.295	803	Glassy aphyric basaltic andesite; talus
P5-640-R2	10:20	24°35.857	176°52.443	729	Aphyric pumice; in situ pyroclastic flow
P5-640-R3	10:45	24°35.832	176°52.465	672	Aphyric pumice; in situ pyroclastic flow
P5-640-R4	10:55	24°35.830	176°52.465	647	Aphyric pumice; in situ pyroclastic flow
P5-640-R5	11:01	24°35.829	176°52.491	637	Aphyric pumice; in situ pyroclastic flow
P5-640-R6	12:17	24°35.435	176°52.779	519	Glassy aphyric basalt; in situ
P5-640-R7	13:10	24°35.351	176°52.398	555	Glassy plag basaltic andesite; in situ
P5-640-R8	13:26	24°35.090	176°51.983	582	Plag-px basaltic andesite; in situ
P5-640-R9	14:20	24°35.224	176°52.290	497	Plagioclase basaltic andesite; in situ
P5-640-R10	15:13	24°35.123	176°52.053	318	Plag basaltic andesite; summit talus
P5-640-R11	15:53	24°35.073	176°51.981	322	Aphyric basaltic andesite; in situ

Appendix 2 – Full Sample Listing

A: Hard Rock and Mineralized Samples (continued)

<u>Sample</u>	<u>Time</u>	<u>Lat (°S)</u>	<u>Long (°W)</u>	<u>Depth</u>	<u>Comments</u>
P5-640-R12	09:02	24°35.771	176°52.375	806	Aphyric basalt; eastern scarp talus
P5-640-Sc#3	10:58	24°35.829	176°52.487	642	Basaltic ash bed; in situ
P5-640-Sc#4	14:55	24°35.16	176°52.12	399	Fe-oxyhydroxide crust
P5-641-R1	10:38	24°33.822	176°54.945	1007	Plag andesite; lithic from pyro. flow
P5-641-R2	11:54	24°33.689	176°54.723	679	Plagioclase andesite; talus
P5-641-R3	12:18	24°33.658	176°54.690	624	Aphyric pumice; in situ pyroclastic flow
P5-641-R4	13:25	24°33.622	176°54.660	572	Aphyric pumice; in situ pyroclastic flow
P5-641-R5	14:45	24°33.956	176°54.876	1135	Aphyric pumice; in situ pyroclastic flow
P5-641-R6	15:33	24°33.846	176°54.745	911	Aphyric pumice; in situ pyroclastic flow
P5-641-R7	11:54	24°33.689	176°54.723	679	Dolerite; lithic from pyroclastic flow
P5-641-R8	11:54	24°33.689	176°54.723	679	Aphyric pumice; top of pyroclastic flow
P5-641-R9	11:54	24°33.689	176°54.723	679	Aphyric basalt; top of pyroclastic flow
P5-641-R10	11:54	24°33.689	176°54.723	679	Aphyric pumice; top of pyroclastic flow
P5-641-R11	10:38	24°33.822	176°54.945	1007	Plagioclase andesite; in situ
P5-641-R12	11:54	24°33.689	176°54.723	679	Aphyric basalt; top of pyroclastic flow
P5-641-R13	11:54	24°33.689	176°54.723	679	Glassy basaltic breccia; top pyro. flow
P5-641-R14	11:54	24°33.689	176°54.723	679	Plag dacite; top of pyroclastic flow
P5-641-R15	12:18	24°33.658	176°54.690	624	Basalt-pumice lapilli; in situ ash bed
P5-641-Sc#3	14:45	24°33.956	176°54.876	1134	Silty clay and sand
P5-641-Sc#5	11:11	24°33.798	176°54.836	925	Aphyric pumice lapilli; in situ ash bed
P4-137-R1	14:29	24°48.443	177°00.003	555	Anhydrite chimney
P4-137-R2	17:03	24°48.450	176°59.985	540	Anhydrite-chalcopyrite-sphalerite spire
P4-137-Sc#5	15:45	24°48.450	176°59.985	540	Anhydrite from knocking over spire
P4-138-R1	10:35	24°48.476	177°00.003	541	Barite-anhydrite-sph-py-cpy spire
P4-138-R2	10:56	24°48.476	177°00.003	542	Barite-anhydrite-sph-py chimney
P4-138-R3	12:53	24°48.401	177°00.137	415	Fe-oxyhydroxide crust; green smectite
P4-138-R4	14:24	24°48.251	177°00.114	393	Barite crust; 130°C
P4-138-Sc#5	12:53	24°48.401	177°00.137	415	Green clay
P4-139-R1	11:23	21°08.973	175°44.934	209	Pervasively altered dacite; dissem. py
P4-139-R2	12:49	21°09.128	175°44.604	161	Coarse ash, weakly cemented
P4-139-Sc#4	10:01	21°09.119	175°44.703	197	Clay and sulfur-rich ash
P4-139-Sc#5	11:58	21°09.047	175°44.859	196	Clay and sulfur-rich ash
P4-141-R1	13:12	21°09.340	175°44.633	198	Altered ash; thin pyrite crust
P4-141-R2	13:25	21°09.316	175°44.659	155	Altered ash; dissem. pyrite
P4-141-R3	16:22	21°09.270	175°44.702	199	Bedded lapilli-ash; native sulfur
P4-141-R4	16:30	21°09.270	175°44.702	199	Native sulfur with embedded fresh ash
P4-141-Sc#5	14:02	21°09.293	175°44.655	198	Clay with altered lithic fragments
P4-141-Sc#4	16:05	21°09.270	175°44.702	199	Fresh glassy ash; trace sulfur
P4-142-R1	09:18	21°09.143	175°43.497	383	Aphyric pumice; talus
P4-142-R2	10:10	21°09.179	175°43.956	275	Fresh to altered lava pebbles, clay, py
P4-142-R3	13:00	21°09.292	175°44.654	197	Ash; partly sulfur-cemented, barite, py
P4-142-R4	16:14	21°09.252	175°44.706	196	Sulfur-cemented ash; fresh glass
P4-142-Sc#2	12:00	21°09.575	175°44.676	200	Fresh coarse ash, native sulfur; 30°C
P4-142-Sc#3	12:34	21°09.292	175°44.654	197	Temp. 152°C; gn GT, yl and bl MS
P4-142-Sc#4	14:01	21°09.292	175°44.654	200	Took gn GT
P4-143-R1 (1)	09:25	21°07.36	175°43.82	429	Plagioclase andesite; talus
P4-143-R1 (2)	09:25	21°07.36	175°43.82	429	Aphyric andesite; talus
P4-143-R1 (3)	09:25	21°07.36	175°43.82	429	Plagioclase andesite; talus
P4-143-R1 (4)	09:25	21°07.35	175°43.82	429	Aphyric andesite; talus
P4-143-R1 (5)	09:25	21°07.36	175°43.82	429	Olivine-plagioclase andesite; talus
P4-143-R1 (6)	09:25	21°07.36	175°43.82	429	Plagioclase andesite; talus
P4-143-R2	10:15	21°07.868	175°43.584	450	Aphyric andesite from a dyke
P4-143-R3	10:35	21°07.809	175°43.605	430	Finely bedded dark green ash
P4-143-R4	11:58	21°07.81	175°43.59	434	Two altered lava fragments in ash
P4-143-R5	11:15	21°07.80	175°43.57	424	Altered lava from volcanoclastic seds
P4-143-R6	11:20	21°07.81	175°43.56	420	Plagioclase basaltic andesite; in situ

Appendix 2 – Full Sample Listing

A: Hard Rock and Mineralized Samples (continued)

<u>Sample</u>	<u>Time</u>	<u>Lat (°S)</u>	<u>Long (°W)</u>	<u>Depth</u>	<u>Comments</u>
P4-143-R7	12:02	21°07.80	175°43.59	405	Plagioclase basalt; in volc seds
P4-143-R8	12:05	21°07.80	175°43.59	405	Altered lava in volcanoclastic seds
P4-143-R9	12:25	21°07.80	175°43.59	370	Plagioclase basalt; in situ
P4-143-R10	12:52	21°07.61	175°43.61	314	Volcanoclastic breccia
P4-143-R11	13:00	21°07.60	175°43.60	314	Volcanoclastic sandstone
P4-143-R12	13:20	21°07.72	175°43.50	269	Poorly bedded coarse ash; px crystals
P4-143-R13	13:30	21°07.68	175°43.53	255	Poorly bedded coarsh ash, lapilli
P4-143-R14	13:45	21°07.584	175°43.541	217	Finely bedded coarse ash, fine ash
P4-143-R15	14:30	21°07.85	175°43.55	380	Aphyric andesite from a dyke
P4-143-R16	14:45	21°07.881	175°43.532	421	Friable plagioclase-pyroxene cumulate
P4-143-R17	15:45	21°08.18	175°43.38	430	Plagioclase basalt; in situ
P4-143-R18	16:00	21°08.246	175°43.349	434	Altered volcanoclastic sediment (ash)

B: Biological Samples

<u>Sample</u>	<u>Time</u>	<u>Lat (°S)</u>	<u>Long (°W)</u>	<u>Depth</u>	<u>Comments</u>
P5-636-A1	14:31	24°48.336	177°01.089	969	Serpulidae (Polychaeta; 4)
P5-637-A1	12:20	24°48.297	177°01.145	985	Bythograeidae (2)
P5-637-A2	12:20	24°48.297	177°01.145	985	Polynoidae (Polychaeta)
P5-637-A3	12:20	24°48.297	177°01.145	985	Polychaeta
P5-637-A4	14:05	24°48.501	177°01.215	725	Scalpellomorpha (Cirrepedia on R3)
P5-637-A5	14:05	24°48.501	177°01.215	725	Verrucomorpha? (Cirrepedia on R3)
P5-637-A6	14:05	24°48.501	177°01.215	725	Alvinellidae (Polychaeta on R1)
P5-638-A1	14:08	24°48.269	177°00.108	399	Bythograeidae (4; 2 are juveniles)
P5-638-A2	13:22	24°48.265	177°00.208	418	Galatheidae (collected from coral)
P5-638-A3	13:22	24°48.265	177°00.208	418	Caryophylliidae (Lopehelia-yellow?)
P5-639-A1					Brachyuran crabs (biobox)
P5-639-A2					Polynoidae (2; biobox)
P5-639-A3					Mussels (8; on rocks in biobox)
P5-639-A4					Limpets (25; on rocks in biobox)
P5-639-A5	11:43			540	Asteroidea
P5-639-A6	13:13	24°48.170	177°00.010	400	Ophiuroidea; on gorgonian
P5-639-A7	13:06			409	Echinoidea
P5-639-A8					Polychaete
P5-639-A9					Polychaete
P5-639-A10					Barnacle
P5-639-A11	13:19	24°48.269	177°00.100	405	Hydrozoa
P5-639-A12	13:13	24°48.170	177°00.010	400	Gorgonacea
P5-639-A13	15:46	24°48.403	177°00.165	426	Vent worms
P5-639-A14	15:46	24°48.403	177°00.165	426	Brachyuran; several on vent worms
P5-639-A15					Galatheidae (2; on rocks)
P5-639-A16					Worms (2; on rocks)
P5-640-A1	10:43	24°35.824	176°52.463	642	Crinoidea (white, stalked)
P5-640-A2	14:35	24°35.187	176°52.203	434	Gorgonacea (green)
P5-640-A3	12:27	24°35.429	176°52.773	520	Caryophylliidae (Lophelia-like, dead)
P5-640-A4	16:10	24°35.046	176°51.960	340	Serpulidae (most likely dead)
P5-640-A5	13:26	24°35.090	176°51.983	582	Vermetidae (Spirorbis? on R8)
P5-640-A6	13:26	24°35.090	176°51.983	582	Porifera (on R8)
P5-640-A7	13:26	24°35.090	176°51.983	582	Bryozoa? (on R8)
P5-640-A8	12:17	24°35.435	176°52.780	519	Ophiuroidea (on R6)
P5-641-A1	11:54	24°33.689	176°54.723	679	Polychaete (on R9)
P5-641-A2	11:54	24°33.689	176°54.723	679	Caryophylliidae (unusual; on R12)
P5-641-A3	11:54	24°33.689	176°54.723	679	Bivalve (unusual; on R12)
P5-641-A4	11:54	24°33.689	176°54.723	679	Bivalve (2; unusually small; on R12)
P5-641-A5	14:45	24°33.956	176°54.876	1135	Porifera (on R5)



Appendix 2 – Full Sample Listing

B: Biological Samples (continued)

<u>Sample</u>	<u>Time</u>	<u>Lat (°S)</u>	<u>Long (°W)</u>	<u>Depth</u>	<u>Comments</u>
P5-641-A6	11:54	24°33.689	176°54.723	679	Caryophiliidae #1 (on R9)
P5-641-A7	11:54	24°33.689	176°54.723	679	Caryophiliidae #2 (on R9)
P5-641-A8	11:54	24°33.689	176°54.723	679	Bivalve (unusual; 1 valve only; on R9)
P5-641-A9	11:54	24°33.689	176°54.723	679	Caryophiliidae (dead; on R14)
P5-641-A10	11:54	24°33.689	176°54.723	679	Caryophiliidae (5; all small; on R14)
P4-137-A1	14:45	24°48.443	176°00.003	555	Bathymodiolus
P4-137-A2	14:45	24°48.443	176°00.003	555	Asteroidea
P4-137-A3	14:45	24°48.443	176°00.003	555	Sipunculans (from byssal thread of A1)
P4-137-A4	14:45	24°48.443	176°00.003	555	Mussel (on A1)
P4-137-A5	14:45	24°48.443	176°00.003	555	Polynoidae
P4-137-A6	17:03	24°48.450	176°59.985	549	Polynoidae (on R2)
P4-138-A1	09:47	24°48.412	176°59.961	558	Bythograeidae (3)
P4-138-A2	09:47	24°48.412	176°59.961	558	Bathymodiolus
P4-138-A3					Polynoidae
P4-138-S1		24°48.412	176°59.961		Mussel shells
P4-139-A1	14:46	21°09.293	175°44.655	200	Caridea (on mussels)
P4-139-A2	14:46	21°09.293	175°44.655	200	Platyhelminthes? (red; on mussels)
P4-139-A3	14:46	21°09.293	175°44.655	200	Limpets (118; on mussels)
P4-139-A4	14:46	21°09.293	175°44.655	200	Bathymodiolus (juvenile; on mussels)
P4-139-A5 to A25	14:46	21°09.293	175°44.655	200	Bathymodiolus (21 specimens)
P4-139-A26	14:46	21°09.293	175°44.655	200	Platyhelminthes? (red; on mussels)
P4-141-A1 to A5	13:01	21°09.339	175°44.629	198	Mussels (5 specimens)
P4-141-A6	13:01	21°09.339	175°44.629	198	Platyhelminthes (red; on mussel)
P4-141-A7	13:01	21°09.339	175°44.629	198	Limpets (2; on mussels)
P4-141-A8	14:02	21°09.293	175°44.655	198	Polychaetes (from Sc#5)
P4-141-A9	13:01	21°09.339	175°44.629	198	Polynoidae?
P4-141-A10	13:01	21°09.339	175°44.629	198	Polychaetes
P4-142-A1	13:00	21°09.292	175°44.654	197	Brachyuran crabs (from mussel beds)
P4-142-A2	13:00	21°09.292	175°44.654	197	Limpets (from mussel beds)
P4-142-A3 to A9	13:00	21°09.292	175°44.654	197	Bathymodiolus (7 frozen specimens)

APPENDIX 3: PHOTOLOGS OF RECOVERED SAMPLES


Appendix 3a:	Photolog of Volcano 19 samples	Pages 1–14
Appendix 3b:	Photolog of Volcano 18s samples	Pages 15–21
Appendix 3c:	Photolog of Volcano 1 samples	Pages 22–30

	<p><u>P5-635-R1</u> 14 x 11 x 7 cm black plagioclase basalt. 15% plagioclase phenocrysts up to 2 mm across (fine grained), trace yellow-green olivine phenocrysts <1 mm across. Vesicular with 15% large flow aligned gas cavities to 2 cm long, but some at <1 mm scale (2 populations?). A dense pillow-shaped block. Strongly weathered brown-black surface to 1 mm depth, but block interior fresh. From the lower SE cliff on the inner western caldera wall.</p>
	<p><u>P5-636-R1</u> 10 cm siliceous volcanic clast in clay-altered ash matrix (possible dacite or silicified andesite). 5% small vesicles (2–4 mm). 1% fine-grained disseminated pyrite. From south wall of deep crater on west flank of Volcano 19.</p>
	<p><u>P5-636-R2</u> Fe-oxyhydroxide crust with thin Mn coating. From biological sample at the base of a 1-m Fe-oxyhydroxide chimney. From Fe-oxide chimney field on south wall of deep crater, west flank of Volcano 19.</p>
	<p><u>P5-636-R3</u> 12 x 9 x 7 cm dark blue-grey aphyric basalt. Aphyric and holocrystalline, this outcrops as a 3 m wide dyke with well-developed rectilinear jointing and the sample represents a half (triangular) piece of one such block. The rock contains several flow aligned gas cavities up to 1.5 cm long and is relatively lightweight. Strongly weathered surface with abundant black Fe-Mn dust, but interior fresh and rind thickness <1 mm. Collected from a dyke on the lower south wall of the western caldera.</p>






Appendix 3a – Photolog of Volcano 19 samples

	<p><u>P5-636-Sc#1</u> Bacterial floc collected in small depression between talus blocks at the edge of the large discontinuous zone of Fe-oxyhydroxide chimneys. Gelatinous, Fe-stained bacteria (for D. Fortin, UniOttawa). Fe-oxide field on south wall of deep crater.</p>
	<p><u>P5-636-Sc#5</u> Clay-altered ash (lapilli-sized) covering sample R1. Lapilli-sized fragments in a matrix of light grey clay, with minor silica, pyrite, celadonite (?). Rare quartz crystals (?) in ash. Fe-oxide field on south wall of deep crater.</p>
	<p><u>P5-636-Sc#5 pan</u> Heavy minerals panned from 636-Sc#5. Pyrite with brown crystals (oxidized pyrite?).</p>
	<p><u>P5-637-R1</u> Fe-oxyhydroxide vent from the top of 7 m spire. Outer coating of Fe-oxyhydroxide and Mn. Interior is completely filled with fine, porous Fe-oxyhydroxide-stained silica (+/- filamentous bacteria). From Fe-oxide chimney field on south wall of large crater on west flank of Volcano 19.</p>
	<p><u>P5-637-R2</u> Massive silica-barite+pyrite/marcasite crust from 112°C vent. Top surface is coated in Fe-oxides. Bottom surface was in the upflow of the vent, with a coating of sulfide worm cases. From central part of Fe-oxide chimney field, south wall of deep crater on west flank of Volcano 19.</p>


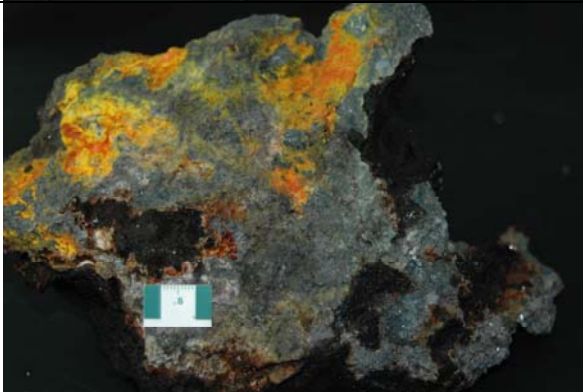



Appendix 3a – Photolog of Volcano 19 samples

	<p><u>P5-637-R2 pc</u> Coarse crystals of barite (dark, Fe-stained) from underside of barite-silica crust.</p>
	<p><u>P5-637-R3</u> 18 x 6 x 5 cm gabbro. 70% plagioclase up to 3 mm across, 25% black tabular pyroxene typically with 2 mm c-axes but locally to 1 cm, and 5% black amphibole with c-axes generally <2 mm. Some of the "plagioclase" population are greyer and possibly quartz. Local domains of the jointed block have coarser or finer grained crystals but domain boundaries are irregular and poorly defined. Weakly weathered surface but fresh interior. Talus, southern rim western caldera.</p>
	<p><u>P5-637-Sc#2</u> Fe-oxyhydroxide crust from 31°C vent (filamentous bacteria coated in Fe-oxyhydroxides, for D. Fortin, UniOttawa). From edge of Fe-oxide chimney field on south wall of large crater on west flank of Volcano 19.</p>
	<p><u>P5-637-Sc#3</u> Miscellaneous loose material from adjacent to dike with nearby bacterial mat. Mostly Fe-oxyhydroxide crust, Fe-oxide coated lapilli-sized ash, pumice fragments. One larger clast (3 cm) of qtz-chlorite-altered volcanic rock with a thin (1 mm) pyrite vein. From rim of deep pit crater on west flank of Volcano 19.</p>
	<p><u>P5-637-Sc#4</u> Assorted small pieces from the southern rim of the western caldera designed to collect "pumice". The "pumice" actually consists of 85% plagioclase crystals to 1 mm across and 15% green amphibole-epidote?-chlorite? after mafics, the latter often oxidised to reddish brown. The cumulates are fairly friable and decompose to sand during washing. The four largest and most lithified pieces were bagged separately from the bulk.</p>




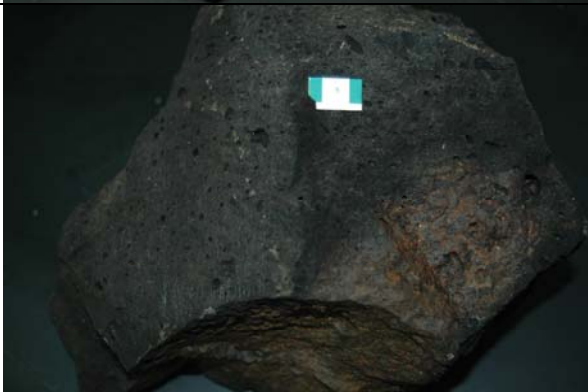

Appendix 3a – Photolog of Volcano 19 samples

	<p><u>P5-638-R1</u> 6 x 5 x 4 cm very dark blue-grey plagioclase basalt. 10% plagioclase phenocrysts to 2 mm across, often tabular. 10% vesicles mostly <1 mm across but a second population of rare big gas cavities up to 7 cm across. Surface has much yellow-orange clays from nearby hydrothermal venting, but the block interior below a rind <1 mm thick is completely fresh. Talus collected from near the base of the shute, thought at the time to be altered.</p>
	<p><u>P5-638-R2</u> Fe- and Mn-oxide crust from 69°C vent. Fe-oxide-cemented ash with an outer coating of Mn-oxides. From the summit area of the main cone of Volcano 19.</p>
	<p><u>P5-638-R2 pc</u> Underside of crust showing Fe-oxide cemented sand-sized ash.</p>
	<p><u>P5-638-R3</u> Top of 1 m-high barite chimney. Outer surface consists of fine-grained yellow-colored barite+silica. From the northern vent site (base of barite tower near marker #37) on the volcanic ridge at the summit of Volcano 19.</p>
	<p><u>P5-638-R3</u> Interior of barite chimney top showing very fine-grained, porous dendritic barite. Small cavities are lined by black crystals of sphalerite or sphalerite-encrusted crystals of barite.</p>






Appendix 3a – Photolog of Volcano 19 samples

	<p><u>P5-638-R4 (upper surface)</u> Barite-silica crust with Fe- and Mn-oxide coating from the southern venting area near marker #38. Very similar to P5-637-R2 (deep crater vent site).</p>
	<p><u>P5-638-R4 (underside)</u> Underside of crust showing massive, fine-grained barite+silica.</p>
	<p><u>P5-638-Sc#5 pc</u> Collection of small gas outlets in barite crust at the top of the large 10 m spire (245°C, near marker #37). The 3-5 mm outlets appear to be associated with two-phase venting and "bubbling" from the top of the spire. Several pcs of fine-grained barite contain up to 5% very fine, disseminated black sphalerite.</p>
	<p><u>P5-639-R1</u> 21 x 12 x 10 cm dark grey plagioclase basalt. 10% plagioclase phenocrysts up to 2 mm thick. 20% vesicles up to 7 mm across but rock remains dense. Black weathering rind <1 mm thick and weakly weathered brownish for a further 2 mm into the rock. Collected from a large unsorted talus pile near the main cone summit.</p>
	<p><u>P5-639-R2</u> 16 x 12 x 8 cm blue-grey plagioclase basalt. 10% plagioclase phenocrysts up to 2 mm across. 30% vesicles up to 2 mm across but rock remains dense. Rock has a breccia along one side of variably altered lava clasts, suggesting it represents either the top or bottom of an aa lava flow. Up to 1 cm of reddish-brown hydrothermal sediment overlies a brown-yellow weathering rind up to 1 cm thick. From the same talus pile as 639-R1.</p>

Appendix 3a – Photolog of Volcano 19 samples

	<p><u>P5-639-R3</u> Two pieces 14 x 6 x 5 cm and 13 x 11 x 4 cm respectively of dark blue-grey plagioclase basalt. 10% plagioclase phenocrysts up to 2 mm across. 15% vesicles to 1 cm across. Black Fe-Mn rind <1 mm thick, but light brown weathering persists for 5 mm into the block. Collected in situ from the summit ridge of Volcano 19.</p>
	<p><u>P5-639-R4</u> 12 x 7 x 6 cm dark blue-grey aphyric basalt. Trace plagioclase phenocrysts to 2 mm across. 50% small vesicles up to 2 mm across, but most are <1 mm across and the rock remains dense. 2% disseminated pyrite throughout the rock, <1 mm across. Rock is coated by orange hydrothermal Fe-Mn precipitates and clay up to 2 cm thick. From the summit ridge of Volcano 19.</p>
	<p><u>P5-639-R5</u> 13 x 9 x 8 cm dark grey plagioclase basalt. 10% plagioclase phenocrysts up to 2 mm across. Rock is a subrounded clast with onion-skin structure, pull-aparts near the surface and 20% vesicles <1 mm across in the core. Pull-aparts have disseminated fine grained pyrite <<1 mm across, and pyrite also occurs in some vesicles near the rock surface. A 1 mm thick alteration rind to bluish-grey covers the rock. From the summit ridge of Volcano 19.</p>
	<p><u>P5-639-R6</u> 20 x 18 x 14 cm dark grey plagioclase-olivine basalt. 10% plagioclase phenocrysts up to 2 mm across and 2% light green olivine phenocrysts up to 2 mm across. 10% vesicles up to 5 mm long, commonly >2 mm in length, and weakly flow aligned. Brown-black weathering rind 1 mm thick. Collected in situ from a vertical dyke on the summit ridge of Volcano 19.</p>
	<p><u>P5-639-R7</u> 6 x 4 x 2 cm dark blue-grey plagioclase basalt. 20% plagioclase phenocrysts up to 3 mm across set in a dark grey scoriaceous matrix with 30% vesicles <1 mm across. Sample is the outer rind of a pillow-like block with ropey surface texture. Interior is discolored yellow-orange with Fe staining along fractures. Orange weathering rind is 2 mm thick. From the summit ridge of Volcano 19.</p>




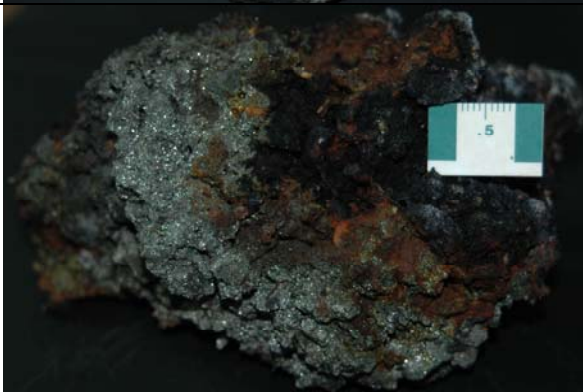

Appendix 3a – Photolog of Volcano 19 samples

	<p><u>P5-639-R8</u> Fe-oxide and Mn crust on indurated scoriaceous material and ash; cemented by Fe oxides. Small 2 cm Mn-oxide outlet on the surface of the crust. Volcaniclastic material ranges in size from 0.5 to 3 cm. Many clasts altered to Fe-oxides. Cone/summit ridge of Volcano 19.</p>
	<p><u>P5-639-R9</u> 19 x 11 x 6 cm black plagioclase basalt. 5% plagioclase phenocrysts up to 2 mm across set in a black glassy scoriaceous matrix. Locally pull-aparts with weakly developed devitrification banding up to 1 cm wide along parallel lines. Dark brown-black weathered surface and also weathered along pull-aparts. From the summit ridge of Volcano 19.</p>
	<p><u>P5-639-R10</u> Fine-grained ash altered to dark grey with minor disseminated pyrite (very fine grained). Minor white clay-altered sand grains. Homogeneous clay-rich matrix. Coated in 0.5 cm Fe-oxides. Cone/summit ridge of Volcano 19.</p>
	<p><u>P5-639-R11</u> Fine-grained ash altered to dark grey with minor disseminated pyrite (very fine grained). Minor white clay-altered sand grains. Homogeneous clay-rich matrix. Coated in 0.5 cm Fe-oxides. Similar to 639-R10 but less sulfide. Cone/summit ridge of Volcano 19.</p>
	<p><u>P5-639-R12</u> 12 x 12 x 8 cm dark blue-grey plagioclase basalt. 15% plagioclase phenocrysts up to 2 mm across. 10% vesicles with irregular shapes grading to pull-aparts up to 1 cm long, weakly flow aligned. A dense jointed block with brown staining along internal joints and fractures. Dark brown weathering rind <1 mm thick. From the flank below the NE summit of Volcano 19.</p>



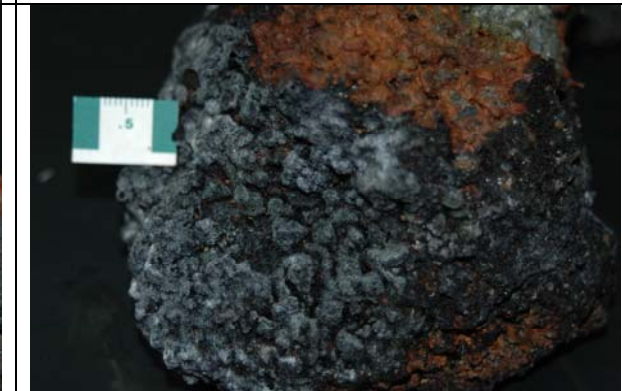



Appendix 3a – Photolog of Volcano 19 samples

	<p><u>P5-639-R13</u> 12 x 11 x 9 cm blue-grey plagioclase basalt. 15% plagioclase phenocrysts up to 2 mm across. 10% vesicles up to 5 mm across but most are much smaller, and weakly flow aligned. Disseminated fine grained pyrite <1 mm across occurs as coatings on some vesicles near the rock surface and along some internal fractures. The rock has a 1 mm thick orange rind of hydrothermal sediment and Fe-Mn oxyhydroxides. From the top of a vertical cliff on the summit ridge of Volcano 19.</p>
	<p><u>P5-639-R14</u> 12 x 7 x 6 cm dark blue-grey plagioclase basalt. 5% plagioclase phenocrysts up to 2 mm across. 30% vesicles to 3 mm across but the rock remains dense. Trace disseminated fine grained pyrite <1 mm across throughout the rock. Locally internal fractures are altered to yellowish green, and the rock has a 1-2 mm thick orange hydrothermal coating of Fe-Si oxyhydroxide and clay. From the summit ridge of Volcano 19.</p>
	<p><u>P5-639-R15</u> 9 x 8 x 4 cm (actually 2 broken pieces) dark grey plagioclase basalt. 5% plagioclase phenocrysts up to 2 mm across. 10% vesicles to 5 mm across. Ropey textured surface. Yellow-brown weathering and clays developed on internal joints, and much of the interior is weathered light grey. A difficult piece to work with! Reddish-black weathering rind 2 mm thick. From the summit ridge of Volcano 19.</p>
	<p><u>P5-639-R16</u> 6 x 5 x 5 cm blue-grey plagioclase andesite. 15% plagioclase phenocrysts up to 2 mm across. 20% vesicles but nearly all are <1 mm across and the rock remains dense. A square jointed block with brown-red Fe staining throughout much of the interior. Reddish-black weathering rind <1 mm thick. From the summit ridge of Volcano 19.</p>
	<p><u>P5-639-R17</u> 11 x 8 x 5 cm dark blue-grey plagioclase basalt. 5% plagioclase phenocrysts up to 2 mm across. 15% vesicles to 3 mm across but the rock remains dense. Trace disseminated fine grained pyrite <1 mm in vesicles and fractures within 5 mm of the rock surface. The rock has a dark brown rind of hydrothermal clay and Fe-Mn hydroxide <1 mm thick. SW rim of a pit crater with an outcropping dyke.</p>








Appendix 3a – Photolog of Volcano 19 samples

	<p><u>P5-639-R18</u> Indurated volcanoclastic material underneath Fe- and Mn-oxide crust. Up to 1 cm Fe-Mn-oxide crust on fine-grained altered ash. Some lapilli-sized clasts still relatively fresh. Cone/summit ridge of Volcano 19.</p>
	<p><u>P5-639-R19</u> Indurated volcanoclastic material underneath Fe- and Mn-oxide crust. 0.5 cm-1cm layer of pyrite (plus minor silica) cementing the ash immediately below the upper Fe-Mn-oxide crust. Some clasts are unaltered. Near marker #38.</p>
	<p><u>P5-639-R20</u> Massive piece of grey indurated volcanoclastic material in a patchy matrix of fine-grained grey barite and minor pyrite. Relict vesicles and cavities coated by pyrite or barite. Thin outer coating of Fe-oxides. Near marker #38.</p>
	<p><u>P5-639-R21</u> Indurated lapillistone fragmental cemented by Fe-oxides. One part of the sample has volcanic clasts entirely cemented by pyrite/marcasite. Individual lapilli are coated by pyrite and marcasite. Near marker #38.</p>
	<p><u>P5-639-R21</u> Close-up view of 639-R21 pyrite/marcasite.</p>

Appendix 3a – Photolog of Volcano 19 samples

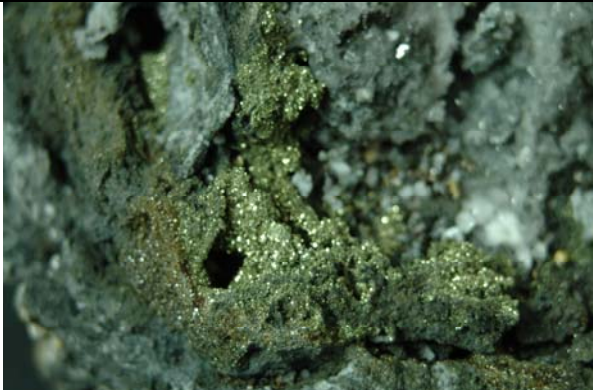
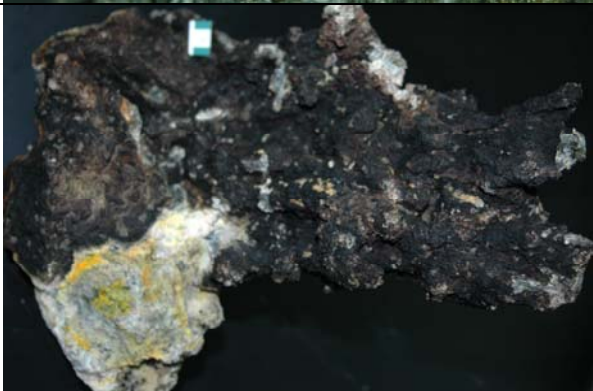
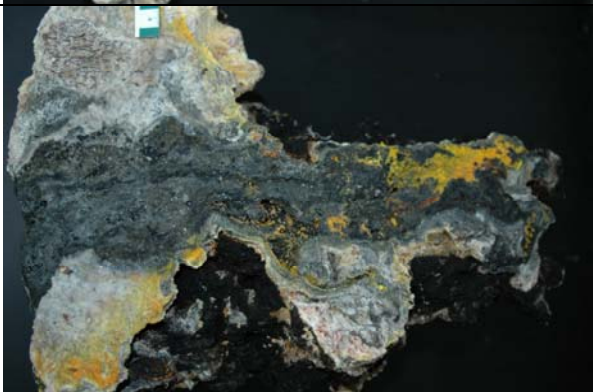
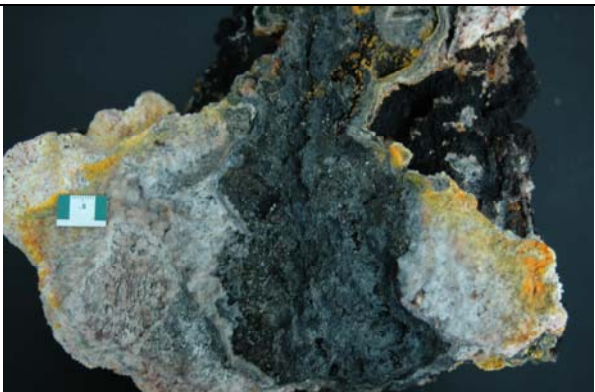


	<p><u>P5-639-R22</u> Indurated lapillistone fragmental cemented by dark grey Mn (+/- clay). Part of the sample is cemented by fine-grained pyrite similar to 639-R21. Outer coating of Fe-oxides associated with oxidation of sulfides. Near marker #38. Below left: close up of 639-R22 pyrite. Below right: close up of 630-R22 Fe-oxides.</p>
	
	<p><u>P4-137-R1</u> Small 30-cm-high anhydrite chimney from 1m sq, venting area in sediment. From pit crater at summit of Volcano 19.</p>
	<p><u>P4-137-R2a</u> Pieces of the large spire with visible 2-phase venting: (a) soft anhydrite from the top of the spire. From pit crater at summit of Volcano 19.</p>
	<p><u>P4-137-R2b</u> Pieces of the large spire with visible 2-phase venting: (b) left and below left- several small pieces of harder chimney wall lined with fine-grained chalcopyrite; below right- larger piece of chimney wall with sphalerite/wurtzite.</p>

Appendix 3a – Photolog of Volcano 19 samples



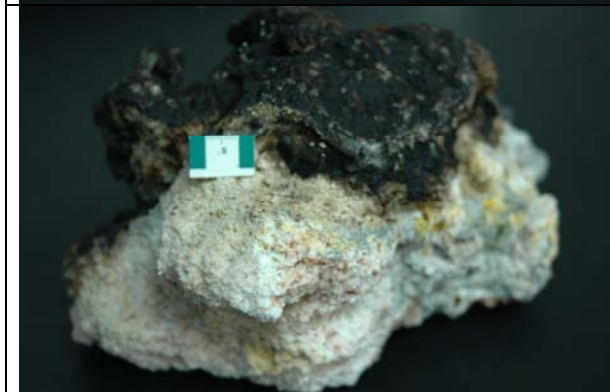

	
	<p><u>P4-137-R2c</u> Pieces of the large spire with visible 2-phase venting: (c) one large coarsely crystalline, massive anhydrite sample with chalcopyrite and sphalerite/wurtzite from the base of the spire. Below left: close-up of 137-R2c anhydrite and cpy. Below right: close-up of 137-R2c anhydrite.</p>
	
	<p><u>P4-137-Sc#5</u> Soft anhydrite from collapsed material produced by knocking over the large spire.</p>
	<p><u>P4-138-R1a</u> Small, 30 cm barite-anhydrite chimney with sphalerite-pyrite inner core from high-temperature vents in pit crater. 2-3 cm barite+anhydrite outer wall with 3 cm wide porous core of fine-grained sphalerite (+wurtzite) and minor pyrite-marcasite. Small satellite chimney. Next two rows below- close-ups and different views of 138-R1a concentrating on the cross-section.</p>

	
	
	<p>P4-138-R1b Small, 20 cm anhydrite chimney with sphalerite-lined orifice from high-temperature vents in pit crater. Inner conduit is lined by dark brown sphalerite+wurtzite crystals. Below left- the inner conduit of 138-R1b. Below right- anhydrite-sphalerite on 138-R1b.</p>
	
	<p>P4-138-R1c Small, 20 cm anhydrite chimney with sphalerite-pyrite-chalcopryite inner core from high-temperature vents in pit crater. Inner wall is lined by dark brown sphalerite+wurtzite crystals and fine-grained chalcopryite.</p>

Appendix 3a – Photolog of Volcano 19 samples



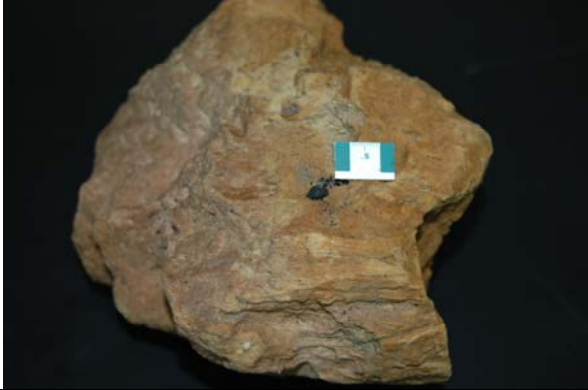


	<p><u>P4-138-R1c</u> Close-up of chalcopyrite on 138-R1c.</p>
	<p><u>P4-138-R2a</u> 30 cm high barite chimney from "razorback" spire near P4-137-R2 (two-phase vent in pit crater). Outer walls of barite with minor anhydrite and inner core of porous fine-grained sphalerite (\pmwurtzite) and minor pyrite-marcasite, similar to 138-R1a.</p>
	
	<p><u>P4-138-R2b</u> Base of barite-anhydrite chimney from spire near P4-137-R2 (two-phase vent in pit crater), similar to 138-R1a.</p>
	<p><u>P4-138-R2b</u> Close-up of other side of 138-R2b.</p>

Appendix 3a – Photolog of Volcano 19 samples




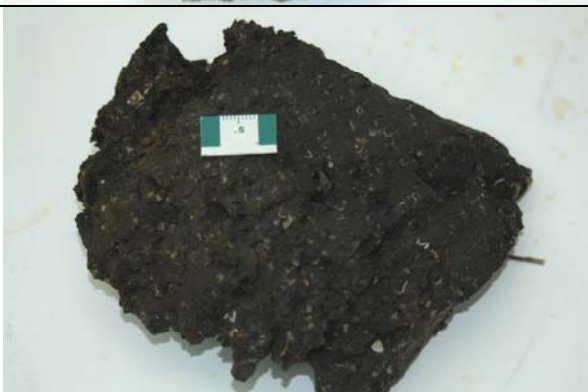

	<p><u>P4-138-3</u> Fe-oxide crust from area surrounding marker #38, with distinctive green clay underneath the Fe-oxide crust (probable ferrous iron-bearing smectite).</p>
	<p><u>P4-138-4</u> Barite crust from collapsed chimney in the northern vent field at the summit of Volcano 19 (barite tower, near marker #37). The barite crust is from an older chimney that appears to be weathering (the barite is corroded and anhydrite may have been dissolved from this piece). Below left and right- views of 138-4 from different angles.</p>
	

End of Photolog for Volcano 19.






Appendix 3b – Photolog of Volcano 18s samples

	<p><u>P5-640-R1</u> 13 x 5 x 4 cm black aphyric basaltic andesite. Glassy lava with trace pyroxene to 2 mm across. Surface is black-brown weathered glass rind up to 2 mm thick. A talus boulder at 803 mbsl below the Eastern Scarp.</p>
	<p><u>P5-640-R2</u> 15 x 9 x 9 cm pale yellow aphyric pumice. Trace black pyroxene to 1 mm across. Poor devitrification banding in shades of pale yellow and grey; the grey bands up to 4 mm wide but mostly thinner and discontinuous. 20% flow aligned vesicles to 1 cm long. Brown weathered surface, pale yellow interior and creamish core. Two lithic pebbles (andesite, basalt) are incorporated in the pumice, 15 mm and 7 mm across respectively. Block from lower part of the pyroclastic flow, 729 mbsl.</p>
	<p><u>P5-640-R3</u> 15 x 13 x 10 cm pale yellow-pink aphyric pumice. Trace black pyroxene to 1 mm across. Weathered brown surface rind <1 mm thick underlain by a weakly weathered yellow shell and fresh pink core. 20% strongly flow aligned vesicles to 1 cm long. Weak devitrification banding from pink to pale grey shades, but bands are discontinuous. A dark brown basalt scoria fragment 3 mm across is incorporated in the pumice as a xenolith. Subwelded block from middle of the pyroclastic flow, 672 mbsl.</p>
	<p><u>P5-640-R4</u> 10 x 5 x 4 cm cream grey aphyric pumice. Trace black pyroxene up to 1 mm across. 20% elongate flow aligned vesicles to 1 cm long. Surface weakly weathered to light brown, but this rind is <1 mm thick. Block from upper part of the pyroclastic flow immediately below the first basalt bed, 647 mbsl.</p>
	<p><u>P5-640-R5</u> 13 x 9 x 5 cm dark grey aphyric pumice. Fine devitrification banding in shades of dark to light grey, typically 1 mm thick. 20% vesicles mostly spherical and 1-2 mm in diameter but grade to large cavities up to 3 cm across at the core. Pseudo-columnar jointing well-developed on one face. Weakly weathered yellowish surface rind <1 mm thick. The darkest material from the core of the large "basalt" lens within the upper pyroclastic flow, 637 mbsl.</p>






Appendix 3b – Photolog of Volcano 18s samples

	<p><u>P5-640-R6</u> 10 x 9 x 5 cm black aphyric basalt. Trace plagioclase phenocrysts to 2 mm across. A weathered brown glass crust surface with ropey texture 2-3 mm thick. Highly vesicular; 20% vesicles mostly <1 mm across together with a few large ones ranging in size up to the core cavity at 3 cm across, yet the block remains dense. This is one of the largest basalt bombs within the explosion pit, ~522 mbsl.</p>
	<p><u>P5-640-R7</u> 12 x 11 x 4 cm black plagioclase basaltic andesite. 10% plagioclase phenocrysts up to 2 mm across. A glassy matrix with weak devitrification banding in shades of dark grey. Numerous incipient pull-aparts that are locally iron-stained brown. Surface very weakly weathered, with a distinctive coral on it. Thick aa flow front at the western base of the Eastern Flank Cone, 555 mbsl.</p>
	<p><u>P5-640-R8</u> 20 x 15 x 10 cm black plagioclase-pyroxene basaltic andesite. 10% plagioclase phenocrysts to 2 mm across and 2% black pyroxene phenocrysts to 2 mm across. A massive non-vesicular flow with incipient pull-aparts. Weak devitrification banding with a few convolute dark grey bands up to 5 mm wide. Brownish weakly weathered surface with much biology. Thick aa flow front at the SW base of the Eastern Flank Cone, 582 mbsl.</p>
	<p><u>P5-640-R9</u> 12 x 9 x 3 cm brownish black plagioclase basaltic andesite. 10% plagioclase phenocrysts up to 2 mm across. Matrix somewhat scoriaceous with incipient pull-aparts in bands, a typical aa flow. Weakly weathered brownish surface rind <1 mm thick, and a prominent puff ball at one end. Outcrops as an in situ lava block on the mid-western flank of the Eastern Flank Cone, 497 mbsl.</p>
	<p><u>P5-640-R10</u> 15 x 12 x 6 cm black plagioclase basaltic andesite. 5% plagioclase phenocrysts up to 2 mm across, trace black pyroxene up to 2 mm across. 10% oval vesicles up to 1 cm across, but most 2 mm across. Surface is overlain by a 4 mm thick light orange clay layer that weathers to black. Piece to MH. Talus from western summit lava flow, 318 mbsl (seen in situ above at 305 mbsl).</p>






Appendix 3b – Photolog of Volcano 18s samples

	<p><u>P5-640-R11</u> 13 x 7 x 6 cm dark grey aphyric basaltic andesite. A dense non-vesicular flow fragment with a 3-4 mm thick yellow-brown alteration rind. Disseminated fine grained pyrite occurs along internal joints and fracture surfaces, but the surrounding matrix looks fresh. Piece to MH. Eastern summit lava flow at a ledge part way down the NE crater, 322 mbsl.</p>
	<p><u>P5-640-R12</u> 13 x 8 x 7 cm black aphyric basalt. Trace black pyroxene up to 2 mm across. Non-vesicular but many small incipient pull-aparts. Weakly weathered brown-black surface rind 2 mm thick with much biology. Large gashes near the surface up to 1 cm long are typically filled with white zeolite or yellowish clay. A talus boulder at 803 mbsl below the eastern scarp.</p>
	<p><u>P5-640-Sc#3</u> Black volcanic ash and sand. From a well-bedded 10 cm thick ash bed immediately overlying the 640-R4 pumice outcrop and representing the lowest stratigraphic occurrence of basaltic material in the pyroclastic flow sequence. Sampled at 642 mbsl.</p>
	<p><u>P5-640-Sc#4</u> Soft Fe-oxyhydroxide crust from the lower part of the Fe-crust area on the western mid-flank of the Eastern Flank Cone. Temperature probe reported 14.4°C (= ambient sea water). At 399 mbsl.</p>
	<p><u>P5-641-R1</u> 11 x 8 x 5 cm dark grey plagioclase andesite. Subrounded block with white clay patches but fresh interior. 5% plagioclase phenocrysts to 2 mm across, often rounded with a "melted" appearance. Trace green-white clots to 3 mm across after mafics (ol, cpx), and trace cream pumice xenoliths to 5 mm across and usually subrounded. A mixed magma? Block is much fractured; 5% small elongate vesicles grade to pull-aparts up to 3 mm long. Clast within the altered pyroclastic flow at 1007 mbsl.</p>






Appendix 3b – Photolog of Volcano 18s samples

	<p><u>P5-641-R2</u> 17 x 10 x 9 cm blue-grey plagioclase andesite. A dense well rounded boulder with spherical weathering and a black rind <1 mm thick. Block interior is fresh. 15% plagioclase phenocrysts to 2 mm across set in a very fine grained matrix of black-green pyroxene (<1 mm across) and light grey holocrystalline material. The rock appears silicified and may be a "cooked" lithic block from the pyroclastic flow. Talus boulder overlying the top of the main pyroclastic flow sequence at 679 mbsl.</p>
	<p><u>P5-641-R3</u> 9 x 8 x 5 cm aphyric pumice. Somewhat weathered clast with a brown surface grading to a light yellow-grey interior. Trace black px(?) to 1 mm across. 30% flow aligned vesicles up to 2 cm long. White pumice below a fallout bed at the top of the main pyroclastic flow, 624 mbsl.</p>
	<p><u>P5-641-R4</u> 11 x 7 x 6 cm aphyric pumice. Somewhat weathered light brown clast grading to a light grey interior. Trace black clots to 1 mm across. 20% elongate vesicles up to 1 cm long. Clast from 3 m below the top of the upper pyroclastic flow, 572 mbsl.</p>
	<p><u>P5-641-R5</u> 15 x 9 x 6 cm aphyric pumice. Somewhat weathered clast with a dark brown surface grading to interior shades of yellow, but the core is ~fresh and light yellow with a prominent 4 mm wide dark grey devitrification band. Trace black clots to 1 mm across. 20% vesicles flow aligned and up to 2 cm long. Has a sponge attached to one end of the clast. Clast from base of cliff in the altered pyroclastic flow, 1135 mbsl.</p>
	<p><u>P5-641-R6</u> 14 x 12 x 5 cm aphyric pumice. Clast has a dark brown weathered surface rind 5 mm thick, but the interior is fresh cream pumice. Trace black rod-like px to 3 mm long. Local domains 1-3 mm across of grey devitrified pumice, but no banding. 20% stretched flow aligned vesicles up to 1 cm long. Clast from the main pyroclastic flow, 911 mbsl.</p>

Appendix 3b – Photolog of Volcano 18s samples

	<p><u>P5-641-R7</u> 12 x 10 x 5 cm dolerite. Very hard and very fine grained (<<1 mm) holocrystalline block with rectilinear jointing. No phenocrysts. Surface is weathered black with attached bivalves and corals but the rind is <1 mm thick; interior is dark green suggesting pervasive chlorite (piece to MH). Talus boulder overlying the top of the main pyroclastic flow sequence at 679 mbsl.</p>
	<p><u>P5-641-R8</u> 13 x 7 x 6 cm aphyric pumice. Black weathering rind <1 mm thick over ~fresh interior of light grey to dark grey devitrification banded pumice. Darker beds are 1 mm across whereas the lighter beds are up to 5 mm wide. 10% elongate vesicles parallel to the devitrification banding and up to 5 mm long. Talus boulder overlying the top of the main pyroclastic flow sequence at 679 mbsl.</p>
	<p><u>P5-641-R9</u> 16 x 12 x 10 cm dark grey aphyric basalt. An irregularly shaped angular block with a black weathering rind <1 mm thick. Trace light green olivine phenocrysts up to 2 mm across. 5% vesicles ranging from very small to 7 cm in length and flow aligned. Talus boulder overlying the top of the main pyroclastic flow sequence at 679 mbsl.</p>
	<p><u>P5-641-R10</u> 10 x 8 x 5 cm aphyric pumice. Black weathering rind <1 mm thick over fresh interior of dark grey to light grey devitrification banded pumice. Mostly dark grey, whereas the lighter beds are thinner and up to 5 mm thick. 20% elongate vesicles parallel to the devitrification banding and up to 5 mm long. This is the darkest pumice recovered during the dive. Talus boulder overlying the top of the main pyroclastic flow sequence at 679 mbsl.</p>
	<p><u>P5-641-R11</u> 12 x 8 x 6 cm dark grey plagioclase andesite, very similar to P5-641-R1. White clay patches but fresh interior. 5% plagioclase phenocrysts to 2 mm across, often rounded with a "melted" appearance. Trace green-white clots to 3 mm across after mafics (ol, cpx). Local domains to 1 cm across of pumice or white dacite, some subrounded but others subangular. 5% small vesicles grading to pull-aparts to 3 mm long; block breaks readily along these. Clast within the altered pyroclastic flow at 1007 mbsl.</p>

Appendix 3b – Photolog of Volcano 18s samples

	<p><u>P5-641-R12</u> 30 x 16 x 15 cm grey aphyric basalt. A dense rectilinear block with strong internal jointing; surface light green to <1 mm depth (piece to MH). Interior fresh but brown Fe staining along joints. Trace plagioclase phenocrysts up to 1 mm across. A large dark green gabbroic xenolith 2.5 cm across is composed of 60% plag, 35% cpx and 5% opx all up to 1 mm across. Rock matrix is holocrystalline (dolerite?). Talus overlying the top of the main pyroclastic flow sequence at 679 mbsl.</p>
	<p><u>P5-641-R13</u> 12 x 10 x 6 cm dark green breccia. The breccia consists of subrounded black glassy aphyric basalt clasts up to 5 mm across and rare subangular pumice and andesite clasts set in a yellow-brown matrix of hyaloclastite. Probably an agglomerate of spatter. Talus boulder overlying the top of the main pyroclastic flow sequence at 679 mbsl.</p>
	<p><u>P5-641-R14</u> 12 x 11 x 7 cm greenish cream plagioclase dacite. A well rounded boulder with a dark weathering rind <1 mm thick. 10% plagioclase phenocrysts up to 2 mm across set in a holocrystalline matrix. The rock is possibly silicified and most likely represents a "cooked" lithic block from the pyroclastic flow. Talus boulder overlying the top of the main pyroclastic flow sequence at 679 mbsl.</p>
	<p><u>P5-641-R15</u> 11 x 9 x 9 cm fallout bed composed of subrounded to subangular aphyric pumice and black aphyric basalt clasts. Well compacted, clasts 0.5–2.0 cm in diameter. Heterolithic, with pumice clasts varying from yellow to grey (fresh) and basalt clasts from dense to scoriaceous. Top 1 cm is finer grained and mostly weathered brown-black basalt clasts 1-3 mm across ("basaltic" appearance from the sub). Immediately overlying 641-R3 at the top of the main pyroclastic flow, 624 mbsl.</p>
	<p><u>P5-641-Sc#3</u> Brown silty clay with numerous volcaniclastic fragments ranging up to coarse sand size. Bluish silty clay from the base of the cliff in the altered pyroclastic flow, 1135 mbsl (immediately below sample 641-R5).</p>

Appendix 3b – Photolog of Volcano 18s samples








P5-641-Sc#5




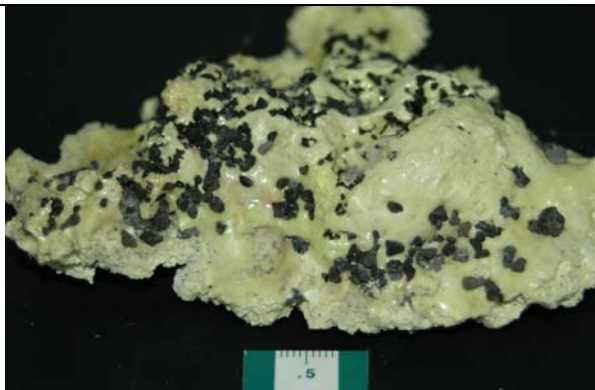


Pebbles of fresh cream to light grey aphyric pumice with local dark domains <0.1 mm across. Apparent white "vein" within the altered pyroclastic flow, now interpreted as a fallout bed, at 925 mbsl.

End of Photolog for Volcano 18s.



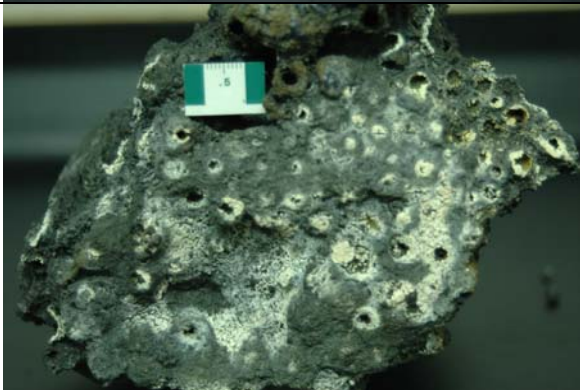

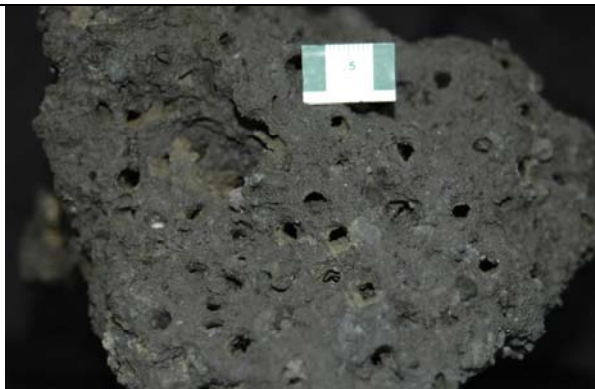

Appendix 3c – Photolog of Volcano 1 samples

	<p><u>P4-139-R1</u> Intensely altered dacite(?) block from escarpment northeast of pit craters. Completely altered to friable, grey clay, with minor disseminated pyrite.</p>
	<p><u>P4-139-R2</u> Semiconsolidated coarse ash with a clay-rich matrix from the main venting area surrounding the pit craters.</p>
	<p><u>P4-139-Sc#4</u> Clay-rich and sulfur rich ash and mud from the main venting area surrounding the pit craters.</p>
	<p><u>P4-139-Sc#5</u> Clay-rich and sulfur rich ash and mud from the main venting area surrounding the pit craters.</p>
	<p><u>P4-141-R1</u> Indurated volcanic ash; components partly altered and covered by thin rim of pyrite/marcasite. Thin (0.2–0.5 cm) oxidation rim on surface.</p>

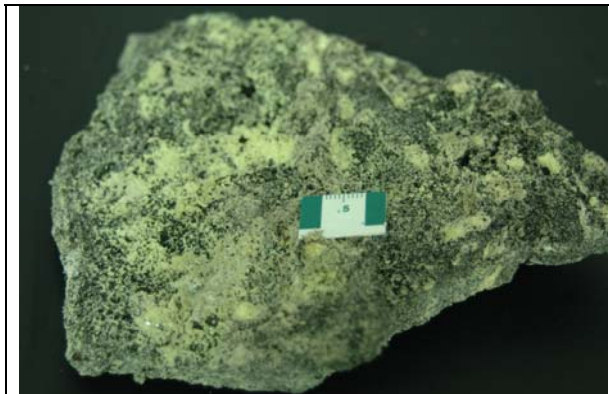
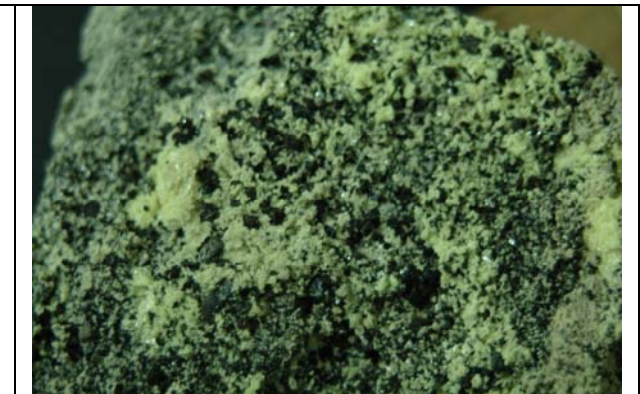




Appendix 3c – Photolog of Volcano 1 samples

	<p><u>P4-141-R2</u> Indurated volcanic ash; few larger components; bleached, clay alteration, silicification; disseminated pyrite/marcasite. Thin (0.2 cm) oxidized crust on surface.</p>
	<p><u>P4-141-R3, R4</u> Crust of native sulphur-indurated sand-lapilli-sized volcaniclastite. Crust of native sulphur up to 0.5 cm thick. Below left- close-up view of R3 volcaniclastite. Below right- close-up view of R4 native sulphur.</p>
	
	<p><u>P4-141-Sc#4</u> Black volcanic sand with few altered components and fragments of thin native sulphur crust.</p>
	<p><u>P4-141-Sc#5</u> Light grey-yellow, fine-grained hydrothermal mud, silt and sand. Few fragments of indurated native sulphur crusts.</p>






Appendix 3c – Photolog of Volcano 1 samples

	<p><u>P4-142-R1</u> 13 x 13 x 6 cm pale grey aphyric pumice. Devitrification banding, with a few dark grey bands up to 0.5 cm thick. 20% flow aligned vesicles up to 1 cm long. Surface weathered dark brown to 0.5 cm depth but interior fresh. A water-logged float block of uncertain origin (possibly not Volcano 1).</p>
	<p><u>P4-142-R2</u> Pebble-sized volcaniclastic talus sampled from a loose bed and disintegrated during the dive. Pebbles are vesicular, glassy to intensely red-stained and altered. Few pebbles consist of hydrothermally indurated (pyrite, clay minerals) volcanic ash.</p>
	<p><u>P4-142-R3</u> Indurated volcanic ash, hydrothermally altered and indurated by native sulphur, pyrite, barite, clay minerals; these are best developed as linings along gas bubble tracks penetrating the ash from below to the surface. Below left- cross-section along gas tracks. Below right- empty gas bubbles.</p>
	
	<p><u>P4-142-R4</u> Sulfur-rich crusts and sulfur-cemented black sand from the main venting areas in the mussel field. Fresh glass is preserved in the molten sulfur on the undersides of the crust. Below left- sulfur-rich crust. Below right- sulfur-cemented black volcanic sand.</p>






Appendix 3c – Photolog of Volcano 1 samples

	
	<p><u>P4-142-Sc#2</u> Loose black volcanic coarse-grained sand, few altered components; several larger pieces of molten native sulphur partly indurating the volcanoclastic material.</p>
	<p><u>P4-143-R1 (1)</u> 10 x 5 x 3 cm black plagioclase andesite. 30% plagioclase phenocrysts up to 4 mm across and trace dark green pyroxene phenocrysts set in a black glassy matrix. Non-vesicular with randomly spaced sub-parallel shear planes. Slight weathering to shades of brown on some surfaces. Talus from base of inner NE caldera wall.</p>
	<p><u>P4-143-R1 (2)</u> 14 x 10 x 3 cm grey aphyric andesite. Trace plagioclase phenocrysts to 2 mm across. Dense lava block with well-developed shear planes semi-regularly spaced at 5 mm and very fine grained holocrystalline groundmass. Probably a dyke. Surface moderately weathered to reddish brown but fresh below 1 mm depth. Talus from base of inner NE caldera wall.</p>
	<p><u>P4-143-R1 (3)</u> 11 x 7 x 3 cm black plagioclase andesite. 5% plagioclase phenocrysts to 2 mm across. Dense non-vesicular block bounded by sub-parallel shear planes. Traces of disseminated pyrite along some shears, but no associated discoloration or alteration of the groundmass. Surface weathered reddish brown to <1 mm depth. Talus from base of inner NE caldera wall.</p>






Appendix 3c – Photolog of Volcano 1 samples

	<p><u>P4-143-R1 (4)</u> 9 x 8 x 7 cm slightly reddish dark grey aphyric andesite. Trace plagioclase phenocrysts to 2 mm across. Vesicular, with 10% small vesicles to 1 mm across forming an integral part of the groundmass fabric. Surface weakly weathered to orange-brown locally, but weathering is minimal. Talus from base of inner NE caldera wall.</p>
	<p><u>P4-143-R1 (5)</u> 9 x 8 x 5 cm dark grey olivine-plagioclase andesite. 15% plagioclase phenocrysts to 3 mm across and 5% yellow-green olivine phenocrysts to 2 mm across. 5% irregularly shaped vesicles up to 1 cm long and grading into incipient pull-aparts. Surface and fracture planes weathered reddish brown to <1 mm depth. Talus from base of inner NE caldera wall.</p>
	<p><u>P4-143-R1 (6)</u> 8 x 8 x 7 cm grey plagioclase andesite. 10% plagioclase phenocrysts and trace black pyroxene phenocrysts up to 2 mm across. Moderately vesicular lava with 10% flow aligned vesicles to 2 mm long. Block interior is fresh, but surface is weathered reddish brown to 2 mm and yellow staining along interior fractures hosts trace disseminated pyrite. Talus from base of inner NE caldera wall.</p>
	<p><u>P4-143-R2</u> 20 x 8 x 6 cm grey aphyric andesite. Trace plagioclase phenocrysts up to 2 mm across. A jointed holocrystalline dense block from a dyke. Surface and joints weathered dark brown to 2 mm depth, but block interior is fresh. Sampled from a dyke on the inner NE caldera wall.</p>
	<p><u>P4-143-R3</u> 13 x 8 x 7 cm block of finely layered yellowish dark green ash. Individual beds range from <0.1 to 1.2 mm thick and are weakly graded, with all material of fine ash size. Surface weathered dark brown. Sampled from an in situ outcrop adjacent to a dyke on the inner NE caldera wall.</p>




Appendix 3c – Photolog of Volcano 1 samples

	<p><u>P4-143-R4</u> Base of the caldera wall. Hydrothermally altered lava fragment in a layered ash sequence.</p>
	<p><u>P4-143-R5</u> Hydrothermally altered lava fragment in the pyroclastic flow sequence.</p>
	<p><u>P4-143-R6</u> 9 x 6 x 5 cm dark grey plagioclase basaltic andesite. 5% plagioclase phenocrysts up to 3 mm across. Glassy matrix with numerous flow-aligned pull-aparts grading from incipient planes to voids up to 2 cm long by 0.5 cm wide. Surface weakly weathered to a lighter shade of grey, but interior fresh. An in situ flow from the inner NE caldera wall.</p>
	<p><u>P4-143-R7</u> 20 x 10 x 6 cm black plagioclase basalt. 20% plagioclase phenocrysts up to 4 mm (most 2 mm) set in a fresh black glassy matrix. Part of a non-vesicular aa flow, locally breaking up along flow aligned pull-apart planes with glassy margins. No evidence of any weathering. A large clast within the volcanoclastic sediment sequence on the inner NE caldera wall.</p>
	<p><u>P4-143-R8</u> White altered lava block in the volcanoclastic sediments.</p>

Appendix 3c – Photolog of Volcano 1 samples

	<p><u>P4-143-R9</u> 13 x 9 x 6 cm black plagioclase basalt. 10% plagioclase phenocrysts up to 3 mm across, but these form an irregular plagioclase-rich (20%) domain ~9 x 4 x 3 cm associated with shearing and the enclosing plagioclase-poor (5%) non-vesicular dense lava. The plagioclase-rich domain has 10% oval voids to 5 mm across, whereas the surrounding lava has sparse pull-aparts to 1 cm in length. Weakly weathered dark grey surface. Lava flow overlying volcanoclastic sediments, inner NE caldera wall.</p>
	<p><u>P4-143-R10</u> 14 x 13 x 5 cm block of orange to dark green volcanoclastic sediment. Angular to sub-angular dark grey lithic clasts of aphyric and sparsely plagioclase-phyric basaltic andesite up to 9 mm across are set in a matrix of poorly bedded orange to dark green coarse ash. Friable. One large clast of subangular aphyric basaltic andesite 8 x 7 x 4 cm is embedded in the sediment with a weakly weathered dark grey surface. Volcanoclastic sediment sequence on the inner NE caldera wall.</p>
	<p><u>P4-143-R11</u> 19 x 13 x 11 cm block of brown volcanoclastic sandstone. Weakly calcite-cemented sand-sized grains of weathered lava; massive with no evidence of bedding or grading. Block remains weakly friable. Surface weathered black to a depth of 0.1 mm but fresh below that. Sampled from the inner NE caldera wall.</p>
	<p><u>P4-143-R12</u> 18 x 11 x 6 cm block of orange to dark green volcanoclastic sediment. Most of the block comprises poorly bedded orange-stained dark green coarse ash and is friable. Within this is a 2 cm thick bed of coarser ash containing abundant fresh dark green-black pyroxene crystals up to 5 mm long. Local domains bearing pyroxene crystals also occur elsewhere in the block. Sampled from the inner NE caldera wall.</p>
	<p><u>P4-143-R13</u> 18 x 14 x 7 cm block of dark green volcanoclastic sediment. Angular to sub-angular dark grey lithic clasts of aphyric and sparsely plagioclase-phyric basaltic andesite up to 8 mm across are set in a matrix of poorly bedded dark green coarse ash. Friable. Surface weathered dark orange to 4 mm depth, but block interior is quite fresh. Sampled from the inner NE caldera wall.</p>

Appendix 3c – Photolog of Volcano 1 samples

	<p><u>P4-143-R14</u> 19 x 9 x 6 cm block of finely layered orange-stained dark green volcanoclastic sediment. Individual beds are predominantly unsorted coarse ash up to 1 cm thick separated by thin (<0.1 mm) fine ash beds. Weakly consolidated and friable. Surface weathered dark brown to orange. Sampled from an outcrop at the summit of the inner NE caldera wall.</p>
	<p><u>P4-143-R15</u> 20 x 9 x 6 cm reddish grey aphyric andesite. Dense jointed block from a dyke, featuring numerous dark grey shear planes ~0.1 mm thick and spaced at semi-regular 5 mm intervals. Surface and joints weakly weathered orange-dark green to a depth of <0.1 mm; block interior is fresh. Sampled from the "staircase" formation on the inner NE caldera wall.</p>
	<p><u>P4-143-R16</u> 18 x 14 x 6 cm subrounded friable block consisting exclusively of white plagioclase and black pyroxene crystals. Block consists of equant plagioclase crystals (70%) and lath-like to stubby black pyroxene crystals (30%). Block is massive, with no bedding, grading or development of domains with different crystal sizes. Poorly lithified and friable. Clearly represents material from the magma chamber walls. Minor staining to orange-brown along some joints. Sampled as talus from the inner NE caldera wall.</p>
	<p><u>P4-143-R17</u> 9 x 7 x 6 cm black plagioclase basalt. 10% plagioclase phenocrysts up to 3 mm across, but their distribution ranges from 20% in shear zones decreasing to 5% in the intervening dominant zones of non-vesicular dense lava. The shear zones are typically 5 mm wide and feature incipient pull-aparts and 10% voids up to 2 mm across. These shear zones are spaced at semi-regular intervals of 1 cm. The block is fresh with minimal surface weathering. Lava flow from the inner NE caldera wall.</p>
	<p><u>P4-143-R18</u> 17 x 11 x 6 cm subrounded block of green volcanoclastic sediment. Block consists of angular to sub-angular, light colored (mostly yellow shades) clasts of deeply weathered (altered?) lava up to 4 mm across set in a matrix of dark yellowish green clay. No bedding or grading. Well-cemented (carbonate) and the matrix is weakly chlorite-altered. Surface is the same as the block interior. A talus block near the base of the inner NE caldera wall.</p>

End of Photolog for Volcano 1.

Appendix 4 – Quick Look Reports

- Sledenia fish
- One small shark (1 m)

Near the low-temperature vent field during P5-636 (observer and pilot report):

- 3 pink crabs (up to 15 cm diameter, including legs), possibly Brachyuran(?) among Fe-oxyhydroxide chimneys
- Single swimming scale worm (Polynoidae?)
- Clumps of small (3 cm) contorted worm tubes in fractures in basalt and on rocks near bacterial mat and Fe-oxyhydroxide precipitates (possibly Siboglinidae polychaete worms similar to those normally associated with vents); dead
- Clumps of live Seripulidae filter feeders at the base of an Fe-oxyhydroxide chimney (sampled)

Midwater organisms observed in video (L. Lundsten, MBARI):

- Munopsidae (Isopoda)
- Calycophorae (Siphonophora)
- Bathylagidae (?)
- Trachymedusae (Medusae)
- Crossota? (Medusae)
- Sergestidae (Decapoda)
- Mysida (Decapoda)
- Chaetognatha (Arrow Worms)
- Appendicularia (Larvaceans)

Benthic organisms observed in video (L. Lundsten, MBARI):

- Brisingidae (Asteroidea)
- Zoarcidae? (Eelpout fishes; possibly Ophidiiformes though difficult to see)
- Lepidisis (unbranched Isididae upon rockwall)
- Anthomastus (Octocorallia - I think)
- Porifera (possible, though no good close-ups)

Mission Evaluation

Limitations, failures, operational problems:

None.

Recommendations for corrective action or improvement:

None.

In your opinion, did the mission essentially achieve its purpose?

Yes, for all objectives.

Compare actual work accomplished with that planned:

Because of the exploratory nature of the dive, limited sampling was undertaken.

DIVE #3:

P5-637

Location: Volcano 19- caldera
Latitude (on-bottom): 24°48.110'S
Latitude (off-bottom): 24°48.383'S
Time (on-bottom): 10:27
Bottom Duration: 6 hours, 18 mins

Date: June 14, 2005
Longitude (on-bottom): 177°01.173'W
Longitude (off-bottom): 177°01.066'W
Time (off-bottom): 15:45
Maximum Depth: 1012 mbsl

Project: SITKAP
Principal Investigator: Prof. Peter Stoffers
Address: Institut für Geowissenschaften
Universität Kiel
Olshausenstr. 40
24098, Kiel
GERMANY

Appendix 4 – Quick Look Reports

- Bathylagidae (?)
- Trachymedusae (Medusae)
- Crossota? (Medusae)
- Sergestidae (Decapoda)
- Mysida (Decapoda)
- Chaetognatha (Arrow Worms)
- Appendicularia (Larvaceans)

Benthic organisms observed in video (L. Lundsten, MBARI):

- Brisingidae (Asteroidea)
- Zoarcidae? (Eelpout fishes, possibly Ophidiiformes though difficult to see)
- Lepidisis (unbranched Isididae upon rockwall)
- Anthomastus (Octocorallia - I think)
- Porifera (Possible, though no good close-ups)

Mission Evaluation

Limitations, failures, operational problems:

None.

Recommendations for corrective action or improvement:

None.

In your opinion, did the mission essentially achieve its purpose?

Yes, for all objectives.

Compare actual work accomplished with that planned:

Actual work fully met the expectations.

DIVE #4:

P5-638

Location:	Volcano 19- caldera to summit	Date:	June 16, 2005
Latitude (on-bottom):	24°48.073'S	Longitude (on-bottom):	177°00.688'W
Latitude (off-bottom):	24°48.400'S	Longitude (off-bottom):	177°00.160'W
Time (on bottom):	09:09	Time (off-bottom):	16:10
Bottom Duration:	7 hours, 01 mins	Maximum Depth:	980 mbsl

Project:	SITKAP		
Principal Investigator:	Prof. Peter Stoffers		
Address:	Institut für Geowissenschaften Universität Kiel Olshausenstr. 40 24098, Kiel GERMANY		
Phone:	+49-431-880 2850		
Observer:	Gary Massoth		
Address:	Institute of Geological and Nuclear Sciences 69 Gracefield Road PO Box 30-368 Lower Hutt NEW ZEALAND		
Pilot 1:	Terry Kerby	Pilot 2:	Steve Price

Dive Objectives:

The goals of this dive were: (1) to explore the east wall of the caldera to further pinpoint the source of 880 ± 35 m plume, (2) to proceed up the shute and investigate the prominent sub-vertical wall (dyke?) that forms its upper part, (3) to explore the summit of the volcano, and (4) to sample hydrothermal fluids, minerals, and biota.

Observations, findings, etc:

The dive commenced moving upslope from below the base of lower north escarpment on the NE caldera floor. Climbed to 890 mbsl and proceeded north until encountered altered rock from above. Also noted dense 'smoke' in same region as saw during dive 635, so went downslope to 969 mbsl in search of vents, which were not found. Climbed back normal to slope heading NW to 890 mbsl, then south to base of wall in the upper part of the shute which is a columnar jointed rock face that was ascended for 70+ m. From this point worked way to base of main upper escarpment at 647 mbsl. Climbed directly up, observing little rock but primarily compacted breccia until about 504 mbsl when an FeOOH vent patch (venting at 79°C) was found and sampled for fluids. Rose to the summit, crossing rock and FeOOH crust to a pinnacle at 384 mbsl where a 14 m-high barite chimney was observed and sampled. Tmax was 245°C and phase separated flow was evident as bubbles. Transited to the south summit and sampled crust, but barely explored before leaving the seafloor.

Species List:

Samples Collected:

- P5-638-A1 Bythograeidae (4); 13:51, 399 mbsl, 24° 48.269'S, 177° 00.108'W
- P5-638-A2 Galatheidae (3); found on coral
- P5-638-A3 Caryophiliidae (Lophelia?); 13:22, 418 mbsl, 24° 48.265'S, 177° 00.208'W

Midwater organisms observed in video (L. Lundsten, MBARI):

- Pyrosoma
- Cylothone
- Appendicularia
- Munnopsidae
- Mysida
- Bathylagidae?
- Pasiphaeidae
- Chaetognatha
- Tomopteris
- Euphasiid?

Benthic organisms observed in video (L. Lundsten, MBARI):

- Green headed eels - numerous
- Synaptibranchidae
- Holothuroidea
- Asteroidea
- Serpulidae - on columnar jointing
- Caryophiliidae (cup corals)
- Gorgonacea (small white)
- Squiliformes (cat shark)
- Lepidisis
- Trachymedusae (on rock)
- Brisingidae
- Ophiuroidea
- Bathypathes
- Crinoidea (white stalked, frilly)
- Keratoisis?
- Palanuridae
- Galatheidae (red, long arms)

Mission Evaluation

Limitations, failures, operational problems:

The snorkels on both the Major and Gas-Tight samplers were positioned with the intake sloped downward, rather than upward, during sampling. This may hinder flushing of the snorkel and increase the effective dead volumes of these samplers.

Recommendations for corrective action or improvement:

Appendix 4 – Quick Look Reports

Valuable time on the seafloor could be saved when working in confined areas by communicating only the decimal minutes when sending and confirming position information.

In your opinion, did the mission essentially achieve its purpose?

Yes.

Compare actual work accomplished with that planned:

The primary objectives of observing the shute, west wall escarpments and locating sites of hydrothermal discharge at the summit were fully accomplished. Ancillary rock sampling in the summit area was deferred to a subsequent dive due to time limitations.

DIVE #5:	P5-639		
Location:	Volcano 19- summit	Date:	June 17, 2005
Latitude (on-bottom):	24°48.555'S	Longitude (on-bottom):	177°00.426'W
Latitude (off-bottom):	24°48.402'S	Longitude (off-bottom):	177°00.165'W
Time (on-bottom):	09:27	Time (off-bottom):	16:20
Bottom Duration:	6 hours, 53 mins	Maximum Depth:	585 mbsl
Project:	SITKAP		
Principal Investigator:	Prof. Peter Stoffers		
Address:	Institut für Geowissenschaften Universität Kiel Olshausenstr. 40 24098, Kiel GERMANY		
Phone:	+49-431-880 2850		
Observer:	Dr. Roger Hekinian		
Address:	Keryunan 24290, Saint Renan FRANCE		
Pilot 1:	Terry Kerby	Pilot 2:	Max Cremer

Dive Objectives:

To explore the youngest volcanic crater located on the eastern side of the summit. Since the shallowest part of the volcanic cone is at about 380 mbsl, a contour depth of 500–550 mbsl was chosen to circumnavigate the southern portion of the summit (WP1 to WP3). Field observations of the morphology and structure of the three summit highs and several small pit craters <300 m in diameter are planned. Search and sample volcanic rocks associated with the various structures and the hydrothermal fields. In addition, it was intended to delineate the extent of hydrothermal activity on the summit by sampling and temperature probing at various locations. Another goal was to define the geological setting in which the hydrothermal fields, Fe-Si oxyhydroxide and active barite chimneys found during dive P5-638 were formed (WP 7 and WP8).

Observations, findings, etc:

The dive was launched in very good weather conditions, allowing a bottom time of about 6 hours. About half of the summit was circumnavigated at a contour depth of 500–550 mbsl. This survey included the southern portion of the summit area where extensive Fe-Si oxyhydroxide crusts, small mounds and small ridges occur. The area covered by Fe-Si oxyhydroxide shows sporadic and diffuse low temperature (<30°C) venting associated with bacterial mats. Along the SE flank two small pit craters of 40 and 70 m depth were explored. They are moderately sedimented and the volcanics are covered by Fe-Si oxyhydroxide crust. A few dyke swarms and talus of massive lava outcrop at the rims of the pit craters. The northern rim of the most easterly located pit-crater (WP3) shows diffuse venting at 537 mbsl with abundant biology (dead clams and a live starfish). The three highs forming the summit were explored. The NE high consists of a plateau covered by Fe-oxyhydroxide crust colonized by small corals and has no trace of hydrothermal activity. The Fe-oxyhydroxide crust lying on top of scoriaceous "aa" lava flows is exposed along an E–W trending fault scarp. The central high with barite chimneys formed on top of massive lava flows along a SW–NE (N020°) oriented ridge, probably associated with a fault. The SW high, where

Appendix 4 – Quick Look Reports

active venting and barite was found during dive P5-638, consists also of Fe-oxyhydroxide crust on top of massive basaltic flows exposed along E–W fault scarps. A small low temperature (26.7°C) hydrothermal field was found at 426 mbsl on the most SW tip of the summit. This field occurs in a "caved-in" lobate lava flow. Several biological specimens were collected from the hydrothermal field.

Species List:

Samples collected:

- P5-639-A1ab Brachyuran crabs; in biobox
- P5-639-A2 Polynoidae (2); in biobox
- P5-639-A3 Mussels (8); from rocks in biobox
- P5-639-A4 Limpets (25); from rocks in biobox
- P5-639-A5 Asteroidea; 11:43, 540 mbsl
- P5-639-A6 Ophiuroidea; found in gorgonian
- P5-639-A7 Echinoidea; 13:06, 409 mbsl
- P5-639-A8 Polychaete
- P5-639-A9 Polychaete
- P5-639-A10 Barnacle
- P5-639-A11 Hydrozoa
- P5-639-A12 Gorgonacea; 13:13, 400 mbsl, 24° 48.170'S, 177° 00.010'W
- P5-639-A13 Vent worms; 15:46, 426 mbsl, 24° 48.403'S, 177° 00.165'W
- P5-639-A14 Brachyuran; several, found on vent worms
- P5-639-A15 Galatheididae (2); found on rocks
- P5-639-A16 Worms (2); found on rocks

Midwater organisms observed in video (L. Lundsten, MBARI):

- Munnopsidae
- Salpida
- Siphonophora
- Mysida
- Chaetognatha
- Euphausiid
- Ctenophora?
- Trachymedusae

Benthic organisms observed in video (L. Lundsten, MBARI):

- Elasmobranchii (mostly small, numerous)
- Ophiuroidea
- Hermit crab (large, 10:23)
- Caryophylliidae (Lophelia like, abundant)
- Solaster? (10:30)
- Gorgonacea (small, white)
- Anthomastus? (white, 10:33)
- Caridea
- Galatheididae (long armed, red)
- Clams (numerous, unusual, roundish, all dead, 11:33)
- Mussels (elongate, all dead, 11:33)
- Chaunax? (red)
- Asteroidea (like sample asteroid - dense)
- Pleuronectiformes
- Gorgonacea (dense, smaller at first then larger, like sample)
- Porifera?
- Zooanthid anemones? (very dense on dikes, yellow)
- Bythograeidae (at vents where worms were collected)

Mission Evaluation

Limitations, failures, operational problems:

None.

Appendix 4 – Quick Look Reports

- P5-640-A3 Caryophylliidae (lophelia like, dead) 12:27, 520 m
- P5-640-A4 Serpulidae (most likely dead)
- P5-640-A5 Vermetidae (from R8)
- P5-640-A6 Porifera (from R8)
- P5-640-A7 Bryzoan? (from R8)
- P5-640-A8 Ophiuroidea (from R6)

Midwater organisms observed in video (L. Lundsten, MBARI):

- Mysida (Decapoda)
- Chaetognatha (Arrow Worms)
- Appendicularia (Larvaceans)
- Salpida
- Cydippida?

Benthic organisms observed in video (L. Lundsten, MBARI):

- Crinoidea (white stalked, numerous)
- Actinaria
- Caridea
- Galatheidae (long arms, red)
- Chrysogorgiidae 11:16, 637m
- Echinoidea
- Hydractinia (large)
- Cerianthidae
- Elasmobranchii
- Ophiuroidea
- Gorgonacea
- Paguroidea (hermit crab)
- Narella?
- Caryophylliidae (lophelia like)
- Anthomastus?
- Gorgonacea (green, sampled)
- Polychaete (tubes only, all animals were dead)
- Porifera

Mission Evaluation

Limitations, failures, or operational problems noted:

None.

Recommendations for corrective action or improvement:

None.

In your opinion, did the mission essentially achieve its purpose?

Yes.

Compare actual work accomplished with the work that was expected to be accomplished.

The ground track was exactly as planned. A major surprise with the scarp exposing a pyroclastic flow sequence rather than stacked lavas, but in hindsight not unexpected.

DIVE #7:

P5-641

Location:	Volcano 18s- caldera wall	Date:	June 19, 2005
Latitude (on-bottom):	24°33.974'S	Longitude (on-bottom):	176°55.055'W
Latitude (off-bottom):	24°33.802'S	Longitude (off-bottom):	176°54.714'W
Time (on-bottom):	09:22	Time (off-bottom):	15:56
Bottom Duration:	6 hours, 34 mins	Maximum Depth:	1223 mbsl

Project: SITKAP
Principal Investigator: Prof. Peter Stoffers

Appendix 4 – Quick Look Reports

Address: Institut für Geowissenschaften
Universität Kiel
Olshausenstr. 40
24098, Kiel
GERMANY

Phone: +49-431-880 2850

Observer: Dr. Tim Worthington

Address: Institut für Geowissenschaften
Universität Kiel
Olshausenstr. 40
24098, Kiel
GERMANY

Pilot 1: Terry Kerby

Pilot 2:

Steve Price

Dive Objectives:

Explore and sample a series of stacked lava flows and chlorite-clay material overlain by the caldera forming pyroclastic flow sequence. These outcrop along a series of 3 ridges at the mid- to upper slopes, inner north caldera wall (WP-1 to WP-10). This is the main aim of the dive. Contour around the inner caldera wall at 910 mbsl to explore for a hydrothermal system known to be present somewhere within the caldera at this depth (WP-10 to WP-12). Explore and sample stacked lava flows on a steep ridge on the inner NE caldera wall (WP-12 to WP-13). If warranted and time permits, continue from here to the summit (WP-14 onwards) to further examine the caldera forming pyroclastic flow sequence.

Observations, findings:

The dive was launched in good weather conditions, allowing a bottom time of 6.4 hours. The prime objectives were achieved. The pyroclastic flow sequence was found to be more complex than previously suspected. At least 3 distinct units are present. The lower unit varies from slightly to pervasively altered with local development of sericitic clay veins are rarely chlorite. This alteration is most severe at 920 mbsl but was found over a total range of 843-1020 mbsl. Above this is an unaltered pyroclastic unit with a subwelded middle section, readily distinguished by the presence of basalt clasts within the uppermost 50 m and overlain by basaltic talus. A further thinner pyroclastic flow sequence, with a mixed population of pumice and ~10% basaltic clasts, caps this unit. The same sequence was observed on a parallel ascent of the inner wall later in the day positioned further to the east.

Species List:

Samples collected:

- P5-641-A1 Polychaete (from R9)
- P5-641-A2 Caryophiliidae (unusual, from R12)
- P5-641-A3 Unusual bivalve (from R12, 12:00, 675m)
- P5-641-A4 Unusual bivalves (2, from R12)
- P5-641-A5 Porifera (from R5)
- P5-641-A6 Caryophiliidae #1 (from R9)
- P5-641-A7 Caryophiliidae #2 (from R9)
- P5-641-A8 Unusual bivalve (1 valve, from R9)
- P5-641-A9 Caryophiliidae (dead, from R9)
- P5-641-A10 Caryophiliidae (5, from R14)

Midwater organisms observed in video (L. Lundsten, MBARI):

- Mysida (Decapoda)
- Munnopsidae (isopoda, numerous)
- Appendicularia (Larvaceans)
- Salpida
- Lobata
- Aeginura?

Benthic organisms observed in video (L. Lundsten, MBARI):

- Cerianthidae
- Crinoidea (white stalked, numerous)

Appendix 4 – Quick Look Reports

- Actiniaria
- Gorgonacea (whip)
- Paguroidea (hermit crab)
- Caryophiliidae (Iophelia like)
- Anthomastus?
- Gorgonacea (green, sampled)
- Porifera
- Synaptobranchiidae
- Ophidiiformes? 10:37, 1008 m
- Iridigorgia
- Asteroidea
- Zoarcidae

Mission Evaluation

Limitations, failures, or operational problems noted:

None.

Recommendations for corrective action or improvement:

None.

In your opinion, did the mission essentially achieve its purpose?

Yes.

Compare actual work accomplished with the work that was expected to be accomplished.

Time did not permit more than two ascents of the inner caldera wall, but this was anticipated and the results were more than satisfactory.

DIVE #8:

P4-137

Location:	Volcano 19- summit	Date:	June 20, 2005
Latitude (on-bottom):	24°48.395'S	Longitude (on-bottom):	176°59.997'W
Latitude (off-bottom):	24°48.450'S	Longitude (off-bottom):	176°59.985'W
Time (on-bottom):	14:00	Time (off-bottom):	17:17
Bottom Duration:	3 hours, 17 mins	Maximum Depth:	540 mbsl

Project:	SITKAP
Principal Investigator:	Prof. Peter Stoffers
Address:	Institut für Geowissenschaften Universität Kiel Olshausenstr. 40 24098, Kiel GERMANY
Phone:	+49-431-880 2850
Observer:	Prof. Mark Hannington
Address:	Dept of Earth Sciences Marion Hall, University of Ottawa 140 Louis Pasteur Ottawa, Ontario K1N 6N5 CANADA

Pilot 1:	Terry Kerby	Pilot 2:	Max Cremer
-----------------	-------------	-----------------	------------

Dive Objectives:

Land close to the eastern crater at its SE corner to sample clams (WP1). Transit to the area of active venting at the southern end of the summit (WP2, 430 mbsl). Investigate the possibility of more vigorous venting near the southern field. Transit to the large barite chimneys (WP3, marker #37, 385 mbsl). Investigate smaller chimneys surrounding the main "barite tower". Sample a range of chimney types, knocking over one or two with active flow to create better vents for fluid

sampling. Re-sample vigorous flow at the top of the large tower. If time permits, investigate areas of the cone along the 450–500 mbsl contour for additional venting.

Observations, findings, etc:

The dive was delayed due to a problem with the manipulator (Titan) on Pisces V and the morning was spent switching to Pisces IV. Pisces IV was launched in good weather conditions at about 13:15, allowing a bottom time of 3.5 hours (extended to 17:15). The original objectives were not fully achieved, owing to the shortness of the dive and because of unexpected findings in the pit crater SE of the summit ridge. A vigorous high-temperature vent (~270°C) was located on the SW slope of the pit in which clams had been observed during P5-639. The vents occur in an area of sedimented talus, close to the projection of the E–W trending dikes noted on the east wall of the pit. A large area of sedimented talus (approx. 50 m x 50 m) at the SW corner of the pit is littered with clams and mussels, partially buried in the sediment. Outside the area of sediment, more diffuse venting was observed in the bare talus. Several fractures and ridges in the sediment-covered talus are punctuated by active venting through holes in the sediment and small (<1 m) anhydrite spires leading up to the rim of the pit. One sample of a smaller spire was collected (R1) and a minimum temperature of 200°C was measured in the flow after the chimney was sampled (only the low-temperature read-out was available, so the actual temperature of the vent was likely higher). Marker #40 (560 mbsl) was deployed immediately down slope from this vent. Near the center of the area of diffuse venting, on the sedimented slope, two large anhydrite spires (one active and one inactive) were found on low mounds of anhydrite debris (collapsed material from former chimneys). The active vent comprises a single large spire, about 1.5 m tall (narrow at the base and branching into 3 spires at the top). Several smaller active chimneys occur through the anhydrite talus at the base of the larger spire. Three small 2-phase vents (flame-like steam venting) were observed on the spire. When knocked over, an open hole at the base of the spire (~10 cm diameter) began to vent vigorous 2-phase fluid. Two major samples and two gas-tight samples were collected in this hole. A precise temperature could not be measured, but 2-phase venting at this depth (540 mbsl) indicates a minimum temperature of about 260–270°C. Several small pieces of the large spire that was knocked over were collected: R2 (a) several friable anhydrite-rich pieces from the top of the chimney, (b) several small pieces of chalcopyrite-lined chimney wall, and (c) one large coarsely crystalline, massive anhydrite sample with chalcopyrite and sphalerite/wurtzite from the base of the spire. A short transit upslope from the vent revealed several additional patches of venting. At the rim of the pit venting was no longer observed, but the rim is covered in thick deposits of Fe-Mn crust. No Fe-Mn crusts were observed in the pit, suggesting that the crater and active hydrothermal vents may be relatively recent features associated with late intrusions of dikes.

Species List:

Samples collected:

- P4-137-A1 Bathymodiolus (1 sample but 3 frozen gill & adductor, 3 70% ethanol gill & adductor)
- P4-137-A2 Asteroidea
- P4-137-A3 Sipunculans (from bisset thread and mantle of mussel)
- P4-137-A4 Mussel (juvenile from bisset thread of adult)
- P4-137-A5 Polynoidae
- P4-137-A6 Polynoidae (from R2)

Midwater organisms observed in video (L. Lundsten, MBARI):

- Mysida (Decapoda)

Benthic organisms observed in video (L. Lundsten, MBARI):

- Bythograeidae
- Polynoidae (numerous at vents, red)
- Asteroidea
- Clam shells – all dead
- Pleuronectiformes (numerous)
- Ophiuroidea

Mission Evaluation

Limitations, failures, operational problems:

Appendix 4 – Quick Look Reports

Absence of a high-temperature probe. Otherwise none.

Recommendations for corrective action or improvement:

None.

In your opinion, did the mission essentially achieve its purpose?

Yes. The results were quite different from the planned objectives, owing to the discovery of the new vent.

Compare actual work accomplished with that planned:

An excellent collection of both waters and hydrothermal precipitates was recovered, together with biological samples from the vicinity of the vents.

DIVE #9: P4-138

Location:	Volcano 19- summit	Date:	June 21, 2005
Latitude (on-bottom):	24°48.455'S	Longitude (on-bottom):	176°59.923'W
Latitude (off-bottom):		Longitude (off-bottom):	
Time (on-bottom):		Time (off-bottom):	
Bottom Duration:	7 hours, 30 mins	Maximum Depth:	562 mbsl

Project: SITKAP
Principal Investigator: Prof. Peter Stoffers
Address: Institut für Geowissenschaften
Universität Kiel
Olshausenstr. 40
24098, Kiel
GERMANY

Phone: +49-431-880 2850
Observer: Lonny Lundsten
Address: Monterey Bay Aquarium Research Institute
7700 Sandholdt Road
Moss Landing
California 95039
UNITED STATES

Pilot 1: Terry Kerby **Pilot 2:** Colin Wollerman

Dive Objectives:

To land close to the SE corner of the young crater on the eastern summit and sample bivalves (WP1). Transit to the area of active venting at the southern end of the summit (WP2, 430 mbsl). Investigate the possibility of more active venting near the southern field. Transit to the large barite chimneys (WP3, Marker 37, ~385 mbsl). Investigate smaller chimneys surrounding the main barite tower. Sample a range of chimney types, knocking over one or two with active flow to create better vents for fluid sampling. Resample vigorous flow at the top of the large tower. If time permits, investigate areas of the cone along the 450–500 mbsl contour for additional venting.

Observations, findings, etc:

The dive was launched in excellent weather conditions, allowing a bottom time of about 7.5 hours. We descended near the 560 mbsl eastern crater to the SE of the summit in the hopes of finding more mussels and live clams. We found clam shells and mussel shells lying upon the sediment, though all were dead. We sampled a few shells, which can be used for identification purposes. Numerous diffuse venting sites existed and some small chimneys were observed. One Bathymodiolus mussel was sampled. We began making our way toward M38 and although we did not find it, we were very near to it. We sampled the temperature of several vent sites along the way and also took chimney samples at a few locations. We observed that a chimney structure seen the previous day that had been knocked over had “re-grown” by about 30 cm overnight. We also observed a small flame structure at one of the vents. We began making our way towards the Tower site since it was getting late in the day and we needed to take water samples at that location. While on route to the Tower, we were in a field of diffuse venting with flanges regularly distributed upon the seafloor and noticeable schlurring at each one. Just below the thin crust on the surface we

found the sediment to be bright green and very deep. We took a scoop of sediment and a sample of the crust at this unusual location. After arriving at the Tower site we knocked over several chimneys, hoping that we could create a more robust flow for sampling, though it didn't work as well as we had hoped. We sampled fluids at a chimney (white major, blue gas tight), which had a temp of 130°C. We decided to head back towards the high temp (flame structure) that we had seen earlier in the vicinity of M38 to get our final water samples. On the approach to M38 we observed a nice chimney structure with a very large flame and black smoke emanating from a vent near the seafloor. We observed this structure for sometime and sampled with a Major (blue) and a Gas Tight (green). At this point we proceeded in the direction of M38, located the site and left the benthos.

Species List:

Samples collected:

- P4-138-A1 Bythograeidae (3, 9:47, 558m)
- P4-138-A2 Bathymodiolus (9:47, 558m)
- P4-138-A3 Polynoidae
- P4-138-S1 Mussel and clam shells (all dead)

Midwater organisms observed in video (L. Lundsten, MBARI):

- Mysida (Decapoda)
- Salpida (numerous)

Benthic organisms observed in video (L. Lundsten, MBARI):

- Bythograeidae
- Polynoidae (numerous at vents, red)
- Asteroidea
- Clam shells – all dead
- Pleuronectiformes (numerous)
- Ophiuroidea

Mission Evaluation

Limitations, failures, operational problems:

None.

Recommendations for corrective action or improvement:

Visibility on the observer site could be improved.

In your opinion, did the mission essentially achieve its purpose?

Yes, for all objectives.

Compare actual work accomplished with that planned:

The dive plan was followed.

DIVE #10:

P4-139

Location: Volcano 1- summit craters
Latitude (on-bottom): 21°09.660'S
Latitude (off-bottom): 21°09.293'S
Time (on-bottom): 08:39
Bottom Duration: 7 hours, 05 mins

Date: June 23, 2005
Longitude (on-bottom): 175°44.202'W
Longitude (off-bottom): 175°44.655'W
Time (off-bottom): 15:44
Maximum Depth: 365 mbsl

Project: SITKAP
Principal Investigator: Prof. Peter Stoffers
Address: Institut für Geowissenschaften
Universität Kiel
Olshausenstr. 40
24098, Kiel
GERMANY

Appendix 4 – Quick Look Reports

Phone: +49-431-880 2850
Observer: Dr. Ulrich Schwarz-Schampera
Address: Federal Institute for Geosciences and Natural Resources
BGR
Stilleweg 2
30655, Hannover
GERMANY

Pilot 1: Terry Kerby

Pilot 2:

Steve Price

Dive Objectives:

Transit from the drop point (WP1) to the ridge NE of the south cone, then to the area of active venting found by RCV-314 searching for active vents. Transit NW along the ridge to the area of strongest venting (WP2, 190 mbsl; according to plume mapping and RCV-314), searching for the origin of smoke observed during RCV-314. Continue to the area of altered talus, sampling the talus material and locating its origin. Continue to the northern end of the hydrothermal field near WP3 (260 mbsl) sampling where appropriate. Continue SE to WP4 (140 mbsl), heading 100°, along the eastern ridge to locate the plume source at 220 mbsl and the origin of smoke seen there during RCV-314.

Observations, findings, etc:

The reconnaissance dive at Volcano 1 was launched in excellent weather conditions, allowing a bottom time of about 7 hours. The dive started in a water depth of 365 m half-way to the crater valley from the southern caldera floor. There were no indications of the hydrothermal activity suggested by the plume survey. The slope is covered by monotonous talus of scoriaceous ash. We then followed the approximate track of RCV-314, which discovered a plume and smoke of possibly hydrothermal origin as well as a large area of white bacterial mats. Owing to the fact that the dive track was shifted to the NE, the only the rims of the bacterial mats were observed. The location of the strongest hydrothermal plume at a water depth of 172 m, which also was observed during the RCV track, was surveyed several times (5x) but evidence for any hydrothermal venting was not observed apart from a significant reduction in visibility. The survey then proceeded towards the north and back to the SE to WP4, only noting more monotonous talus of scoriaceous ash. On the following track to the SW crossing the central crater NE of the young south cone we discovered a large area (several hundred metres diameter) of diffuse hydrothermal venting (clear water and gas bubbles) with a dense population of mussels (*Bathymodiolus* sp.), associated with shrimps, crabs, and fish. Venting occurs at temperatures between 23 and 52°C. The distribution of the mussels is heterogeneous and associated with the higher temperatures. In between and underneath the mussel fields, precipitates of native sulfur and barite (?) were seen. These are the locations of the highest temperature venting (52°C). The dive ended when a partial breakdown of the hydraulic system occurred, causing the immediate return of the Pisces IV to the surface.

Species List:

Samples collected:

- P4-139-A1 Caridea (found on mussels)
- P4-139-A2 Platyhelmenthes?, Red worms (found in mussels, usually on gills)
- P4-139-A3 Limpets (118, found on mussels)
- P4-139-A4a,b Juvenile mussels (found on larger mussels)
- P4-139-A5-A25 Bathymodiolus (1 adductor & gill frozen, 1 adductor & gill 70% Eth)
- P4-139-A26 Platyhelmenthes? (from mantle cavity of Mussel)

Midwater organisms observed in video (L. Lundsten, MBARI):

- Salpida (numerous)

Benthic organisms observed in video (L. Lundsten, MBARI):

- Cerianthidae? (white, numerous)
- Caridea (at base of Cerianthidae)
- Asteroidea
- Actiniaria
- Gorgonacea (corkscrew whips, numerous)
- Nidaliidae (soft corals, numerous)
- Echinoidea

- Porifera
- Gastropoda
- Bathymodiolus (mussel beds, dense)
- Limpets (dense, on mussels and rocks)
- Grouper (many)

Mission Evaluation

Limitations, failures, operational problems:

Partial failure of the hydraulic system.

Recommendations for corrective action or improvement:

None.

In your opinion, did the mission essentially achieve its purpose?

Yes, for the objectives of a reconnaissance dive.

Compare actual work accomplished with that planned:

Actual work fully met the expectations for a reconnaissance dive.

DIVE # (aborted): P4-140

Location:	Volcano 1- summit craters	Date:	June 24, 2005
Latitude (on-bottom):	21°09.362'S	Longitude (on-bottom):	175°44.520'W
Latitude (off-bottom):	21°09.362'S	Longitude (off-bottom):	175°44.520'W
Time (on-bottom):	08:20	Time (off-bottom):	08:40
Bottom Duration:	0 hours, 20 mins	Maximum Depth:	200 mbsl

Project: SITKAP
Principal Investigator: Prof. Peter Stoffers
Address: Institut für Geowissenschaften
Universität Kiel
Olshausenstr. 40
24098, Kiel
GERMANY
Phone: +49-431-880 2850
Observer: Dr. Mark Schmidt
Address: Institut für Geowissenschaften
Universität Kiel
Olshausenstr. 40
24098, Kiel
GERMANY
Pilot 1: Terry Kerby

Pilot 2: Max Cremer

Dive Objectives:

The goals of the dive were: (1) to explore the extension of the mussel field and localize the plume source in the southern and central craters; (2) to sample the vent fluids and gases; and (3) to collect rock samples from the northern slope of the south cone.

Observations, findings, etc:

None, due to electrical and hydraulic failures causing immediate termination of the dive.

Species List:

Midwater organisms observed in video (L. Lundsten, MBARI):

- Mysida

Benthic organisms observed in video (L. Lundsten, MBARI):

- Bacterial mat (dense, filamentous, white)

Appendix 4 – Quick Look Reports

- P4-141-A7 Limpets; 2, found on mussels
- P4-141-A8 Polychaetes; from Sediment Scoop 5 with lots of sulfur
- P4-141-A9 Polynoidae?
- P4-141-A10 Polychaetes

Midwater organisms observed in video (L. Lundsten, MBARI):

- Mysida

Benthic organisms observed in video (L. Lundsten, MBARI):

- Bacterial mat (dense, filamentous, white)
- Pennatulacea (small)
- Bathymodiolus (dense)
- Pleuronectiformes (numerous in mussel beds)
- Asteroidea
- Limpets (numerous on mussels)
- Gorgonacea (corkscrew whip)
- Gastropoda
- Brachyuran crabs (numerous in mussel beds)
- Echinoidea
- Grouper sp.1
- Grouper sp.2
- Elasmobranchii
- Idols
- Wrasses
- Moray eels
- Numerous other tropical fish of various (unknown) species

Mission Evaluation

Limitations, failures, operational problems:

None.

Recommendations for corrective action or improvement:

None.

In your opinion, did the mission essentially achieve its purpose?

Yes, for the objectives of reconnaissance and sampling.

Compare actual work accomplished with that planned:

Actual work fully met the expectations for a reconnaissance and sampling dive.

DIVE #12:

P4-142

Location:	Volcano 1- summit craters	Date:	June 25, 2005
Latitude (on-bottom):	21°09.130'S	Longitude (on-bottom):	175°43.480'W
Latitude (off-bottom):		Longitude (off-bottom):	
Time (on-bottom):		Time (off-bottom):	
Bottom Duration:	8 hours, 13 mins	Maximum Depth:	438 mbsl

Project:	SITKAP
Principal Investigator:	Prof. Peter Stoffers
Address:	Institut für Geowissenschaften Universität Kiel Olshausenstr. 40 24098, Kiel GERMANY
Phone:	+49-431-880 2850
Observer:	Rennie Vaiomo'unga
Address:	Ministry of Lands, Survey and Natural Resources

Appendix 4 – Quick Look Reports

PO Box 5
Nuku'alofa
KINGDOM OF TONGA
Terry Kerby

Pilot 1:

Pilot 2:

Steve Price

Dive Objectives:

Start from the eastern end of the semi-circular ridge in the southern part of the Volcano 1 caldera (WP1), then proceed west along the ridge towards the crater chain to the hydrothermal field near WP2. Proceed to WP3 and WP4 in the southern crater for further sampling of the mussel fields and venting. Then continue to WP5 and sampling the venting water, gases, altered rocks and biology. Also complete a survey of the central and southern craters contouring along the southern crater walls.

Observations, findings, etc:

We landed at 340 mbsl east of WP1 and started moving upslope SW to WP1. This area was covered by ashes and sediments with brown clay (21° 09.143'S, 175° 43.497'W). We collected pumice at 383 mbsl. Continued up and discovered a red and tan bedding layer exposed under the sediment (21° 09.178'S, 175° 43.956'W, 275 mbsl). On the summit of ridge (WP4) at 131 mbsl we moved SW down to the mussel bed area. We entered white clouds at 156 mbsl and at 170 mbsl visibility dropped to 2 m. Around the base of north slope at 203 mbsl mussel shell fragments and some live mussels were seen. Flat sandy bottom with sediment mounds, depressions, and signs of hydrothermal alteration (21° 09.251'S, 175° 44.660'W). Then moving to the dense mussel bed at 200 mbsl (21° 09.282'S, 175° 44.680'W). At M41 (200 mbsl) we collected Sediment Scoop #2 of what appear to be elemental sulfur fragments (21° 09.288'S, 175° 44.676'W). We then located the venting site with strong flow at 197 mbsl with a temperature of 152°C. We collected blue Major, yellow Major and green Gastight water samples at 21° 09 292'S, 175° 44.654'W together with a sulfurous rock 3 m from the vent.

Then proceeding to M43 at 199 mbsl where the temperature was 71°C in the main bubble vent. We collected blue Gastight, mussels and grabs (21° 09.270'S, 175° 44.727'W). Proceeding upslope to the NW to a ridge at 184 mbsl. This drops a bit to the north with white silt moving up in a slight current from the north (21° 09.200'S, 175° 44.740'W). Continuing down NW into a crater through a dense silt layer to its base at 226 mbsl (21° 09.200'S, 175° 44.740'W). Then proceeding upwards to the west out of the crater to a ridge in clear water at 203 mbsl (21° 09.098'S, 175° 44.844'W). Contouring back to the SE 200 mbsl up to the ridge with a white plume at 199 mbsl (21° 09.174'S, 175° 44.737'W), then back to the west up the slope of the cone to 180 mbsl. Only oxide crust here and out of the dense plume (21° 09.176'S, 175° 44.807'W). Proceeding SE into a dense bed of dead mussels at 196 mbsl (21° 09.244'S, 175° 44.763'W). Then moved back to the SE to the mussel bed and discovered a large clear batch of white deposits with heavy diffuse venting coming from a large area about 4 m across in the middle of a dense mussel bed at 198 mbsl. Visibility appears diminished and slightly smoky (21° 09.279'S, 175° 44.696'W). Finally back to M43 and take a scoop and gas sample, then moved SW to 143 mbsl and left the bottom.

Species List:

Samples collected:

- P4-142-A1 Brachyuran crabs (from mussel beds)
- P4-142-A2 Limpets (from mussels)
- P4-142-A3 Bathymodiulus (7, frozen whole)
- P4-142-A4 – A9 Bathymodiulus

Midwater organisms observed in video (L. Lundsten, MBARI):

- Mysida
- Salpida

Benthic organisms observed in video (L. Lundsten, MBARI):

- Bacterial mat (dense, filamentous, white)
- Pennatulacea (small)
- Bathymodiulus (dense)
- Caryophiliidae
- Caridea (numerous at vent)
- Ophiuroidea

Appendix 4 – Quick Look Reports

- Actiniaria (white, red)
- Pleuronectiformes (numerous in mussel bed)
- Asteroidea
- Limpets (numerous on mussels)
- Gorgonacea (corkscrew whip)
- Gorgonacea (white, fan like)
- Gastropoda
- Brachyuran crabs (numerous in mussel beds)
- Serranidae - Grouper (dense near vent)
- Elapidae, Hydrophiinae – sea snake 11:43
- (numerous other tropical fish, but I don't know the species)

Mission Evaluation

Limitations, failures, operational problems:

None.

Recommendations for corrective action or improvement:

None.

In your opinion, did the mission essentially achieve its purpose?

Yes, for all objectives.

Compare actual work accomplished with that planned:

The dive plan was followed. No venting was found along the semi-circular ridge, but all other areas were as expected.

DIVE #13:

P4-143

Location:	Volcano 1- NE caldera wall	Date:	June 26, 2005
Latitude (on-bottom):	21°07.936'S	Longitude (on-bottom):	175°43.820'W
Latitude (off-bottom):	21°08.246'S	Longitude (off-bottom):	175°43.349'W
Time (on-bottom):	09:02	Time (off-bottom):	15:49
Bottom Duration:	6 hours, 47 mins	Maximum Depth:	585 mbsl

Project: SITKAP
Principal Investigator: Prof. Peter Stoffers
Address: Institut für Geowissenschaften
Universität Kiel
Olshausenstr. 40
24098, Kiel
GERMANY

Phone: +49-431-880 2850
Observer: Dr. Roger Hekinian
Address: Keryunan
24290, Saint Renan
FRANCE

Pilot 1: Terry Kerby

Pilot 2: Max Cremer

Dive Objectives:

The objectives were: (1) to land at the foot of the inner NE caldera wall near the site of SO-167 dredge DR-9 at 460 mbsl and undertake stratigraphic sampling of lavas along the exposed fault scarp, (2) to explore the intersection between the caldera floor and the inner caldera walls in order to detect any signs of hydrothermal activity near 460–470 mbsl, (3) to explore the eastern inner caldera wall at the 440 mbsl contour line heading SSE (150°), and (4) to perform systematic observations and sampling of the inner caldera walls.

Observations, findings, etc:

Appendix 4 – Quick Look Reports

The dive was launched in moderate weather conditions, allowing 7 hours on the bottom. The dive explored a portion of the west-facing inner caldera wall. A complete geological section was completed along a section of the eastern wall between 450 and 210 mbsl near WP1. It was found that the upper part of the volcano was constructed during episodic volcanic activity, the main events of which are recorded in the faulted outcrops generated by the violent caldera-forming eruption. Several explosive events generated bedded ash layers alternating with pyroclastic deposits up to 20 meters thick. Dolerite dykes have intruded these deposits throughout the sections explored. In addition, massive lava flows were observed in the lower part of the outcrops. There are also lava flows interbedded within the pyroclastic sequence suggesting periods of quieter volcanism. The top section near the caldera rim is composed of gravel-sized pyroclastic debris made up of ash and scoria-like “aa” fragments. A pre-caldera cone composed of sand-sized sorted pyroclasts was found at 210 mbsl near sample station R13 and R14 (21° 07.84'S, 175° 43.54'W). The intersection between the caldera floor and the inner caldera walls was explored from WP1 southward for about 1 km. The pyroclastic sequence was found to be continuous around the base in this area. A small mound (<100 m in diameter, <20 m-high) covered with yellowish hydrothermal material was found near the intersection of the NE inner caldera wall and the caldera floor. A temperature of 26°C was recorded.

Species List:

Midwater organisms observed in video (L. Lundsten, MBARI):

- Mysida
- Euphausiid - dense

Benthic organisms observed in video (L. Lundsten, MBARI):

- Gorgonacea (corkscrew whip)
- Crinoidea (white, stalked)
- Caryophylliidae (cup corals)
- Brisingidae
- Muranidae? (yellow moray eel)
- Caridea
- Pennatulacea (small)
- Bathymodiolus (dense)
- Caryophylliidae (Lophelia like)
- Syngnathidae? (pipe fish)
- Muraenidae (striped moray eel)
- Crinoidea (orange feather star)
- Scorpaenidae (red)

Mission Evaluation

Limitations, failures, operational problems:

None.

Recommendations for corrective action or improvement:

None.

In your opinion, did the mission essentially achieve its purpose?

Yes, for all objectives.

Compare actual work accomplished with that planned:

The dive plan was followed without any problems.